SANDIA REPORT

SAND86–2742 • UC–700
Unlimited Release
Printed June 1990

Models for Multimegawatt Space Power Systems

Michael W. Edenburn

Prepared by
Sandia National Laboratories
Albuquerque, New Mexico 87185 and Livermore, California 94550
for the United States Department of Energy
under Contract DE-AC04-76DP00789

Issued by Sandia National Laboratories, operated for the United States Department of Energy by Sandia Corporation.

Printed in the United States of America. This report has been reproduced directly from the best available copy.

Available to DOE and DOE contractors from
Office of Scientific and Technical Information
PO Box 62
Oak Ridge, TN 37831

Prices available from (615) 576-8401, FTS 626-8401

Available to the public from
National Technical Information Service
US Department of Commerce
5285 Port Royal Rd
Springfield, VA 22161

NTIS price codes
Printed copy: A05
Microfiche copy: A01

Accession Number: 4426

Publication Date: Jun 01, 1990

Title: Models for Multimegawatt Space Power Systems

Personal Author: Edenburn, M.W.

Corporate Author Or Publisher: Sandia National Laboratories, Albuquerque, NM 87185 Report Number: SAND86-2742

Report Prepared for: US Department of Energy, Office of Scientific and Technical Information, PO Box 62, Oak Ridege, TN 37831

Descriptors, Keywords: Model Multimegawatt Space Power System

Pages: 00080

Cataloged Date: Mar 31, 1993

Document Type: HC

Number of Copies In Library: 000001

Record ID: 26587

SAND86-2742
Printed December 1990

Distribution
Category - 700

MODELS FOR MULTIMEGAWATT SPACE POWER SYSTEMS

Michael W. Edenburn
Advanced Power Systems Division
Sandia National Laboratories
Albuquerque, NM 87185

ABSTRACT

This report describes models for multimegawatt, space power systems which Sandia's Advanced Power Systems Division has constructed to help evaluate space power systems for SDI's Space Power Office. Five system models and models for associated components are presented for both open (power system waste products are exhausted into space) and closed (no waste products) systems:

1. Open, burst mode, hydrogen cooled nuclear reactor - turboalternator system;
2. Open, hydrogen-oxygen combustion turboalternator system;
3. Closed, nuclear reactor powered Brayton cycle system;
4. Closed, liquid metal Rankine cycle system; and
5. Closed, in-core, reactor thermionic system.

The models estimate performance and mass for the components in each of these systems.

ACKNOWLEDGEMENTS

This document has grown from the modeling efforts of Steve Hudson and Al Marshall as well as the author. Their contributions were critical. The author thanks Steve Hudson and Frank Thom for their detailed review of the document. Because of their efforts, many errors have been corrected and many issues have been clarified. The author is greatful to Sandy Portlock for her editorial efforts and to Lou Cropp, who gave considerable support to the document's creation.

This work was performed at Sandia National laboratories, which is operated for the U.S. Department of Energy under contract #DE-AC04-76DP00789, for the Strategic Defense Initiative Space Power Office's Independent Evaluation Group. Sandia is teamed with NASA's Lewis Research Center for this effort.

TABLE OF CONTENTS

LIST OF TABLES

LIST OF FIGURES

INTRODUCTION

Sandia National Laboratories' Advanced Power Systems Division performs system analysis for the Strategic Defense Initiative (SDI) Space Power Office's Independent Evaluation Group (IEG) to help SDI evaluate multimegawatt space power system concepts. These systems are ultimately planned to power space based antiballistic missile weapons and their associated surveillance and command satellites. The purpose of the evaluation is to identify promising technologies and concepts which will lead to more effective, less expensive space power systems. Identifying these technologies and concepts will help the SDI direct their space power development program.

Proposed multimegawatt space power concepts take a variety of forms. Primary energy sources proposed include reactors, chemicals, the sun, and various energy storage devices such as batteries, flywheels, and large, cryogenic inductors. Turbines with generators, thermionics, thermoelectrics, alkali metal thermoelectrics, thermophotovoltaics, magnetohydrodynamics, and others have been proposed as energy converters. Two basic types of systems are needed--"continuous" power systems to provide power over a long time for general service loads and "burst" power systems to provide power to weapons for a several minute battle engagement.

We have constructed models for some of the proposed power systems to help us in our evaluation efforts. We call these modeled systems reference systems because we believe they represent some of the more likely candidates for space power, and we will use them as a reference of comparison to measure the merit of other proposed system concepts. The modeled systems are listed below.

"Continuous" power systems (Closed)
- Gas cooled reactor powered Brayton cycle
- Liquid metal cooled reactor powered Rankine cycle
- Liquid metal cooled reactor thermionic system

"Burst" power systems (Open)
- Gas cooled reactor powered open turbine-generator
- Hydrogen-oxygen combustion open turbine-generator

An open system is one that dumps turbine exhaust into space. These systems consist of a power source, power conversion components, and power conditioning. They do not include the component for which the power is being generated such as a weapon or a radar. We calculate system performance, system weight, and a very rough estimate of system cost using the models.

This report will describe the five models, and we believe they will be useful to the SDI's technology development program.

GAS COOLED REACTOR POWERED BURST SYSTEM

The power source for this system is a hydrogen cooled reactor. Hot hydrogen leaves the reactor and is expanded in a turbine which produces shaft power to run a generator or alternator. After expansion, the hydrogen is exhausted into space. Figure 1 shows a simple schematic of this system. The figure shows that the hydrogen originates in a refrigerated tank and that it cools the weapon, power conditioning unit, and generator before entering the reactor. The weapon, having an efficiency less than unity, dumps heat into the hydrogen which enters as a liquid and passes through a supercritical process as it cools the weapon. The amount of hydrogen required to cool the weapon is determined by the weapon's cooling load and by its prescribed outlet temperature. If the turbine requires more hydrogen than the weapon, makeup hydrogen is supplied from the tank and bypasses the weapon. If the turbine requires less hydrogen than the weapon, the excess hydrogen is dumped into space after cooling the generator. The schematic also shows a flywheel. This energy storage component does not interact with the system in this model but is used to indicate that the system will store energy during brief periods when the weapon is not firing but turning the power system off is not practical. This might happen when the time between bursts of shots is very brief or when a weapon fault is detected. The flywheel contributes a small weight to the system but its true size cannot be determined until a dynamic battle scenario model is constructed. This type of system is intended to power an antiballistic missile weapon. It is believed that a battle engagement will last less than one-half hour and will not be repeated. Thus, the stored hydrogen must last the duration of one battle engagement plus any test time prior to the engagement. The equations that quantify the system's performance are developed below.

The weapon requires continuous electrical power P_W (watts). If the weapon pulses, then P_W is the average power needed but it is still supplied continuously during the battle engagement. The hydrogen flow rate required to cool the weapon is $\dot{m}_W$ (kg/sec) and is found using Equation (1).

$$\dot{m}_W[h(T_{WO}) - h(T_{store})] = P_W\psi + \dot{m}_W S_P \quad , \tag{1}$$

where ψ is the weapon cooling load fraction,
h is the enthalpy of hydrogen (see Appendix G),
T_{WO} is the specified weapon outlet temperature (K),
T_{store} is the hydrogen storage temperature (20 K, storage pressure is assumed to be 1 atm), and
S_P is the pump's power per unit flow rate (Equation 2).

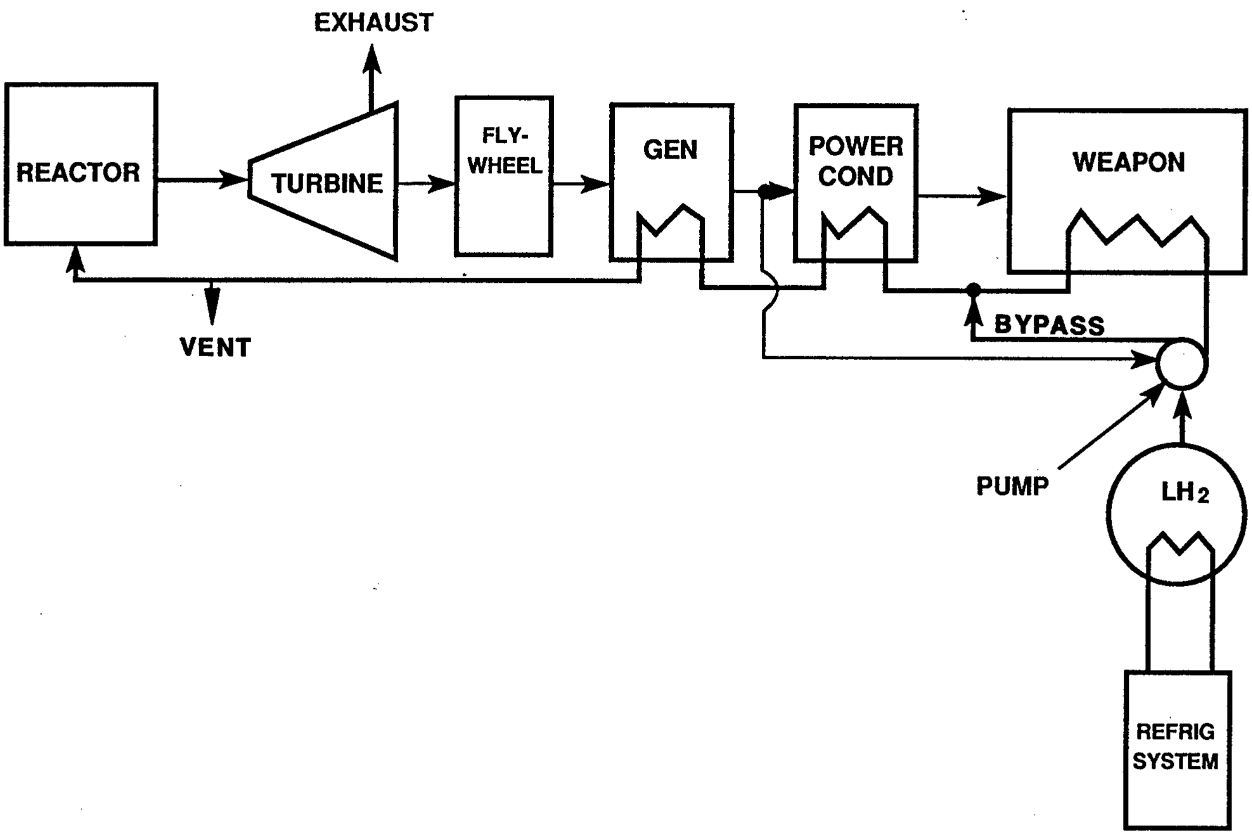

FIGURE 1. Hydrogen Cooled Reactor,
Open Space Power System.

$$S_p = \frac{[P_{ti}(1+dP) - P_{store}]}{0.7 \times \rho_{store}} \quad , \tag{2}$$

where P_{ti} is the turbine inlet pressure (P_a),
dP is the fractional pressure drop across the reactor,
P_{store} is the hydrogen storage pressure (Pa),
ρ_{store} is the hydrogen storage density (kg/m^3), and
0.7 accounts for pump efficiency.

The turbine's outlet temperature T_{to} depends on its inlet temperature T_{ti}, its pressure ratio R_p, and its efficiency.

$$T_{to} = T_{ti} - T_{ti}(1 - R_p^{-\alpha})\eta_t \quad , \tag{3}$$

where η_t is the turbine's efficiency,
α is R/C_p,
R is hydrogen's gas constant, and
C_p is its specific heat (equation 4).

$$C_p = [h(T_{ti}) - h(T_{to})]/(T_{ti} - T_{to}) \quad , \tag{4}$$

The turbine's flow rate is $\dot{m}_t$ (kg/sec), and can be found using Equation (5).

$$\dot{m}_t[h(T_{ti}) - h(T_{to})] = \frac{P_w}{\eta_g \eta_{pc}} + \frac{\dot{m}S_p}{\eta_g} \quad , \tag{5}$$

where η_g is generator efficiency, and
η_{pc} is power conditioning efficiency.
$\dot{m}$ is either the hydrogen flow rate for weapon cooling or for turbine power, whichever is greater.

The energy added to the hydrogen before it reaches the reactor is Q_{th}.

$$Q_{th} = P_w \left(\frac{1}{\eta_g \eta_{pc}} + \psi - 1 \right) + \frac{\dot{m}S_p}{\eta_g} \quad . \tag{6}$$

The reactor's inlet temperature is T_{ri}, which can be found by iteratively solving Equation (7).

$$\dot{m} \left[h(T_{ri}) - h(T_{store}) \right] = Q_{th} \tag{7}$$

The reactor's thermal power is Q_r.

$$Q_r = \dot{m}_t[h(T_{ti}) - h(T_{ri})] \quad . \tag{8}$$

The parameter R_p, the turbine's pressure ratio, must be adjusted to minimize either system weight or cost. As R_p increases, turbine flow rate is reduced, the reactor's thermal power is reduced, and more enthalpy is extracted in the turbine. However, as R_p increases, progressively larger stages must be added to the turbine to accommodate the added hydrogen expansion. Thus, system weight, or cost, has a "U" shaped curve when plotted against R_p, and there is a minimum value which must be determined.

The system model consists of the above equations and models for individual component weights and costs which will be described later. From these equations and models, we constructed a FORTRAN program (REBRST) which runs on the IBM-AT computer to calculate system performance, weight, and cost. The model is interactive and a listing of the self explanatory input sequence is shown in Table 1. The underlined parameters are supplied by the user. The model contains a default set of parameters that can be replaced by following the given instructions.

Table 2 shows a listing of model output. The first section of this table shows the optimization of pressure ratio. As pressure ratio increases, reactor weight and hydrogen cooling system weight decease and power conversion weight increases until pressure ratio gets to 284.9. A pressure ratio of 237.4 was selected to minimize system weight. The second section of the table lists values of selected parameters for the optimum system.

Table 3 summarizes the component weight and cost models that were used in the system model.

The reactor model was written by Al Marshall and is described in Marshall (1986). Briefly, it calculates the fuel mass required for each of three limits: end of life criticality, burnup, and specific power removal. The largest of the three is selected and is added to masses for the moderator, structure, reflector, pressure vessel, shield, and miscellaneous items to get a total reactor and shield mass. The specific set of reactor parameters used in this system model are for a hydrogen cooled, LiH moderated, UC fuel, particle bed, burst reactor. The specific parameter values can be found in Marshall's report.

We have augmented Marshall's model in two areas. A specific power calculation has been added, and "wraparound" shield is used when it is lighter than a planar shield.

Specific power is the maximum thermal power per kilogram of fuel that can be removed from the reactor's core without overheating the fuel, or causing an excessive pressure drop. The calculation of this value is described in Appendix A for a hydrogen or helium cooled particle bed reactor.

The wraparound shield model is explained in Appendix B. Marshall's model calculates the weight of a disc shaped shadow shield. When the protection cone angle is large, a wraparound shield will be lighter than a disc shadow shield and is substituted when this is the case.

The turbine model is described in Appendix C. It is based on a stage-by-stage size, weight, and efficiency computation with temperature dependent material strengths, working fluid properties, and working fluid energy extraction. Table 3 describes the models for the flywheel and for the generator which is assumed to have a 95 percent efficiency. Power conditioning weight is assumed to be 0.2 kg/kW. We estimate that beam weapons will require power conditioners that weigh close to 0.5 kg/kW and that kinetic energy weapons will require almost no power conditioning weight. Thus, 0.2 kg/kW is used to represent the range of estimates.

The cooling system consists of hydrogen, an insulated hydrogen tank, a refrigeration system to keep the hydrogen at cryogenic temperatures, and a meteoroid shield. The model for this system is described in Appendix D. The turbine and the weapon may require different quantities of hydrogen. The model uses the greater of the two values to calculate cooling system weight.

The weapon is simply modeled as a cooling load. If its cooling load is 50 percent, then half of the energy used by the weapon must be extracted as heat.

The model also includes cost. While our estimates for these are not yet very accurate, they have been included because we recognize that cost will become the most important factor by which to judge a system. The major cost for previously launched small power system was launch cost which is proportional to weight, but for multimegawatt size, lower specific weight systems, the production cost of the system is also important. Our estimates for launch cost are based on present shuttle launch cost. Aviation Week (1985) estimates that a commercially competitive shuttle launch would cost \$128 million. If a heavy lift shuttle could lift 100 metric tons into low earth orbit, then the launch cost would be \$1280/kg. This is the launch cost used by the model.

TABLE 1

```
THIS PROGRAM MODELS AN OPEN CYCLE SPACE POWER
SYSTEM.  THE SYSTEM CONSISTS OF A HYDROGEN COOLED
REACTOR, A TURBINE, A FLYWHEEL, A GENERATOR,
A POWER CONDITIONER, A WEAPON SUBSYSTEM,
AND A HYDROGEN STORAGE SUBSYSTEM.
PRESSURE RATIO IS OPTIMIZED TO GET EITHER
MINIMUM SYSTEM WEIGHT OR COST.
THE WEAPON IS COOLED BY SUPERCRITICAL HYDROGEN
STORED AT 1 ATM. AS A LIQUID AND PUMPED TO REACH
TURBINE PRESSURE.
THE COOLANT ALSO COOLS THE POWER CONDITIONER
AND THE GENERATOR BEFORE ENTERING THE REACTOR.



ENTER VALUES FOR WEAPON INPUT ELECTRICAL POWER
IN MW AND OPERATING TIME IN HOURS.   100 .2

ENTER "WEIGHT" OR "COST" AS PARAMETER TO BE
  MINIMIZED (IN CAPITAL LETTERS).   WEIGHT

THE FOLLOWING ARE DEFAULT PARAMETER VALUES.
THEY MAY BE CHANGED IF YOU WISH.


CYCLE PARAMETERS:
     1.     1200.00000000 TURBINE INLET TEMP, K
     2.        4.00000000 TURBINE INLET PRESSURE, MPa
     3.   1.00000000E+06 MAXIMUM PRESSURE RATIO
     4.        0.94999999 GENERATOR EFFICIENCY
     5.        0.94999999 POWER CONDITIONING EFFICIENCY
     6.        0.50000000 WEAPON COOLING LOAD FRACTION
     7.      300.00000000 WEAPON OUTLET TEMP, K
     8.       10.00000000 FLYWHEEL ENERGY STORAGE TIME, SEC


TURBINE PARAMETERS:
     9.        4.00000000 NUMBER OF TURBINES
    10.        1.00000000 TURBINE MATERIAL: 1-SUPERALLOY,
                   2-CARBON-CARBON COMPOSITE
    11.     1200.00000000 MAXIMUM DISK TEMPERATURE, K
    12.     1200.00000000 MAXIMUM BLADE TEMPERATURE, K
    13.    10000.00000000 TURBINE SPEED, RPM
    14.        5.00000000 WORK COEFFICIENT


REACTOR PARAMETERS:
    15.        0.93000001 FRACTIONAL FUEL ENRICHMENT
    16.        1.00000000 CRITICAL COMPACT MASS, Kg
    17.        0.40000001 FUEL + MODERATOR VOL FRACT
    18.   2.19999999E-02 FUEL BED LENGTH, m
    19.        0.10000000 REACTOR PRSUR DROP, FRACT OF PIN
    20.        0.25000000 FUEL BURNUP FRACTION LIMIT
    21.       65.50000000 MODERATOR-TO-FUEL RATIO
    22.       93.00000000 MODERATOR MOLECULAR WEIGHT
    23.     5610.00000000 MODERATOR DENSITY, Kg/m3
```

TABLE 1 (cont.)

```
24.    4.99999992E+16 ALLOWED PAYLOAD NEUTRON DOSE, nvt
25.       25.00000000 PAYLOAD SEPARATION DISTANCE, m
26.       15.00000000 PROTECTION CONE HALF ANGLE, DEG
27.        2.00000000 NEUTRON SHIELD MATL-B4C=1, LIH=2
28.    1.00000000E+07 ALLOWED PAYLOAD GAMMA DOSE, R


ENTER THE NUMBER OF PARAMETERS YOU WISH TO CHANGE.   3

ENTER THE           3 PARAMETER NUMBERS.   1 11 12

ENTER THE           3 PARAMETER VALUES.   1150 900 1150


CYCLE PARAMETERS:
     1.     1150.00000000 TURBINE INLET TEMP, K
     2.        4.00000000 TURBINE INLET PRESSURE, MPa
     3.    1.00000000E+06 MAXIMUM PRESSURE RATIO
     4.        0.94999999 GENERATOR EFFICIENCY
     5.        0.94999999 POWER CONDITIONING EFFICIENCY
     6.        0.50000000 WEAPON COOLING LOAD FRACTION
     7.      300.00000000 WEAPON OUTLET TEMP, K
     8.       10.00000000 FLYWHEEL ENERGY STORAGE TIME, SEC

TURBINE PARAMETERS:
     9.        4.00000000 NUMBER OF TURBINES
    10.        1.00000000 TURBINE MATERIAL: 1-SUPERALLOY,
                   2-CARBON-CARBON COMPOSITE
    11.      900.00000000 MAXIMUM DISK TEMPERATURE, K
    12.     1150.00000000 MAXIMUM BLADE TEMPERATURE, K
    13.    10000.00000000 TURBINE SPEED, RPM
    14.        5.00000000 WORK COEFFICIENT

REACTOR PARAMETERS:
    15.        0.93000001 FRACTIONAL FUEL ENRICHMENT
    16.        1.00000000 CRITICAL COMPACT MASS, Kg
    17.        0.40000001 FUEL + MODERATOR VOL FRACT
    18.    2.19999999E-02 FUEL BED LENGTH, m
    19.        0.10000000 REACTOR PRSUR DROP, FRACT OF PIN
    20.        0.25000000 FUEL BURNUP FRACTION LIMIT
    21.       65.50000000 MODERATOR-TO-FUEL RATIO
    22.       93.00000000 MODERATOR MOLECULAR WEIGHT
    23.     5610.00000000 MODERATOR DENSITY, Kg/m3
    24.    4.99999992E+16 ALLOWED PAYLOAD NEUTRON DOSE, nvt
    25.       25.00000000 PAYLOAD SEPARATION DISTANCE, m
    26.       15.00000000 PROTECTION CONE HALF ANGLE, DEG
    27.        2.00000000 NEUTRON SHIELD MATL-B4C=1, LIH=2
    28.    1.00000000E+07 ALLOWED PAYLOAD GAMMA DOSE, R


ENTER THE NUMBER OF PARAMETERS YOU WISH TO CHANGE.   0
```

TABLE 2

PRESSURE RATIO	RCT+SHLD WT (Kg)	POW CONV WT (Kg)	COOL SYS WT (Kg)	TOTAL WT (Kg)	TOTAL COST (M$)
1.200	74782.	38310.	284803.	437685.	1142.
1.440	36241.	37121.	136823.	231203.	701.
1.728	24741.	36836.	92074.	169016.	569.
2.074	19177.	36750.	70299.	138848.	505.
2.488	15880.	36741.	57375.	120996.	467.
2.986	13693.	36773.	48800.	109192.	442.
3.583	12132.	36828.	42688.	100813.	425.
4.300	10959.	36900.	38110.	94565.	412.
5.160	10044.	36984.	34550.	89736.	401.
6.192	9309.	37078.	31703.	85899.	393.
7.430	8705.	37180.	29374.	82785.	387.
8.916	8200.	37290.	27434.	80216.	382.
10.699	7770.	37407.	25793.	78067.	377.
12.839	7399.	37530.	24388.	76249.	373.
15.407	7076.	37660.	23171.	74698.	370.
18.488	6792.	37797.	22108.	73366.	367.
22.186	6541.	37939.	21170.	72215.	365.
26.623	6316.	38089.	20339.	71217.	363.
31.948	6113.	38244.	19596.	70349.	361.
38.338	5931.	38406.	18928.	69592.	360.
46.005	5764.	38575.	18326.	68932.	359.
55.206	5613.	38751.	17780.	68358.	358.
66.247	5496.	38934.	17283.	67884.	357.
79.497	5391.	39124.	16828.	67477.	356.
95.396	5294.	39321.	16411.	67129.	356.
114.476	5205.	39527.	16027.	66835.	355.
137.371	5122.	39740.	15673.	66589.	355.
164.845	5046.	39961.	15346.	66389.	355.
197.814	4975.	40191.	15042.	66229.	355.
237.377	4902.	40431.	14831.	66179.	355.
284.852	4814.	40781.	14831.	66469.	356.
237.377	4902.	40431.	14831.	66179.	355.

THERMODYNAMIC PARAMETERS

WEAPON FLOW RATE-Kg/s	=	10.73518658
TURBINE FLOW RATE-Kg/s	=	10.68002987
TURBINE INLET TEMP-K	=	1150.00000000
TURBINE OUTLET TEMP-K	=	451.15634155
PUMP POWER-MW	=	0.92879885
REACTOR INLET TEMP-K	=	369.53829956
PRESSURE RATIO	=	237.37660217
REACTOR THERMAL POWER-MW	=	124.45237732

REACTOR PARAMETERS

BURNUP MASS-Kg	=	1.16099336E-03
INITIAL CRITICAL MASS-Kg	=	24.81669044
END CRITICAL MASS-Kg	=	24.81677246
TOTAL BRNUP+CRIT MASS-Kg	=	24.81793213
SPECIFIC POWER-W/Kg	=	3.37396975E+06
MASS FOR SPECIFIC POWER LIM-Kg	=	47.95184708

TABLE 2 (cont.)

MASS FOR ALLOWED BURNUP-Kg	=	5.61456382E-03
FUEL MASS-Kg	=	47.95184708
MODERATOR MASS-Kg	=	1155.96496582
STRUCTURE MASS-Kg	=	1373.03930664
REFLECTOR MASS-Kg	=	871.28448486
PRESSURE VESSEL MASS-Kg	=	249.86604309
MISCELLANEOUS MASS-Kg	=	1203.91687012
TOTAL REACTOR MASS-Kg	=	4902.02343750
NEUTRON SHIELD THICKNESS-m	=	0.00000000E-01
NEUTRON SHIELD MASS-Kg	=	0.00000000E-01
GAMMA SHIELD THICKNESS-m	=	0.00000000E-01
GAMMA SHIELD MASS-Kg	=	0.00000000E-01
TOTAL SHIELD MASS-Kg	=	0.00000000E-01
HYDROGEN STORAGE PARAMETERS		
TURBINE		
TANK VOLUME-m3	=	108.30452728
REFRIGERATION SYSTEM POWER-MW	=	7.05457712E-03
HYDROGEN WEIGHT-Kg	=	7689.62158203
TANK WEIGHT-Kg	=	219.85820007
INSULATION WEIGHT-kg	=	352.72885132
REFRIG SYST WEIGHT-KG	=	484.09591675
METEOROID SHIELD WEIGHT-kg	=	6014.22802734
WEAPON		
TANK VOLUME-m3	=	108.86386871
REFRIGERATION SYSTEM POWER-MW	=	7.07885763E-03
HYDROGEN WEIGHT-Kg	=	7729.33447266
TANK WEIGHT-Kg	=	220.99363708
INSULATION WEIGHT-kg	=	353.94287109
REFRIG SYST WEIGHT-KG	=	485.36471558
METEOROID SHIELD WEIGHT-kg	=	6040.93066406
POWER CONVERSION PARAMETERS		
TURBINE STAGES	=	19
TURBINE SPEED-RPM	=	10000.00000000
TURBINE EFFICIENCY	=	0.78069597
TURBINE PRESSURE RATIO	=	237.37660217
TURBINE WEIGHT-Kg	=	6733.51806641
GENERATOR WEIGHT-Kg	=	10619.19628906
FLYWHEEL WEIGHT-Kg	=	3077.87011719
POWER CONDITIONING WEIGHT-Kg	=	20000.00000000

TABLE 2 (cont.)

WEIGHT AND COST SUMMARY		
REACTOR WEIGHT-Kg	=	4902.02343750
SHIELD WEIGHT-Kg	=	0.00000000E-01
POWER CONVERSION WEIGHT-Kg	=	40430.58593750
COOLING SUBSYSTEM WEIGHT-Kg	=	14830.56640625
MISC. WEIGHT-Kg	=	6016.31787109
TOTAL WEIGHT-Kg	=	66179.49218750
REACTOR+SHIELD COST-M$	=	21.56890297
POWER CONVERSION COST-M$	=	245.32461548
COOLING SUBSYSTEM COST-M$	=	0.31664482
FLYWHEEL COST-M$	=	3.07787037
LAUNCH COST-M$	=	84.70974731
TOTAL COST-M$	=	354.99777222

Execution terminated : 0

TABLE 3

Reactor Powered Burst System

Weight and Cost Algorithm Summary

Component	Weight	Cost
Reactor and Shield	Marshall's algorithm (Marshall, 1986)	\$4400/kg (estimate)
Turbine	See Appendix C	\$2000/kg (Gerry, 1985)
Generator	0.1 kg/kW (Gerry, 1985)	\$3000/kg (Gerry, 1985)
Power Conditioning	0.2 kg/kW (estimate)	\$10,000/kg (estimate)
Hydrogen Cooling Subsystem	$W_h = \dot{m}T$ $V = W_h/\rho$ $W_t = 2.03\ V$ $W_i = 15.5\ V^{0.667}$ $W_r = 12.6\ V^{0.667}$+109x10** [0.0468(log(2.78V**0.667))**2.9] $W_s = 107\ V^{0.86}$ W_h = hydrogen mass, kg $\dot{m}$ = hydrogen flow rate, kg/s T = operating time, s V = volume of hydrogen, m^3 ρ = density of liquid H_2, 71 kg/m^3 W_t = tank weight, kg W_i = insulation weight, kg W_r = refrigeration weight, kg W_s = meteoroid shield weight, kg See Appendix D	hydrogen \$28/kg (Bents, 1984) tank \$20/kg (estimate) refrigeration \$640/kg (est.) insulation \$100/kg (est.) shield \$10/kg (estimate)
Miscellaneous	10% of subtotal	
Launch cost		\$1280/kg (Aviation Week, 1985, and heavy lift shuttle)

H2-02 COMBUSTION POWERED BURST SYSTEM

This system is similar to the reactor powered burst system, but instead of a reactor, it has an oxygen subsystem and a hydrogen-oxygen combustor (see Figure 2). The turbine in this system uses the combustion products, a mixture of steam and hydrogen, as a working fluid. If a stoichiometric mixture of hydrogen and oxygen is burned, the combustion product temperature will be too high for a turbine inlet temperature. To cool the combustion products, excess hydrogen is used in the combustion mixture. The ratio, R, of hydrogen to oxygen determines the combustion product temperature (which is also the turbine inlet temperature, T_{ti}). Thus, for a desired combustion product temperature, there is a required ratio of hydrogen to oxygen as specified by equation 9 and derived in Appendix E.

$$R = \frac{0.125[h_H(T)-h_H(T_r)]+1.125h_{COMB}-h_O(T_r)+h_O(T_{so})-1.125[h_S(T)-h_S(T_r)]+S_{po}}{h_H(T) - h_H(T_{ih})}, \qquad (9)$$

where h_{COMB} is the enthalpy of combustion (13400 J/kg H_2O),
T_{ih} is the temperature of the hydrogen entering the combustion chamber,
T is the combustion product temperature,
h_O is the enthalpy of oxygen,
h_S is the enthalpy of steam,
h_H is the enthalpy of hydrogen,
S_{po} is the oxygen pump power per unit of oxygen flow,
T_{so} is the oxygen's storage temperature, and
T_r is the reaction temperature (300 K).

Enthalpy values are specified in Appendix G.

The thermodynamic properties for the combustion products are specified in Appendix E. They are used to calculate turbine performances and weight.

Hydrogen is used to cool the weapon, power conditioning unit, and generator before it enters the combustor. The amount of hydrogen needed depends on weapon efficiency and weapon outlet temperature. The amount of hydrogen needed by the turbine depends on its inlet temperature, pressure ratio, efficiency, and on the ratio of hydrogen to steam in the working fluid. It may need either more or less hydrogen than the weapon. If it needs more, extra hydrogen will be supplied by the hydrogen storage subsystem. If it needs less, some weapon coolant hydrogen will be dumped after cooling the weapon, power conditioning unit, and generator. The hydrogen needed on the platform is the greater of that needed by the weapon and that needed by the turbine.

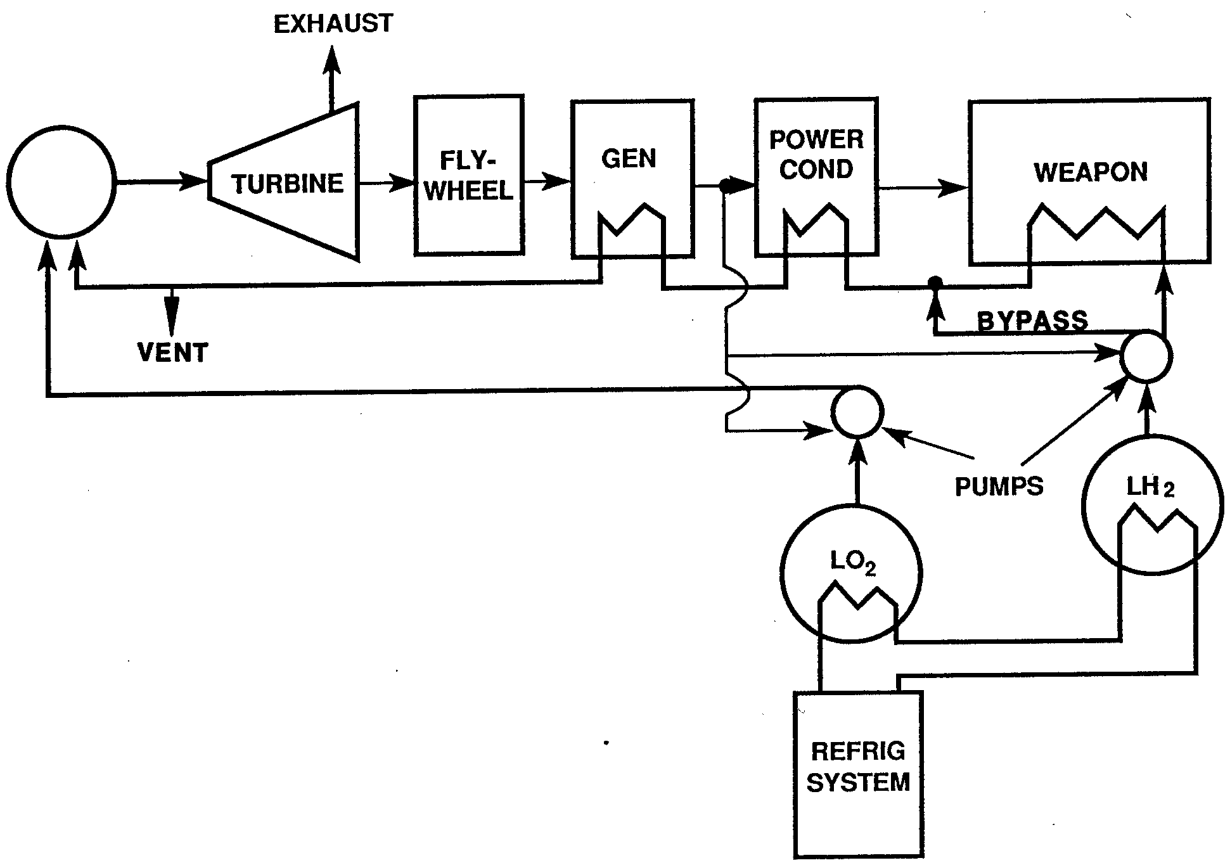

FIGURE 2. H_2-O_2 Combustion, Open Space Power System.

The system includes a flywheel to accommodate short energy transients. It has no effect on system performance in this model. It does, however, add a small amount of weight to the system.

The weapon is presumed to require continuous electrical power, P_w, to fight a battle over a several-minute time interval. The flow rate of coolant hydrogen needed by the weapon is specified by Equation (10).

$$\dot{m}_{hw}[h_H(T_{wo}) - h_H(T_{sh})] = P_w\psi + \dot{m}_{hw}S_{ph} \quad , \tag{10}$$

where $\dot{m}_{hw}$ is the mass flow rate of hydrogen to the weapon (kg/sec),
ψ is the weapon's cooling load fraction,
turbine power, whichever is greater,
T_{wo} is the specified weapon outlet temperature (K),
T_{sh} is the temperature at which liquid hydrogen is stored (20 K), and
S_{ph} is the power divided by flow rate for the hydrogen pump.

The turbine's outlet temperature T_{to} depends on its inlet temperature T_{ti}, its pressure ratio R_p, and its efficiency η_t.

$$T_{to} = T_{ti} - T_{ti}(1 - R_p^{-\alpha})\eta_t \quad , \tag{11}$$

where α is R_g/C_p where R_g is the gas constant and C_p is the specific heat for the steam-hydrogen mixture. C_p is calculated using weighted enthalpy change values (see Appendix G).

The turbine's total flow rate is m_t.

$$\dot{m}_t[h_C(T_{ti}) - h_C(T_{to})] = \frac{P_w}{\eta_g\eta_{pc}} + \frac{\dot{m}_o S_{po}}{\eta_g} + \frac{\dot{m}_h S_{ph}}{\eta_g} \quad , \tag{12}$$

where h_C is the enthalpy of the hydrogen-steam mixture (Appendix E),

$\dot{m}_o$ is the mass flow rate of oxygen,
η_g is the generator efficiency,
η_{pc} is the power conditioning efficiency, and

$\dot{m}_h$ is the flow rate of hydrogen for either weapon cooling or turbine power, whichever is greater.

$$S_{ph} = \frac{(P_{ti} - P_s)}{0.7\rho_H} \quad , \tag{13}$$

$$S_{po} = \frac{(P_{ti} - P_s)}{0.7\rho_O} \quad , \tag{14}$$

where P_{ti} is the turbine inlet pressure (Pa),
P_s is the storage pressure (100,000 Pa),
ρ_H is the density of liquid hydrogen (71 kg/m^3),
ρ_O is the density of liquid oxygen (1142 kg/m^3), and
0.7 represents pump efficiency.

The turbine's hydrogen and oxygen flow rates are found using Equations (15) and (16), respectively.

$$\dot{m}_{ht} = \dot{m}_t \frac{R}{1+R} \quad . \tag{15}$$

$$\dot{m}_o = \frac{\dot{m}_t}{1+R} \quad . \tag{16}$$

The enthalpy change of the coolant hydrogen before it enters the combustor is given by Equation (17).

$$Q_{th} = P_w \left(\frac{1}{\eta_g \eta_{pc}} + \psi - 1 \right) + \frac{\dot{m}_h S_{ph}}{\eta_g} + \dot{m}_o S_{po} \left(\frac{1}{\eta_g} - 1 \right) \quad . \tag{17}$$

The hydrogen enters the combustor at temperature T_{ri} which can be found by iterating Equation (18).

$$\dot{m}_h \left[h_H(T_{ri}) - h_H(T_{sh}) = Q_{th} \right] \quad . \tag{18}$$

Recall the pressure ratio parameter, R_p, that was used to determine turbine outlet temperature. This parameter is a variable and must be adjusted to minimize either system weight or cost. When R_p increases, turbine enthalpy extraction increases, and the flow rates of hydrogen and oxygen decrease. However, when R_p increases, the turbine becomes heavier because it must have additional stages. Because of this, there is an optimum value of R_p that minimizes either system weight or system cost.

The above equations, along with weight and cost models (discussed later), for each of the system components have been combined into a system computer model that calculates performance, weight, and cost. The system model (HOBRST) is written in FORTRAN and runs on an IBM-AT computer. It is interactive and a listing of the self explanatory input sequence is shown in Table 4. The underlined parameters are supplied by the user. The model contains a default set of parameters that can be replaced by following the instructions given while running the program. Table 5 is a listing of model output. The first part of the table shows how the pressure ratio is optimized. The optimum value selected was 114. The rest of the table summarizes values of selected parameters from the optimum system.

The weight and cost models for this system are summarized in Table 6 and consist of hydrogen and oxygen subsystems, a turbine, a generator, power conditioning, and a flywheel. The turbine model is described in detail in Appendix C. The generator and power conditioning unit are both 95 percent efficient. The cryogen (hydrogen and oxygen) storage subsystems consist of the stored liquid, tanks, multilayer insulation, refrigeration units, and meteoroid shields. The weights of hydrogen and oxygen are calculated by multiplying their flow rates by the system's operating time. The other cryogen storage component weights are addressed in detail in Appendix D.

The weapon is modeled as shown in equation 10. It contributes no weight, other than its required coolant, to the system.

The model also includes cost. The cost parameters in the model are very crude at present, but they represent an attempt to consider the parameter that should be the most important discriminator in the future. The launch cost used in the model is a reasonable estimate, $1280/kg, based on current shuttle experience (Ref. 5) projected to a heavy lift vehicle that can put 100 metric tons in orbit.

TABLE 4

```
THIS PROGRAM MODELS AN OPEN CYCLE SPACE POWER
SYSTEM.  THE SYSTEM CONSISTS OF A HYDROGEN--OXYGEN
COMBUSTION TURBINE, A FLYWHEEL, A GENERATOR,
A POWER CONDITIONER, A WEAPON SUBSYSTEM,
AND HYDROGEN AND OXYGEN STORAGE SUBSYSTEMS.
PRESSURE RATIO IS OPTIMIZED TO GET EITHER
MINIMUM SYSTEM WEIGHT OR COST.
THE WEAPON IS COOLED BY SUPERCRITICAL HYDROGEN
STORED AT 1 ATM. AS A LIQUID AND PUMPED TO REACH
TURBINE PRESSURE.
THE HYDROGEN COOLS THE POWER CONDITIONER
AND THE GENERATOR BEFORE ENTERING THE COMBUSTOR.


ENTER VALUES FOR WEAPON INPUT ELECTRICAL POWER
IN MW AND OPERATING TIME IN HOURS.   100 .2

ENTER "WEIGHT" OR "COST" AS PARAMETER TO BE
  MINIMIZED (IN CAPITAL LETTERS).   WEIGHT

THE FOLLOWING ARE DEFAULT PARAMETER VALUES.
THEY MAY BE CHANGED IF YOU WISH.

CYCLE PARAMETERS:
     1.      1200.00000000 TURBINE INLET TEMP, K
     2.         4.00000000 TURBINE INLET PRESSURE, MPa
     3.    1.00000000E+06 MAXIMIUM PRESSURE RATIO
     4.         0.94999999 GENERATOR EFFICIENCY
     5.         0.94999999 POWER CONDITIONING EFFICIENCY
     6.         0.50000000 WEAPON COOLING LOAD FRACTION
     7.       300.00000000 WEAPON OUTLET TEMP, K
     8.        10.00000000 FLYWHEEL ENERGY STORAGE TIME, SEC

TURBINE PARAMETERS:
     9.         4.00000000 NUMBER OF TURBINES
    10.         1.00000000 TURBINE MATERIAL: 1-SUPERALLOY,
                            2-CARBON COMPOSITE

    11.      1200.00000000 MAXIMUM DISK TEMPERATURE, K
    12.      1200.00000000 MAXIMUM BLADE TEMPERATURE, K
    13.     10000.00000000 MAXIMUM TURBINE SPEED, RPM
    14.         4.00000000 WORK COEFFICIENT


ENTER THE NUMBER OF PARAMETERS YOU WISH TO CHANGE.   3

ENTER THE           3 PARAMETER NUMBERS.   1 11 12

ENTER THE           3 PARAMETER VALUES.   1150 900 1150
```

TABLE 4 (cont.)

CYCLE PARAMETERS:

1.	1150.00000000	TURBINE INLET TEMP, K
2.	4.00000000	TURBINE INLET PRESSURE, MPa
3.	1.00000000E+06	MAXIMIUM PRESSURE RATIO
4.	0.94999999	GENERATOR EFFICIENCY
5.	0.94999999	POWER CONDITIONING EFFICIENCY
6.	0.50000000	WEAPON COOLING LOAD FRACTION
7.	300.00000000	WEAPON OUTLET TEMP, K
8.	10.00000000	FLYWHEEL ENERGY STORAGE TIME, SEC

TURBINE PARAMETERS:

9.	4.00000000	NUMBER OF TURBINES
10.	1.00000000	TURBINE MATERIAL: 1-SUPERALLOY, 2-CARBON COMPOSITE
11.	900.00000000	MAXIMUM DISK TEMPERATURE, K
12.	1150.00000000	MAXIMUM BLADE TEMPERATURE, K
13.	10000.00000000	MAXIMUM TURBINE SPEED, RPM
14.	4.00000000	WORK COEFFICIENT

ENTER THE NUMBER OF PARAMETERS YOU WISH TO CHANGE. 0

TABLE 5

PRESSURE RATIO	O2-SYSTEM WT (Kg)	H2-SYSTEM WT (Kg)	POW CONV WT (Kg)	TOTAL WT (Kg)	TOTAL COST (M$)
1.200	194770.	244903.	37394.	524774.	923.
1.440	90008.	119658.	36419.	270694.	592.
1.728	58537.	81011.	36177.	193297.	491.
2.074	43369.	62078.	36100.	155702.	442.
2.488	34443.	50804.	36087.	133467.	413.
2.986	28565.	43310.	36108.	118781.	394.
3.583	24404.	37964.	36148.	108367.	380.
4.300	21304.	33956.	36202.	100608.	370.
5.160	18908.	30840.	36266.	94615.	362.
6.192	17000.	28348.	36338.	89855.	356.
7.430	15447.	26310.	36417.	85992.	352.
8.916	14159.	24614.	36502.	82803.	348.
10.699	13074.	23180.	36593.	80131.	344.
12.839	12148.	21952.	36689.	77868.	342.
15.407	11349.	20890.	36790.	75933.	339.
18.488	10653.	19963.	36897.	74264.	337.
22.186	10042.	19147.	37008.	72817.	336.
26.623	9502.	18423.	37124.	71554.	334.
31.948	9014.	17778.	37246.	70441.	333.
38.338	8590.	17198.	37372.	69476.	332.
46.005	8202.	16676.	37504.	68621.	331.
55.206	7851.	16204.	37642.	67866.	330.
66.247	7532.	15774.	37785.	67200.	330.
79.497	7242.	15381.	37933.	66612.	329.
95.396	6976.	15022.	38088.	66094.	329.
114.476	6764.	14807.	38249.	65802.	329.
137.371	6613.	14807.	38418.	65823.	329.
114.476	6764.	14807.	38249.	65802.	329.

THERMODYNAMIC PARAMETERS

WEAPON FLOW RATE-Kg/s	=	10.71666813
TURBINE FLOW RATE-Kg/s	=	19.30736351
TURBINE HYDROGEN FLOW RATE-kg/S	=	10.62598038
TURBINE OXYGEN FLOW RATE-kg/S	=	8.68138409
HYDROGEN/OXYGEN RATIO	=	1.22399616
TURBINE INLET TEMP-K	=	1150.00000000
TURBINE OUTLET TEMP-K	=	469.77078247
PUMP POWER-MW	=	0.88329923
COMBUSTOR INLET TEMP-K	=	369.64312744
PRESSURE RATIO	=	114.47557831

HYDROGEN STORAGE PARAMETERS

TURBINE

TANK VOLUME-m3	=	107.75642395
REFRIGERATION SYSTEM POWER-MW	=	7.03074411E-03
HYDROGEN WEIGHT-Kg	=	7650.70605469
TANK WEIGHT-Kg	=	218.74552917
INSULATION WEIGHT-kg	=	351.53720093
REFRIG SYST WEIGHT-KG	=	482.85034180
METEOROID SHIELD WEIGHT-kg	=	5988.04345703

TABLE 5 (cont.)

WEAPON		
TANK VOLUME-m3	=	108.67607117
REFRIGERATION SYSTEM POWER-MW	=	7.07070949E-03
HYDROGEN WEIGHT-Kg	=	7716.00097656
TANK WEIGHT-Kg	=	220.61242676
INSULATION WEIGHT-kg	=	353.53549194
REFRIG SYST WEIGHT-KG	=	484.93896484
METEOROID SHIELD WEIGHT-kg	=	6031.96728516
OXYGEN PARAMETERS		
TANK VOLUME-m3	=	5.47337675
REFRIGERATION SYSTEM POWER-MW	=	2.40834124E-04
OXYGEN WEIGHT-Kg	=	6250.59619141
TANK WEIGHT-Kg	=	11.11095428
INSULATION WEIGHT-kg	=	23.92803383
REFRIGERATION SYSTEM WEIGHT-Kg	=	16.51741409
METEOROID SHIELD WEIGHT-kg	=	461.61868286
POWER CONVERSION PARAMETERS		
TURBINE STAGES	=	16
TURBINE SPEED-RPM	=	10000.00000000
TURBINE EFFICIENCY	=	0.82368428
TURBINE PRESSURE RATIO	=	114.47557831
TURBINE WEIGHT-Kg	=	4556.61767578
GENERATOR WEIGHT-Kg	=	10614.64550781
FLYWHEEL WEIGHT-Kg	=	3077.87011719
POWER CONDITIONING WEIGHT-Kg	=	20000.00000000
NOZZLE OUTLET VELOCITY-m/s	=	1934.09130859
WEIGHT AND COST SUMMARY		
POWER CONVERSION WEIGHT-Kg	=	38249.13281250
HYDROGEN SUBSYSTEM WEIGHT-Kg	=	14807.05468750
OXYGEN SUBSYSTEM WEIGHT-Kg	=	6763.77148437
MISC. WEIGHT-Kg	=	5981.99609375
TOTAL WEIGHT-Kg	=	65801.95312500
POWER CONVERSION COST-M$	=	240.95716858
HYDROGEN SUBSYSTEM COST-M$	=	0.62265307
OXYGEN SUBSYSTEM COST-M$	=	1.90524738E-02
FLYWHEEL COST-M$	=	3.07787037
LAUNCH COST-M$	=	84.22650146
TOTAL COST-M$	=	328.90322876

Execution terminated : 0

TABLE 6
Combustion Powered Burst System
Weight and Cost Algorithm Summary

Component	Weight	Cost
Reactor and Shield	Marshall's algorithm (Marshall, 1986)	\$4400/kg (estimate)
Turbine	See Appendix C	\$2000/kg (Gerry, 1985)
Generator	0.1 kg/kW (Gerry, 1985)	\$3000/kg (Gerry, 1985)
Power Conditioning	0.2 kg/kW (estimate)	\$10,000/kg (estimate)
Flywheel	10 kg/kWh (Bents, 1984)	\$1000/kg (estimate)
Hydrogen Storage Subsystem	$W_h = \dot{m}T$ $V = W_h/\rho$ $W_t = 2.03\ V$ $W_i = 15.5\ V^{0.667}$ $W_r = 12.6\ V^{0.667}$+109x10** [0.0468(log(2.78V**0.667))**2.9] $W_s = 107\ V^{0.86}$ W_h = hydrogen mass, kg $\dot{m}$ = hydrogen flow rate, kg/s T = operating time, s V = volume of hydrogen, m^3 ρ = density of liquid H_2, 71 kg/m^3 W_t = tank weight, kg W_i = insulation weight, kg W_r = refrigeration weight, kg W_s = meteoroid shield weight, kg See Appendix D	hydrogen \$28/kg (Bents, 1984) tank \$20/kg (estimate) refrigeration \$640/kg (est.) insulation \$100/kg (est.) shield \$10/kg (estimate)

TABLE 6 (cont.)
Combustion Powered Burst System
Weight and Cost Algorithm Summary

Component	Weight	Cost
Oxygen Storage Subsystem	$W_o = \dot{m}T$ $V_o = W_o/\rho$ $W_t = 2.03\ V_o$ $W_i = 7.7\ V_o^{0.667}$ $W_r = .25 \left[\frac{V_o}{V_{hydrogen}} \right]^{0.667}$ x hydrogen refrigerator weight $W_s = 107\ V_o^{0.86}$ W_o = oxygen mass, kg $\dot{m}$ = oxygen flow rate, kg/s T = operating time, s V_o = volume of oxygen, m^3 ρ = density of oxygen, 1142 kg/m^3 W_t = tank weight, kg W_i = insulation weight, kg	Same as for hydrogen but oxygen cost \$0.2/kg (Gerry, 1985)
Oxygen Storage Subsystem cont.	W_r = refrigeration weight, kg W_s = meteoroid shield weight, kg See Appendix D	
Miscellaneous	10% of subtotal	
Launch cost		\$1280/kg (Aviation Week, 1985) and heavy lift shuttle)

BRAYTON CYCLE CONTINUOUS POWER SYSTEM

The two previously discussed systems, the reactor powered and combustion powered burst systems, both provided a high power level for a short time during a battle engagement. They consumed hydrogen or hydrogen and oxygen for cooling and/or fuel. Continuous power systems, on the other hand, must run for long periods of time and cannot use expendable fuels and coolants, since the quantities needed for long term operation are prohibitive. Because of this, we consider closed thermodynamic cycle nuclear powered, generation systems to be the most likely power source for continuous multimegawatt space power. These systems would use thermal radiators, not expendable coolants, to remove waste heat.

Figure 3 illustrates a closed Brayton cycle power system. A 50% by mass helium xenon mixture is used as the working fluid. It is compressed, heated at constant pressure by a gas cooled reactor, expanded by a turbine, and cooled at constant pressure by a radiator to complete its cycle. Shaft power from the turbine drives the compressor and generator.

Part of the flow leaving the compressor may be diverted to the turbine for blade cooling. Algorithms for calculating the quantity of blade coolant required are given in Appendix C.

Generated electrical power is converted by a power conditioning unit into a form that can be used by the platform's payload. Waste heat from the generator and power conditioning unit is removed by a low temperature radiator.

The efficiency of the Brayton Power Conversion cycle depends on cycle temperatures and the efficiencies of the turbine and compressor,

$$\eta_{cyc} = \frac{\dot{M}(T_{ti}-T_{to}) - \dot{m}(T_{to}-T_{co}) - (\dot{M}+\dot{m})(T_{co}-T_{ci})}{\dot{M}(T_{ti}-T_{co})} \quad , \qquad (19)$$

$$\eta_{cyc} = 1 - \left(1 + \frac{\dot{m}}{\dot{M}}\right)\left(\frac{T_{to} - T_{ci}}{T_{ti} - T_{co}}\right) \quad , \qquad (20)$$

where, $\dot{M}$ is the flow rate through the turbine excluding blade coolant,
$\dot{m}$ is the blade coolant flow rate,
T_{ti} is turbine inlet temperature,
T_{to} is turbine outlet temperature,
T_{co} is compressor outlet temperature,
T_{ci} is compressor inlet temperature,
η_t is turbine efficiency,
η_c is compressor efficiency, and
η_{cyc} is cycle efficiency.

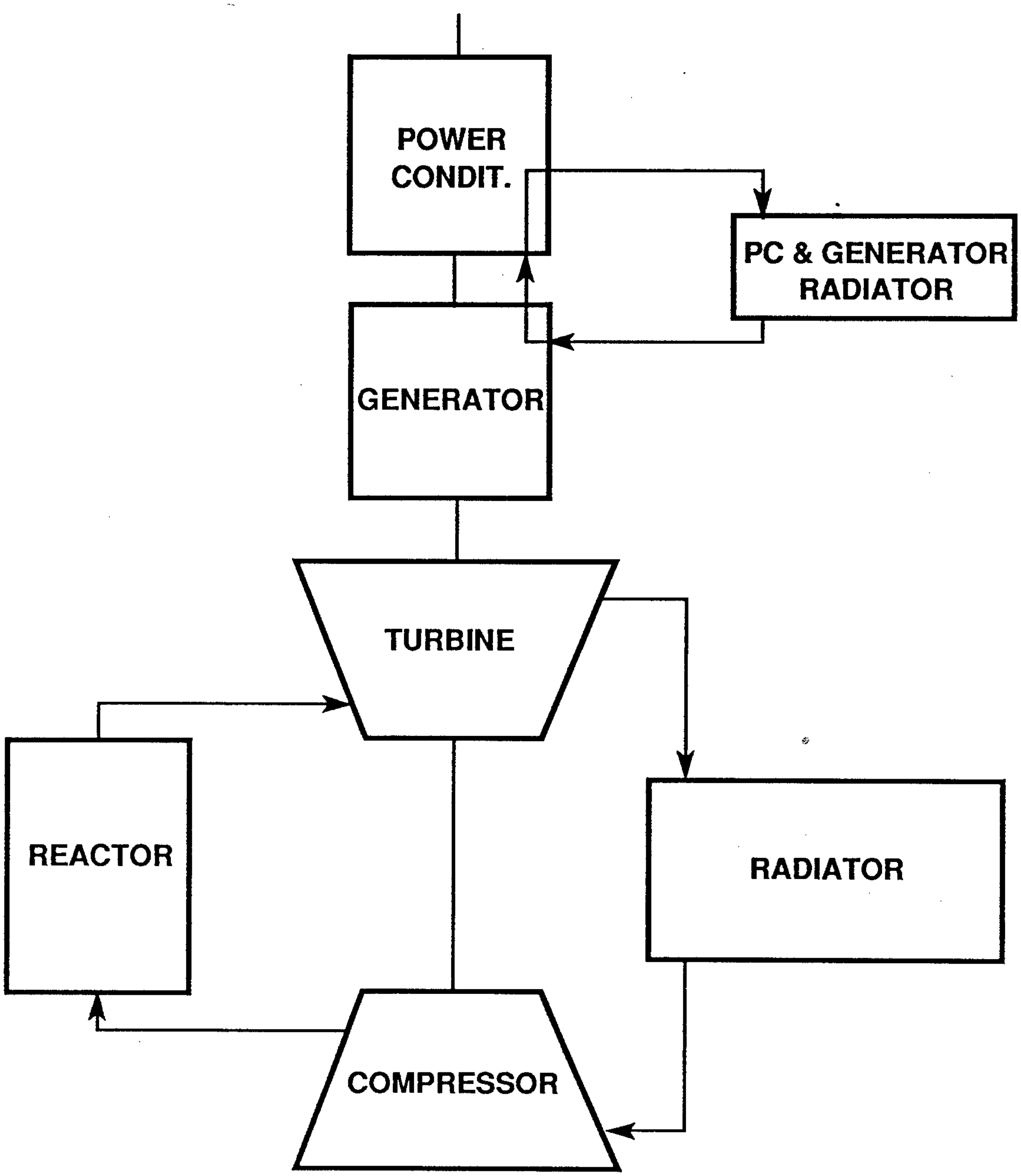

FIGURE 3. Brayton System.

The numerator in Equation (19) is the power extracted by the turbine minus that needed by the compressor. It is the net shaft power delivered by the turbine. Notice that this term includes the enthalpy contribution from the cooling fluid which can either add to or subtract from turbine power, depending on the relative values of T_{to} and T_{co}. The denominator is the power required of the reactor. Note in later equations that the heat generated by the inefficiency of the compressor reduces the energy needed from the reactor.

The turbine and compressor outlet temperatures are given by Equations (21) and (22).

$$T_{to} = (1 - \eta_t + \eta_t P_r^{1/\gamma - 1}) T_{ti} \quad , \tag{21}$$

$$T_{co} = \left\{ 1 - \frac{1}{\eta_c} + \frac{1}{\eta_c [P_r(1 + \Delta P)]^{1/\gamma - 1}} \right\} T_{ci} \quad , \tag{22}$$

where P_r is the turbine's pressure ratio,
γ is the working gas's specific heat ratio, and
ΔP is the pressure loss across the reactor and radiator as a fraction of the turbine's inlet pressure.

Because of the ΔP term, the cycle efficiency depends on pressure losses in the system.

In the cycle analysis T_{ti} is specified, but P_r and T_{ci} are not. They are found by iterating the values of each to minimize system weight. That is, pressure and temperature (T_{ti}/T_{ci}) ratios are optimized to minimize system weight.

System efficiency also depends on generator and power conditioning unit efficiencies.

$$\eta_{sys} = \eta_{cyc} \eta_g \eta_{pc} \quad , \tag{23}$$

where η_g is generator efficiency, and
η_{pc} is power conditioning efficiency.

The thermal power required of the reactor is found by dividing the required electrical power by system efficiency.

$$P_{th} = P_e / \eta_{sys} \quad . \tag{24}$$

The power system's flow rate is found using Equation (25).

$$\dot{M} = P_{th} / C_p \, (T_{ti} - T_{co}) \quad . \tag{25}$$

$\dot{M}$ is the flow rate and C_p is the fluid's specific heat.

As mentioned above, pressure and temperature ratios are optimized to get minimum system weight. As the pressure ratio increases, cycle efficiency increases and the power dumped by the radiator decreases; however, the radiator's temperature also decreases. These two things combine to give radiator weight a "U" shaped function of pressure ratio. The weights of other components enter in various ways, but the end result is that there is a pressure ratio which minimizes system weight. Also, as temperature ratio decreases, cycle efficiency decreases and radiator temperature increases, again producing a "U" shaped function of temperature ratio, and again there is an optimum value of temperature ratio. Actually, pressure and temperature ratios have to be iterated together because the optimum value of one depends on the value of the other.

Our Brayton system model comprises the above performance algorithms, an optimization procedure, and algorithms for the weight of each component (discussed later).

The model was "computerized" for use on an IBM-AT personal computer. It is written in FORTRAN and is interactive. Table 7 shows a typical input sequence. Default values for all parameters except power level and operation time are supplied. The default values may be easily changed. The underlined values were supplied by the user. Table 8 is the output. The first part shows the pressure and temperature ratio optimization. The second part shows selected parameter values for the optimum system.

Table 9 summarizes the weight and cost algorithms used in the model.

The reactor model was formulated by Al Marshall of Sandia National Laboratories and is described in Marshall (1986). It uses a specific power density value as part of its fuel mass calculation. Power density calculation is described in Appendix A. We have augmented Marshall's shield model by adding a wrap-around shield. This is described in Appendix B.

The turbine model is described in Appendix C, and the compressor weight algorithm is summarized in Table 9. The generator, see Table 9, has an efficiency of 95%.

Radiator area depends on the quantity of heat to be dissipated and on the radiator's temperature. The algorithms that calculate radiator area are developed in Appendix E, and radiator weights are summarized in Table 9.

Power conditioning weight depends strongly on the load to be powered, but we have selected 0.2 kg/kW as a place holder until better estimates are made. Power conditioning is assumed to have a 95% efficiency.

The power conditioning unit and generator must be cooled by a radiator. We assume that it is isothermal at 500 K and its area can be calculated like that of a Rankine cycle radiator.

TABLE 7

THIS PROGRAM MODELS A BRAYTON CYCLE SPACE POWER SYSTEM. THE SYSTEM CONSISTS OF A HELIUM COOLED REACTOR, A TURBINE, A COMPRESSOR, A GENERATOR AND A RADIATOR. THE SYSTEM OPERATING PARAMETERS, TEMPERATURE RATIO AND PRESSURE RATIO, ARE OPTIMIZED TO GET EITHER MINIMUM SYSTEM WEIGHT OR COST.

ENTER VALUES FOR ELECTRICAL POWER IN MW AND OPERATING TIME IN HOURS. 10 87600

ENTER "WEIGHT" OR "COST" AS PARAMETER TO BE MINIMIZED (IN CAPITAL LETTERS). WEIGHT

THE FOLLOWING ARE DEFAULT PARAMETER VALUES. THEY MAY BE CHANGED IF YOU WISH.

```
CYCLE PARAMETERS:
     1.     1200.00000000 TURBINE INLET TEMP, K
     2.        2.00000000 TURBINE INLET PRESSURE, MPa
     3.    0.00000000E-01 NOT USED
     4.        0.85000002 COMPRESSOR EFFICIENCY
     5.        0.94999999 GENERATOR EFFICIENCY
     6.        0.94999999 POWER CONDITIONING EFFICIENCY

REACTOR PARAMETERS:
     7.        0.93000001 FRACTIONAL FUEL ENRICHMENT
     8.       18.00000000 CRITICAL COMPACT MASS, Kg
     9.        1.00000000 CRITICAL MASS CORRECTION FACT
    10.        0.12200000 FUEL + MODERATOR VOL FRACT
    11.    2.50000004E-02 FUEL BED LENGTH, m
    12.    2.99999993E-02 REACTOR PRESSUR DROP, FRAC OF PIN
    13.        0.25000000 FUEL BURNUP FRACTION LIMIT
    14.    0.00000000E-01 MODERATOR-TO-FUEL RATIO
    15.    0.00000000E-01 MODERATOR MOLECULAR WEIGHT
    16.        1.00000000 MODERATOR DENSITY, Kg/m3
    17.        4.21999979 STRUCTURE TO FUEL & MOD RATIO
    18.     5560.00000000 STRUCTURE DENSITY, kg/m3
    19.    2.70000007E-02 CORE REMOVAL X-SECTION, cm-1
    20.    9.00000036E-02 CORE GAMMA ATTEN X-SECTION, cm-1
    21.    4.99999992E+16 ALLOWED PAYLOAD NEUTRON DOSE, nvt
    22.       25.00000000 PAYLOAD SEPARATION DISTANCE, m
    23.       15.00000000 PROTECTION CONE HALF ANGLE, DEG
    24.        2.00000000 NEUTRON SHIELD MATL-B4C=1, LIH=2
    25.    1.00000000E+07 ALLOWED PAYLOAD GAMMA DOSE, R

TURBINE PARAMETERS:
    26.        4.00000000 NUMBER OF TURBINES
    27.        1.00000000 TURBINE MATERIAL  1-SUPERALLOY,
                  2-CARBON
    28.     1200.00000000 MAXIMUM BLADE TEMPERATURE-K
```

TABLE 7 (cont.)

```
    29.    10000.00000000 TURBINE SPEED-RPM
    30.        2.00000000 WORK COEFFICIENT

RADIATOR PARAMETERS:
    31.        0.88000000 RADIATOR EMITTANCE


ENTER THE NUMBER OF PARAMETERS YOU WISH TO CHANGE.   0
```

TABLE 8

PRESSURE RATIO	TEMP RATIO	CYCLE EFFIC	RCT+SHLD WT (Kg)	POW CONV WT (Kg)	RADIATOR WT (Kg)	TOTAL WT (Kg)	TOTAL COST (M$)
1.800	2.527	0.137	18872.	17810.	108129.	159291.	357.
2.600	2.924	0.222	12786.	14654.	101952.	142332.	301.
3.400	3.253	0.280	11451.	13982.	115871.	155434.	313.
2.200	2.736	0.184	14849.	15907.	100438.	144313.	315.
3.000	3.095	0.254	11744.	13737.	107592.	146380.	301.
2.400	2.833	0.204	13677.	15226.	100508.	142352.	306.
2.800	3.012	0.239	12083.	14164.	104386.	143696.	299.
2.500	2.879	0.213	13203.	14929.	101087.	142141.	303.
2.700	2.968	0.231	12415.	14400.	103062.	142865.	300.
2.500	1.727	-0.246					
2.500	2.015	0.078	47493.	106478.	160475.	345891.	910.
2.500	2.303	0.157	19759.	28959.	89774.	152341.	371.
2.500	2.591	0.193	14297.	18700.	89085.	134290.	303.
2.500	2.879	0.213	13203.	14929.	101087.	142141.	303.
2.500	2.447	0.178	16215.	22318.	87074.	138167.	323.
2.500	2.735	0.204	13660.	16451.	93976.	136495.	299.
2.500	2.519	0.186	15012.	20272.	87648.	135225.	310.
2.500	2.663	0.199	13949.	17457.	91227.	134896.	300.
2.500	2.555	0.190	14501.	19438.	88270.	134429.	305.
2.500	2.627	0.196	14115.	18044.	90075.	134457.	301.
1.800	2.274	0.121	20833.	23136.	101157.	159639.	375.
2.600	2.632	0.201	13822.	18294.	89256.	133509.	299.
3.400	2.928	0.257	11705.	16656.	96772.	137646.	293.
2.200	2.463	0.165	16175.	20168.	90468.	139493.	321.
3.000	2.786	0.231	12380.	16952.	91924.	133382.	290.
2.800	2.711	0.217	13025.	17574.	90250.	132934.	294.
3.200	2.858	0.245	11854.	16795.	94130.	135057.	290.
2.700	2.672	0.209	13401.	17920.	89655.	133074.	296.
2.900	2.749	0.224	12686.	17252.	91013.	133047.	292.
2.800	1.807	-0.269					
2.800	2.108	0.094	41434.	91382.	147747.	308620.	803.
2.800	2.409	0.179	17971.	26717.	88608.	146626.	351.
2.800	2.711	0.217	13025.	17574.	90250.	132934.	294.
2.800	3.012	0.239	12083.	14164.	104386.	143696.	299.
2.800	2.560	0.201	14828.	20819.	87209.	135142.	310.
2.800	2.861	0.229	12477.	15544.	96150.	136588.	293.
2.800	2.635	0.210	13754.	18988.	88311.	133157.	300.
2.800	2.786	0.224	12726.	16453.	92889.	134276.	292.
2.800	2.673	0.214	13296.	18238.	89186.	132792.	296.
2.800	2.748	0.220	12869.	16983.	91488.	133473.	293.
2.800	2.673	0.214	13296.	18238.	89186.	132792.	296.

CYCLE PARAMETERS

CYCLE EFFICIENCY	=	0.21353653
THERMAL POWER-MW	=	51.88963699
MASS FLOW RATE-Kg/s	=	41.14289474
TURBINE INLET TEMP-K	=	1200.00000000
TURBINE OUTLET TEMP-K	=	820.02722168
COMPRESSOR INLET TEMP-K	=	448.94909668
COMPRESSOR OUTLET TEMP-K	=	728.16864014
PRESSURE RATIO	=	2.79999995

TABLE 8 (cont.)

REACTOR PARAMETERS		
BURNUP MASS-Kg	=	212.02217102
INITIAL CRITICAL MASS-Kg	=	697.88366699
END CRITICAL MASS-Kg	=	712.42236328
TOTAL BRNUP+CRIT MASS-Kg	=	924.44451904
SPECIFIC POWER-W/Kg	=	65079.46484375
MASS FOR SPECIFIC POWER LIM-Kg	=	1036.52551270
MASS FOR ALLOWED BURNUP-Kg	=	1025.33923340
FUEL MASS-Kg	=	1036.52551270
MODERATOR MASS-Kg	=	0.00000000E-01
STRUCTURE MASS-Kg	=	2268.67578125
REFLECTOR MASS-Kg	=	1144.35083008
PRESSURE VESSEL MASS-Kg	=	339.70037842
MISCELLANEOUS MASS-Kg	=	1036.52551270
TOTAL REACTOR MASS-Kg	=	5825.77783203
NEUTRON SHIELD THICKNESS-m	=	0.22490446
NEUTRON SHIELD MASS-Kg	=	877.93627930
GAMMA SHIELD THICKNESS-m	=	7.39577487E-02
GAMMA SHIELD MASS-Kg	=	6592.65576172
TOTAL SHIELD MASS-Kg	=	7470.59179687
RADIATOR PARAMETERS		
INLET TEMPERATURE-K	=	770.83776855
OUTLET TEMPERATURE-K	=	426.50921631
HIGH TEMPERATURE AREA-m2	=	0.00000000E-01
MEDIUM TEMPERATURE AREA-m2	=	1210.29101562
LOW TEMPERATURE AREA-m2	=	7576.68359375
TOTAL AREA-m2	=	8786.97460937
TOTAL WEIGHT-Kg	=	89185.77343750
POWER CONVERSION PARAMETERS		
TURBINE STAGES	=	14
TURBINE SPEED-RPM	=	8266.25000000
TURBINE EFFICIENCY	=	0.93672222
TURBINE PRESSURE RATIO	=	2.79999995
TURBINE COOLANT FLOW RATE-kg/s	=	0.00000000E-01
TURBINE WEIGHT-Kg	=	3221.94262695
COMPRESSOR WEIGHT-Kg	=	9665.82812500
GENERATOR WEIGHT-Kg	=	1052.63159180
POWER CONDITIONING WEIGHT-Kg	=	2000.00000000
GEN & PC RADIATOR WEIGHT-Kg	=	2297.35815430
GEN & PC RADIATOR AREA-m2	=	367.57730103
TOTAL WEIGHT-Kg	=	18237.75976562

TABLE 8 (cont.)

WEIGHT AND COST SUMMARY

REACTOR WEIGHT-Kg	=	5825.77783203
SHIELD WEIGHT-Kg	=	7470.59179687
POWER CONVERSION WEIGHT-Kg	=	18237.75976562
RADIATOR WEIGHT-Kg	=	89185.77343750
MISCELLANEOUS WEIGHT-Kg	=	12071.99023437
TOTAL WEIGHT-Kg	=	132791.89062500

REACTOR+SHIELD COST-M$	=	58.50402451
POWER CONVERSION COST-M$	=	49.39291000
RADIATOR COST-M$	=	17.83715439
LAUNCH COST-M$	=	169.97361755
TOTAL COST-M$	=	295.70770264

Execution terminated : 0

TABLE 9
Brayton System
Weight and Cost Algorithm Summary

Component	Weight	Cost
Reactor and Shield	Marshall's algorithm (Marshall, 1986)	\$4400/kg (estimate)
Turbine	See Appendix C	\$2000/kg (Gerry, 1985)
Generator	0.1 kg/kW (Gerry, 1985)	\$3000/kg (Gerry, 1985)
Power Conditioning	0.2 kg/kW (estimate)	\$10,000/kg (estimate)
Radiator	12 kg/m² for temp > 1000 K 8 kg/m² for 650 < temp < 1000 K 5 kg/m² for temp < 650 K (NASA estimates) multiply by 1.25 for meteoroid loss (estimate) multiply by 1.5 for heat exchanger (estimate) See Appendix F for area calculation	\$200/kg (estimate)
Compressor	3 times turbine (estimate)	\$2000/kg (Gerry, 1985)
PC & Generator Radiator	5 kg/m² (NASA estimate) add 25% for meteoroid loss (estimate)	\$200/kg (estimate)
Miscellaneous	10% of subtotal	
Launch cost		\$1280/kg (Aviation Week, 1985, and heavy lift shuttle)

RANKINE CYCLE CONTINUOUS POWER SYSTEM

Like the nuclear reactor powered Brayton cycle system, the nuclear reactor powered liquid metal Rankine cycle system can potentially provide continuous power for several years. Because of its long operation time, expendables cannot be practically used. Cycle waste heat is rejected by a space radiator, and this is where the Rankine system has a significant advantage over the Brayton system. The Rankine system rejects heat from a condensing working fluid; thus, its radiator is nearly isothermal and radiates much more heat per unit area than a comparable Brayton radiator. Since the Brayton cycle rejects sensible heat from its working fluid, its radiator experiences a substantial temperature drop from the inlet end to the outlet end. Thus, Rankine radiators use much less area than Brayton radiators to reject the same quantity of heat. A major disadvantage of Rankine systems is that the technology associated with using two phase alkaline metals as working fluids in space is not well developed.

We have modeled two types of Rankine systems, direct and indirect, shown in Figures 4 and 5 respectively. The direct system boils potassium in a liquid metal cooled reactor and sends the saturated vapor to a turbine for power generation. Since the fluid leaving the "hot" end of the reactor is unlikely to be pure vapor, a separator is used to separate the saturated vapor from its accompanying liquid. The liquid is recirculated to the "cold" end of the reactor.

The indirect Rankine system uses liquid lithium as a reactor coolant. It transfers heat, via heat exchangers, to the potassium working fluid. Our model of this system allows for nearly any level of superheat as indicated by the temperature entropy diagrams in Figures 6a, 6b, and 6c.

Our model for the Rankine cycle is an approximate one, but it gives very accurate results. We divide the ideal cycle into three zones -- preheat, boil, and superheat -- as shown in Figure 7. Then we calculate the Carnot efficiency for each zone based on the average temperature in that zone. Finally, we weight the three efficiencies by the corresponding enthalpy added to the working fluid in that zone to get the ideal cycle efficiency, and we multiply the ideal cycle efficiency by turbine efficiency to get the cycle efficiency. We have compared this method to one using real enthalpy values for several cases and find that our approximation is usually within 2 to 3 percent of the rigorously derived values. By 2 to 3 percent, we mean that if the rigorous value is 20%, the approximate value will be 19.4%, not 17%. The following steps will show this method in more detail.

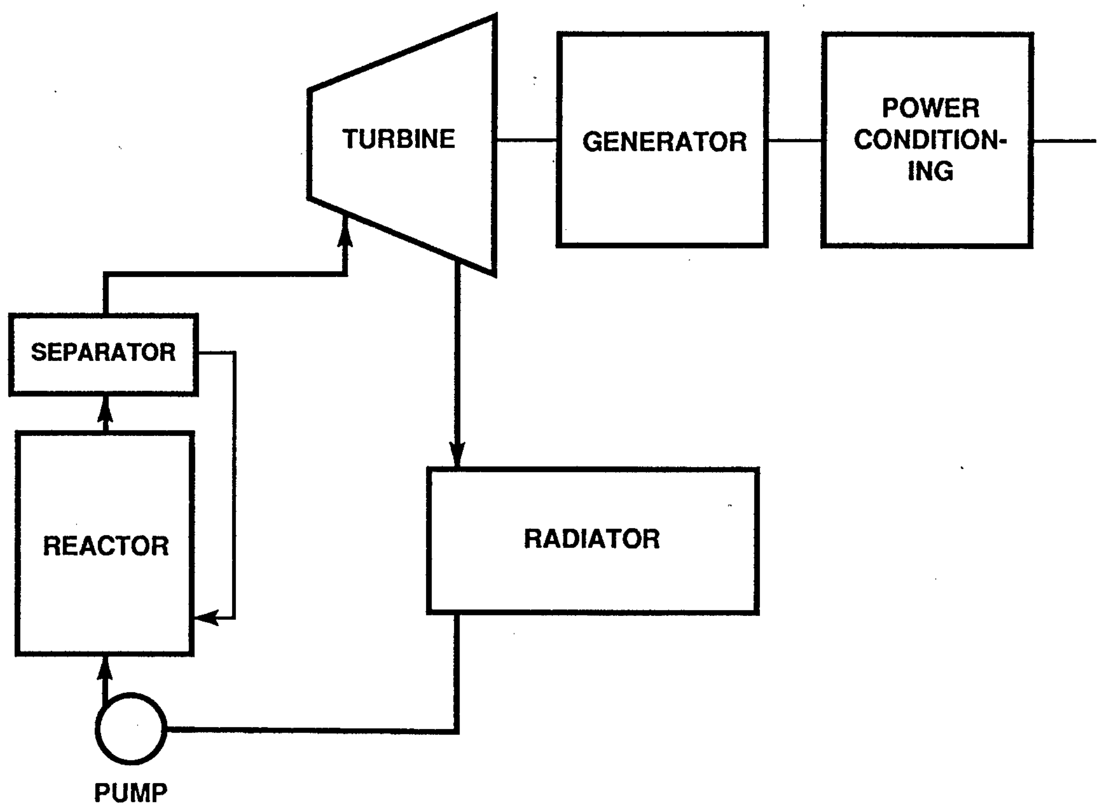

FIGURE 4. Direct Rankine System

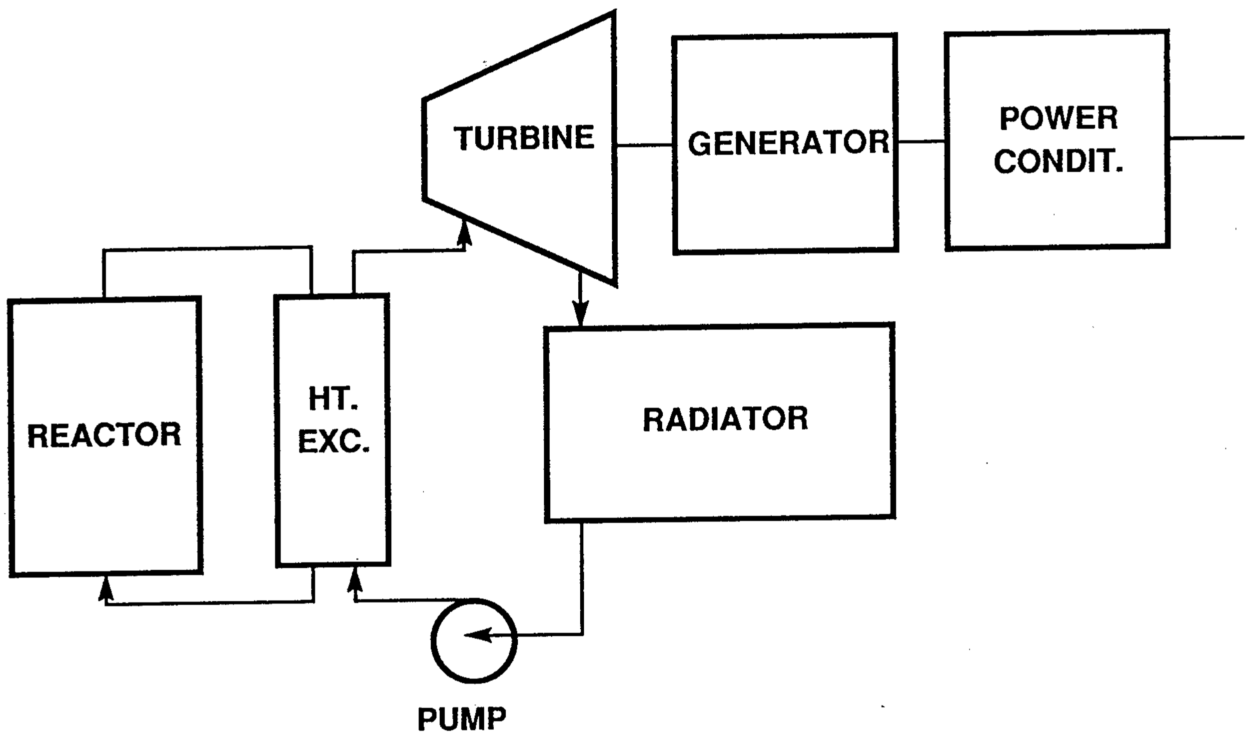

FIGURE 5. Indirect Rankine System

FIGURE 6a. Direct Rankine Cycle and Indirect Cycle Without Superheat

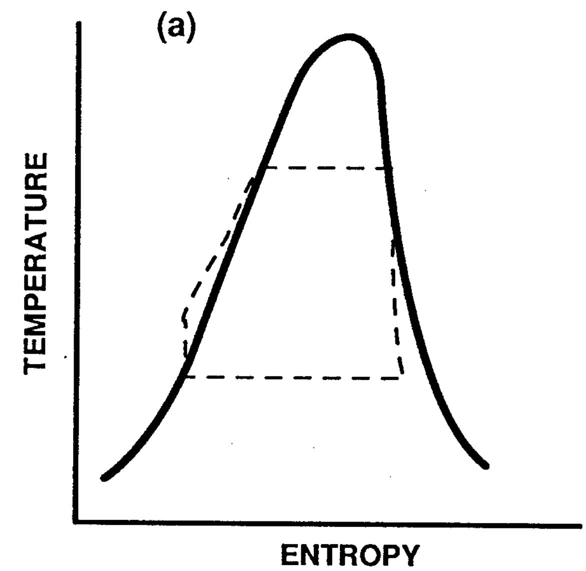

FIGURE 6b. Indirect Rankine Cycle With Some Superheat

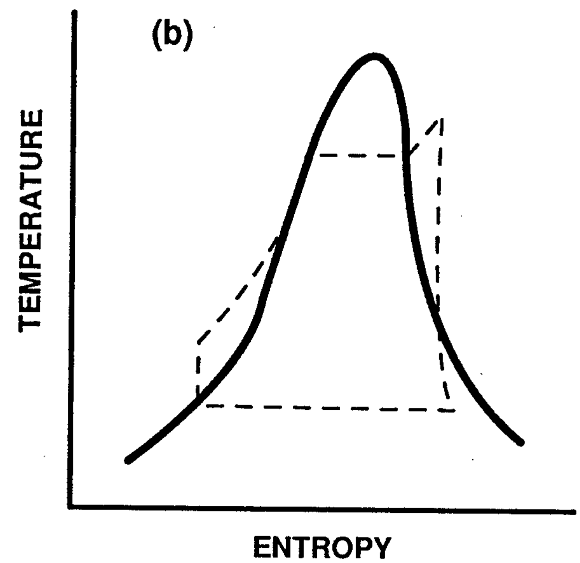

FIGURE 6c. Indirect Rankine Cycle With Superheat

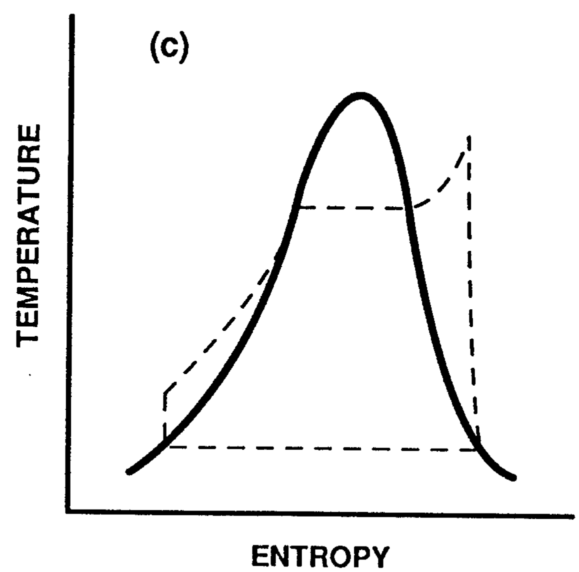

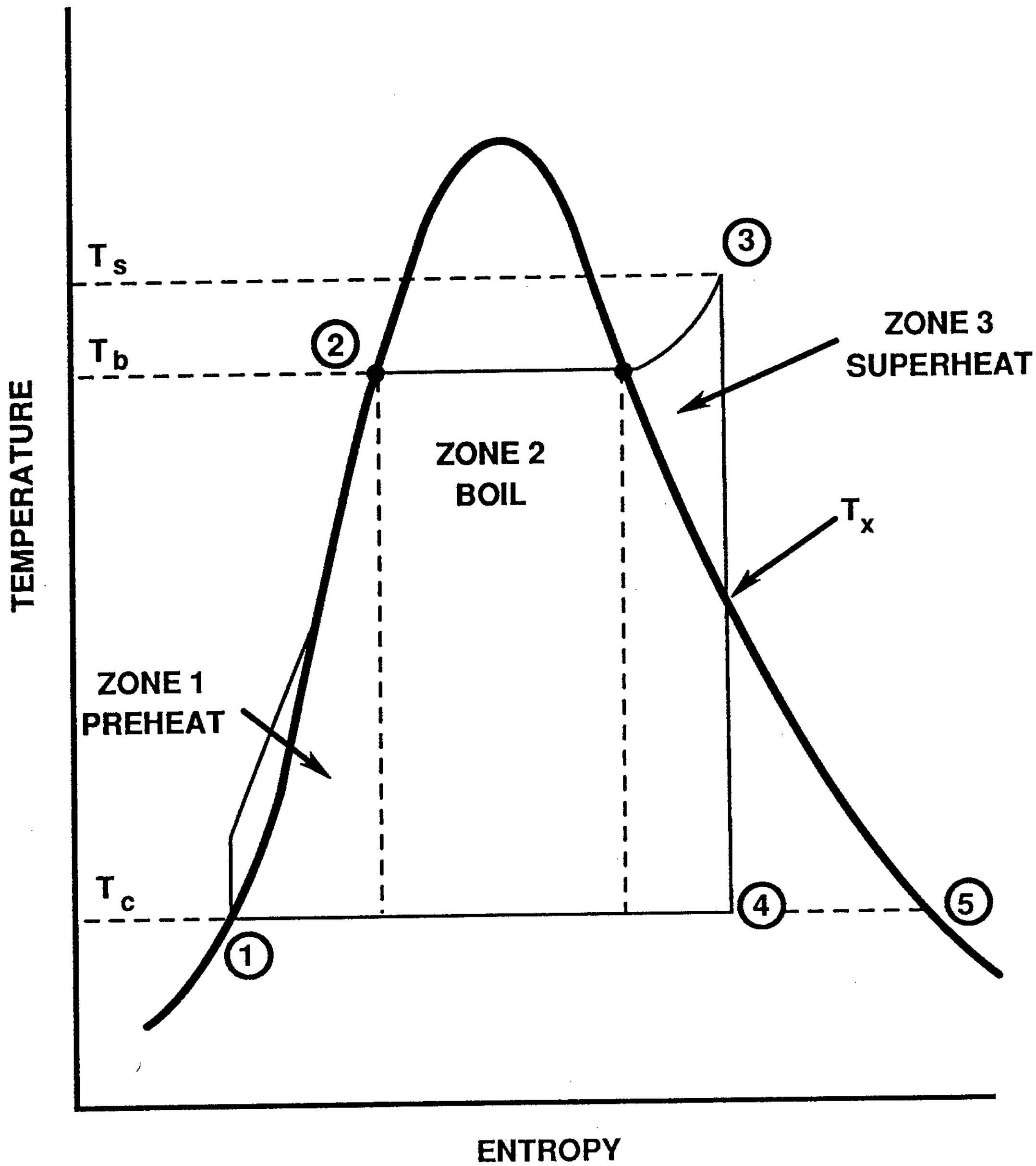

FIGURE 7. Ideal Rankine Cycle

1. Preheat zone -- The equations for this zone are as follows:

$$\eta_p = \frac{.5(T_b + T_c) - T_c}{.5(T_b + T_c)} \quad , \tag{26}$$

where η_p is the efficiency in the preheat zone,
T_b is the boiling temperature, and
T_c is the condensing temperature.

The enthalpy added in this zone is given in equation 27:

$$h_p = C_{pl}(T_b - T_c) \quad , \tag{27}$$

where C_{pl} is the potassium liquid's specific heat (830 J/kg).

2. Boiling zone -- The equations for this zone are as follows:

$$\eta_b = \frac{T_b - T_c}{T_b} \quad , \tag{28}$$

where η_b is the efficiency in the preheat zone.

The boiling enthalpy depends on boiling temperature. Fitting potassium data from Reynolds (1979) gives the following result:

$$h_{fg} = 2.57 \times 10^6 - 640T_b \quad , \tag{29}$$

where h_{fg} is the enthalpy of vaporization for potassium.

3. Superheat zone -- The equations for this zone are as follows:

$$\eta_s = \frac{.5(T_s + T_b) - T_c}{.5(T_s + T_b)} \quad , \tag{30}$$

where η_s is the efficiency in the superheat zone, and
T_s is the peak, or turbine inlet temperature.

The superheat enthalpy is given by:

$$h_s = C_{pg}(T_s - T_b) \quad , \tag{31}$$

where h_s is the superheat enthalpy, and
C_{pg} is the gas specific heat.

C_{pg} was also found by fitting data in Reynolds (1979).

$$C_{pg} = 1.7T_x - .05T_s - .0005T_xT_s \quad . \tag{32}$$

T_x is the saturation temperature of the gas. That is, it is the temperature where the gas will become a saturated vapor if it is expanded isentropically. It was also found by fitting data from Reynolds (1979).

$$T_x = 295\ e^{2.6/S} \quad . \tag{33}$$

$$S = S_o + \ln(T_s/T_b)/1.06 \quad . \tag{34}$$

$$S_o = 2.6/[\ln(T_b) - 5.687] \quad . \tag{35}$$

In these equations, S and S_o are the entropy at T_s and the entropy at T_b respectively.

Equations (26) through (35) and turbine efficiency (see Appendix C) are all we need to estimate cycle efficiency:

$$\eta_{cyc} = \left[\eta_t \frac{h_p\eta_p + h_b\eta_b + h_s\eta_s}{h_p + h_b + h_s} \right] \quad , \tag{36}$$

where η_{cyc} is cycle efficiency, and
η_t is turbine efficiency.

For an example, let T_s = 1200 K, T_b = 1109 K, T_c = 900 K, and η_t = .9. We get the following:

T_x = 1057,
h_s = 100.4 kJ/kg,
η_s = .220,
h_b = 1860 kJ/kg,
η_b = .1885,
h_p = 173.5 kJ/kg,
η_p = .104, and
η_{cyc} = 16.48%.

Using enthalpy and entropy values from Reynolds (1979) and Figure 7:

h_1 = 79.3 kJ/kg,
h_3 = 2225.1 kJ/kg, and
h_5 = 1087.8 kJ/kg.

S_3 = S_4 = 20418 kJ/kg K,
S_1 = .0933 kJ/kg K, and
S_5 = 2.3250 kJ/kg K.

$$x = \text{quality at point } 4 = \frac{S_4 - S_1}{S_5 - S_1} = .8731, \text{ and}$$

$$h_4 = h_1 + x(h_5 - h_1) = 1832.9 \text{ kJ/kg.}$$

We also need pump enthalpy, h_p, which is equal to pressure change times specific volume divided by efficiency (.7).

$P_1 = .025 \times 10^6$ Pa,
$P_2 = .2 \times 10^6$ Pa, and
$v_1 = .001437$ m³/kg.

$$h_{pump} = \frac{(P_2 - P_1)v_1}{.7} = 359 \text{ J/kg}$$

$$\eta_{cyc} = \frac{.9(h_3 - h_4) - h_{pump}}{h_3 - h_1 - h_{pump}} = 16.44\%$$

Thus, our approximate model calculates a cycle efficiency of 16.48%, and a rigorous analysis calculates an efficiency of 16.44% for our example.

In our model, we could specify T_s, which is both the superheat temperature and the turbine inlet temperature, and the boiler temperature, T_b, but we do not. Instead, we specify T_s and the ratio of turbine inlet pressure to saturation pressure at the turbine inlet temperature, and we use this ratio to calculate the boiler temperature. This is done using a derivative of the Clausius-Clapeyron equation which gives the relation between boiling temperature and boiling pressure. For potassium, this equation is as follows:

$$P_{boil} = 1320\ e^{-9760/T_{boil}} \tag{37}$$

Thus:

$$\frac{P_{ti}}{P_s} = \frac{1320\ e^{-9760/T_b}}{1320\ e^{-9760/T_s}}, \tag{38}$$

and

$$T_b = \frac{9760\ T_s}{9760 - T_s \ln(P_{ti}/P_s)}. \tag{39}$$

where P_{ti} is turbine inlet pressure, also the boiler pressure (Pa), and
P_s is the saturated vapor or boiling pressure that corresponds to a temperature of T_s.

If $P_{ti} = P_s$, then the cycle does not use any superheat. As P_{ti}/P_s grows less than 1, the quantity of superheat grows.

Turbine inlet and condenser pressures can be calculated using equation 37:

$$P_{ti} = 1320\ e^{-9760/T_b} \quad , \tag{40}$$

$$P_c = 1320\ e^{-9760/T_c} \quad . \tag{41}$$

The heat which must be supplied by the system's reactor, Q_{rctr}, is given by equation 42:

$$Q_{rctr} = P_e/(\eta_{cyc}\eta_g\eta_{pc}) \quad , \tag{42}$$

where P_e is the electrical power required (W),
η_g is generator efficiency, and
η_{pc} is power conditioning efficiency.

The heat rejected by the radiator, Q_{rad}, is given by equation 43:

$$Q_{rad} = Q_{rctr} - P_e/(\eta_g\eta_{pc}) \quad . \tag{43}$$

Turbine power, P_{turb}, is given by equation 44:

$$P_{turb} = P_e/(\eta_g\eta_{pc}) \quad . \tag{44}$$

Working fluid flow rate, $\dot{m}$, is given by equation 45:

$$\dot{m} = Q_{rctr}/(h_p + h_b + h_s) \quad . \tag{45}$$

This is also the reactor flow rate for the direct cycle, but h_s is zero.

To find the reactor flow rate, $\dot{m}_r$, for an indirect cycle, we have to make some assumptions about heat exchanger effectiveness. Figure 8 shows a temperature-enthalpy plot for the indirect cycle. Working fluid enters the preheater and progresses to the superheater. Reactor fluid flows in the opposite direction, and it must satisfy "pinch point" requirements. That is, T_{pp} must be greater than T_b. Reactor inlet and outlet temperatures and flow rate can be found as follows:

$$T_{pp} = T_c + \frac{T_b - T_c}{\eta_{px}} \quad , \tag{46}$$

$$T_{ro} = T_b + \frac{T_s - T_b}{\eta_{sx}} \quad , \tag{47}$$

where η_{px} is preheater effectiveness (.9), and
η_{sx} is superheater effectiveness (.8).

But we also require that $T_{ro} \geq T_{pp} + 1$.

$$\dot{m}_r = \frac{\dot{m}(h_b + h_s)}{C_{PLi}(T_{ro} - T_{pp})} \quad , \tag{48}$$

where C_{PLi} is the lithium reactor coolant's specific heat.

We also require that $\dot{m}_r$ must not exceed 5 kg/s per MW_{th} generated in the reactor. This 5 kg/s per MW_{th} number represents one of the highest flow rates we have seen for a liquid metal cooled reactor. Higher flow rates may be practical, but we have not yet studied their implications. If we use the flow rate limit, then we must adjust T_{ro}.

If $\dot{m}_r > 5$ kg/MW-s, then $\dot{m}_r = 5$ kg/MW-s, and

$$T_{ro} = T_{pp} + \dot{m}(h_b + h_s)/\dot{m}_r C_{PLi} \quad . \tag{49}$$

The reactor's inlet temperature is given by Equation (50):

$$T_{ri} = T_{pp} - \dot{m}h_p/\dot{m}_r C_{PLi} \quad , \tag{50}$$

and reactor pressure is assumed to be the saturated liquid pressure for lithium at T_{ro}:

$$P_{react} = 7200\ e^{-18100/T_{ro}} \quad . \tag{51}$$

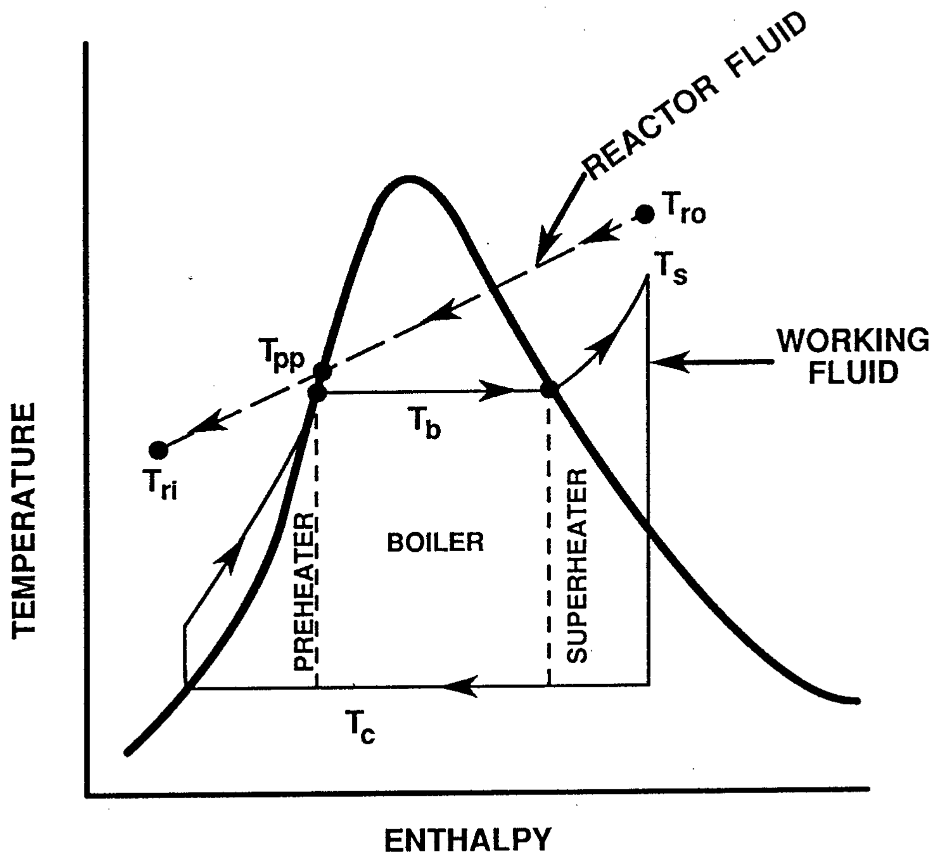

T_{ro} = reactor outlet temperature
T_{ri} = reactor inlet temperature
T_{pp} = pinch point temperature
T_s = superheat (turbine inlet) temperature

FIGURE 8. Indirect Cycle

This is the Clausius-Clapeyron derivative equation for lithium.

Condenser temperature is a variable which can be optimized. As it decreases, the cycle becomes more efficient, reactor mass decreases, and the waste heat which must be removed by the radiator decreases. On the other hand, as condenser temperature decreases, radiator temperature decreases and the radiator can remove less heat per unit area. Thus, there is an optimum condenser temperature which minimizes system mass.

Our Rankine system model was "computerized" for use on the IBM-AT personal computer. It is written in FORTRAN/77 and is interactive. The program uses the above algorithms to determine system performance and parameter values. Then, it estimates mass and cost values for each component and for the system (discussed later). Table 10 shows a typical input sequence for running the computer program which we call "RNKCYC." First, the user is asked to specify a power level in MWe and an operation time in hours (user input is underlined in Table 10). Next, default parameter values are listed and changes are solicited. When all of the changes have been made, the program runs and prints the information shown in Table 11.

The first part of Table 11 shows the optimization of condenser temperature. In this example, the minimum mass system is achieved for a 675 K condenser temperature. Notice that the system mass values decrease until condenser temperature is 825 K. Then, mass starts increasing until it takes a sharp drop at 675 K and starts increasing again. The drop was caused by switching radiator materials from titanium to aluminum. The switch was made because aluminum is used when radiator temperature is below 650 K. (There is a 30 K difference between condenser and radiator temperature.)

The second part of Table 11 lists parameter values for the optimum system.

Table 12 summarizes component mass algorithms which are also described below.

The model assumes the use of a lithium (indirect cycle) or potassium (direct cycle) cooled reactor. The reactor model was formulated by Al Marshall of Sandia National Laboratories and is described in Marshall (1986). As with other reactors already discussed, his model calculates three fuel mass values -- end-of-life criticality, burnup limit, and the specific power fuel requirement -- and uses the largest of the three. To the fuel mass is added moderator mass (if any), structure mass, reflector mass, pressure vessel mass, a miscellaneous mass, and gamma and neutron shield mass.

Radiator mass is calculated using the mass per unit area values in Table 12, and the area algorithms in Appendix F. To the radiator is added a heat exchanger (condenser) mass calculated using the algorithms in Table 12.

Turbine mass algorithms are given in Appendix C. They were derived from algorithms developed by Steve Hudson of Sandia National Laboratories. The direct cycle uses a vapor separator and its mass is calculated using the same algorithms as for a condenser. The indirect cycle does not use a separator but it does use a heat exchanger. Heat exchanger mass algorithms are given in Table 12. Alternator mass is assumed to be 0.1 kg/kWe and is based on a near term, iron core type of alternator. It has an efficiency of 95%.

Power conditioning mass is assumed to be 0.2 kg/kW. This is a place holder and the real value will depend on load characteristics. We assume power conditioning is 95% efficient. The alternator and power conditioning must be cooled and we assume the use of a radiator for this. It rejects heat at 500 K and is assumed to be isothermal. We multiply its area (calculated using the Rankine radiator algorithm in Appendix F) by 1.25 to account for meteoroid losses.

A miscellaneous mass of 10% is added to account for structure, piping, etc.

Costs are estimated, but they are at present very crude and little confidence should be placed in them.

TABLE 10

```
THIS PROGRAM MODELS A RANKINE CYCLE SPACE POWER
SYSTEM.  THE SYSTEM CONSISTS OF A LIQUID METAL
COOLED REACTOR, A TURBINE, A GENERATOR
A RADIATOR, AND POWER CONDITIONING.
THREE TYPES OF CYCLES ARE COVERED:
   1. A DIRECT CYCLE WITH NO SUPERHEAT, A VAPOR
      SEPARATOR, AND LITHIUM AS A WORKING FLUID.
   2. AND AN INDIRECT CYCLE WITH SUPERHEAT, A HEAT-
      EXCHANGER, POTASSIUM AS A WORKING FLUID AND
      LITHIUM AS A REACTOR COOLANT.
CONDENSER TEMPERATURE IS OPTIMIZED
TO GET EITHER MINIMUM SYSTEM WEIGHT OR COST.


ENTER VALUES FOR ELECTRICAL POWER IN MW AND
OPERATING TIME IN HOURS.   10 87600

ENTER "WEIGHT" OR "COST" AS PARAMETER TO BE
  MINIMIZED (IN CAPITAL LETTERS).   WEIGHT

THE FOLLOWING ARE DEFAULT PARAMETER VALUES.
THEY MAY BE CHANGED IF YOU WISH.


CYCLE PARAMETERS:
     1.       1200.00000000 TURBINE INLET TEMP, K
     2.          1.00000000 CYCLE TYPE  1-DIRECT, 2-INDIRECT
     3.          1.00000000 TURBINE INLET/SATURATION PRESSURE
     4.          0.94999999 GENERATOR EFFICIENCY
     5.          0.94999999 POWER CONDITIONING EFFICIENCY


REACTOR PARAMETERS:
     6.          0.93000001 FRACTIONAL FUEL ENRICHMENT
     7.         18.00000000 CRITICAL COMPACT MASS, Kg
     8.      12170.00000000 FUEL DENSITY, kg/m3
     9.          1.00000000 CRITICAL MASS CORRECTION FACT
    10.          0.28000000 FUEL + MODERATOR VOL FRACT
    11.     150000.00000000 FUEL POWER DENSITY, W/kg
    12.      7.00000003E-02 FUEL BURNUP FRACTION LIMIT
    13.      0.00000000E-01 MODERATOR-TO-FUEL RATIO
    14.      0.00000000E-01 MODERATOR MOLECULAR WEIGHT
    15.          1.00000000 MODERATOR DENSITY, Kg/m3
    16.          1.42999995 STRUCTURE TO FUEL & MOD RATIO
    17.       8300.00000000 STRUCTURE DENSITY, kg/m3
    18.          0.83999997 CORE REMOVAL X-SECTION, cm-1
    19.          0.23300000 CORE GAMMA ATTEN X-SECT, cm-1
    20.      4.99999992E+16 ALLOWED PAYLOAD NEUTRON DOSE, nvt
    21.         25.00000000 PAYLOAD SEPARATION DISTANCE, m
    22.         15.00000000 PROTECTION CONE HALF ANGLE, DEG
    23.          2.00000000 NEUTRON SHIELD MATL-B4C=1, LIH=2
    24.      1.00000000E+07 ALLOWED PAYLOAD GAMMA DOSE, R
```

TABLE 10 (cont.)

TURBINE PARAMETERS

25.	4.00000000	NUMBER OF TURBINES
26.	1.00000000	TURBINE MATERIAL 1-Ni, 2-Ta
27.	10000.00000000	TURBINE SPEED, RPM
28.	1.50000000	TURBINE WORK COEFFICIENT
29.	0.00000000E-01	DISK COOL PARAM, 0-NO, 1-YES

RADIATOR PARAMETERS:

30.	0.88000000	RADIATOR EMITTANCE

ENTER THE NUMBER OF PARAMETERS YOU WISH TO CHANGE. 0

TABLE 11

TURBINE TEMP (K)	CONDENSER TEMP (K)	CYCLE EFFIC	RCT+SHLD WT (Kg)	POW CONV WT (Kg)	RADIATOR WT (Kg)	TOTAL WT (Kg)	TOTAL COST (M$)
1200.000	1125.000	0.055	66009.	25568.	39706.	144411.	547.
1200.000	1100.000	0.072	51471.	20769.	32438.	115145.	435.
1200.000	1075.000	0.090	42548.	17918.	28326.	97672.	367.
1200.000	1050.000	0.106	36501.	16045.	25824.	86208.	321.
1200.000	1025.000	0.123	32121.	14733.	16182.	69340.	276.
1200.000	1000.000	0.139	28796.	13774.	15564.	63948.	252.
1200.000	975.000	0.154	26181.	13054.	15248.	59931.	234.
1200.000	950.000	0.170	24068.	12504.	15166.	56912.	220.
1200.000	925.000	0.185	22323.	12080.	15281.	54653.	208.
1200.000	900.000	0.200	20857.	11755.	15573.	53003.	199.
1200.000	875.000	0.214	19606.	11599.	16034.	51962.	192.
1200.000	850.000	0.228	18525.	11528.	16665.	51390.	187.
1200.000	825.000	0.242	17582.	11538.	17474.	51253.	182.
1200.000	800.000	0.256	16750.	11628.	18477.	51540.	180.
1200.000	775.000	0.269	16011.	11799.	19698.	52260.	178.
1200.000	750.000	0.283	15350.	12116.	21170.	53499.	177.
1200.000	725.000	0.296	14754.	12524.	22936.	55235.	178.
1200.000	700.000	0.309	14214.	13036.	25053.	57534.	180.
1200.000	675.000	0.321	13722.	13674.	17248.	49109.	167.
1200.000	650.000	0.334	13272.	14463.	19165.	51591.	170.
1200.000	625.000	0.346	12858.	15438.	21493.	54767.	175.
1200.000	600.000	0.358	12476.	16643.	24341.	58805.	181.
1200.000	575.000	0.370	12121.	18136.	27862.	63932.	190.
1200.000	550.000	0.382	11792.	19997.	32269.	70464.	201.
1200.000	525.000	0.394	11484.	22332.	37867.	78852.	217.
1200.000	500.000	0.405	11196.	25285.	45108.	89748.	237.
1200.000	475.000	0.417	10926.	29056.	54683.	104132.	263.
1200.000	450.000	0.428	10672.	33926.	67707.	123535.	299.
1200.000	425.000	0.440	10431.	40298.	86073.	150483.	349.
1200.000	400.000	0.451	10204.	48760.	113283.	189472.	421.
1200.000	375.000	0.462	9988.	60191.	156547.	249398.	528.
1200.000	350.000	0.473	9783.	75935.	233420.	351051.	704.
1200.000	325.000	0.485	9587.	98114.	400527.	559051.	1047.
1200.000	300.000	0.496	9400.	130189.	997690.	1251007.	2115.
1200.000	675.000	0.321	13722.	13674.	17248.	49109.	167.

CYCLE PARAMETERS

CYCLE EFFICIENCY	=	0.32119268
THERMAL POWER-MW	=	34.49746323
MASS FLOW RATE-Kg/s	=	15.41613865
TURBINE INLET TEMP-K	=	1200.00000000
CONDENSER TEMP-K	=	675.00000000
BOILER TEMP-K	=	1200.00000000
BOILER PRESSURE-MPa	=	0.38753614
CONDENSER PRESSURE-MPa	=	6.93421869E-04
REACTOR OUTLET TEMP-K	=	1200.00000000
REACTOR INLET TEMP-K	=	675.00000000
REACTOR PRESSURE-MPa	=	0.38753614
REACTOR FLOW RATE-kg/s	=	15.41613865

TABLE 11 (cont.)

REACTOR PARAMETERS		
BURNUP MASS-Kg	=	140.95736694
INITIAL CRITICAL MASS-Kg	=	165.93653870
END CRITICAL MASS-Kg	=	175.27770996
TOTAL BRNUP+CRIT MASS-Kg	=	316.23507690
SPECIFIC POWER-W/Kg	=	150000.00000000
MASS FOR SPECIFIC POWER LIM-Kg	=	298.97799683
MASS FOR ALLOWED BURNUP-Kg	=	2434.53515625
FUEL MASS-Kg	=	2434.53515625
MODERATOR MASS-Kg	=	0.00000000E-01
STRUCTURE MASS-Kg	=	2374.32177734
REFLECTOR MASS-Kg	=	1392.97717285
PRESSURE VESSEL MASS-Kg	=	256.64099121
MISCELLANEOUS MASS-Kg	=	2434.53515625
TOTAL REACTOR MASS-Kg	=	8893.01074219
NEUTRON SHIELD THICKNESS-m	=	0.00000000E-01
NEUTRON SHIELD MASS-Kg	=	0.00000000E-01
GAMMA SHIELD THICKNESS-m	=	6.23262003E-02
GAMMA SHIELD MASS-Kg	=	4829.31933594
TOTAL SHIELD MASS-Kg	=	4829.31933594
RADIATOR PARAMETERS		
TOTAL AREA-m2	=	2759.63330078
TOTAL WEIGHT-Kg	=	17247.70703125
POWER CONVERSION PARAMETERS		
TURBINE WEIGHT-Kg	=	5798.25781250
TURBINE SPEED-RPM	=	10000.00000000
TURBINE EFFICIENCY	=	0.78950000
HEAT EXCHANGER WEIGHT-kg	=	0.00000000E-01
VAPOR SEPARATOR WEIGHT-kg	=	1263.01953125
CONDENSER WEIGHT-kg	=	1263.01953125
GENERATOR WEIGHT-Kg	=	1052.63159180
POWER CONDITIONING WEIGHT-Kg	=	2000.00000000
GEN & PC RADIATOR WEIGHT-Kg	=	2297.35815430
GEN & PC RADIATOR AREA-m2	=	367.57730103
TOTAL WEIGHT-Kg	=	13674.28613281
WEIGHT AND COST SUMMARY		
REACTOR WEIGHT-Kg	=	8893.01074219
SHIELD WEIGHT-Kg	=	4829.31933594
POWER CONVERSION WEIGHT-Kg	=	13674.28613281
RADIATOR WEIGHT-Kg	=	17247.70703125
MISCELLANEOUS WEIGHT-Kg	=	4464.43261719
TOTAL WEIGHT-Kg	=	49108.75781250
REACTOR+SHIELD COST-M$	=	60.37825012
POWER CONVERSION COST-M$	=	40.26596069
RADIATOR COST-M$	=	3.44954133
LAUNCH COST-M$	=	62.85920715
TOTAL COST-M$	=	166.95295715

Execution terminated : 0

TABLE 12
Rankine System
Mass and Cost Algorithm Summary

Component	Weight	Cost
Reactor and Shield	Marshall's algorithm (Marshall, 1986)	\$4400/kg (estimate)
Turbine	See Appendix C	\$2000/kg (Gerry, 1985)
Alternator	0.1 kg/kW (Gerry, 1985)	\$3000/kg (Gerry, 1985)
Power Conditioning	0.2 kg/kW (estimate)	\$10,000/kg (estimate)
Radiator	12 kg/m^2 temp > 1000 K 8 kg/m^2 temp 650 to 1000 K 5 kg/m^2 temp < 650 K (NASA estimates) multiply by 1.25 for meteoroid losses (estimate) See Appendix F for area calculation	\$200/kg (estimate)
PC & Alternator radiator	5 kg/m^2 (NASA estimate) add 25% for meteoroid losses	\$200/kg (estimate)
Heat Exchanger	Preheater & Boiler: $.53[(h_P + h_b)\dot{m}/1000]^{.74}$ Superheater: $14(h_s\dot{m}/1000)^{.7}$ (NASA estimates) h_p = preheat enthalpy (J/kg) h_b = boiler enthalpy (J/kg) h_s = superheat enthalpy (J/kg) $\dot{m}$ = flow rate (kg/s)	\$2000/kg (estimate--same as turbine)

TABLE 12 (cont.)
Rankine System
Mass and Cost Algorithm Summary

Component	Weight	Cost
Separator & Condenser	mass = b $Qrad^z$ Q / b / z <.5 / 120 / .42 .5 to .7 / 124 / .46 .7 to 1 / 130 / .60 1 to 3 / 137 / .62 3 to 10 / 113 / .79 10 to 30 / 142 / .69 > 30 / 50 / 1.0 Q = radiator heat rejected (MW_{th}) (NASA estimates)	$2000/kg (estimate--same as turbine
Miscellaneous	10% of subtotal	
Launch cost		$1280/kg (Aviation Week, 1985, and heavy lift shuttle)

THERMIONIC CONTINUOUS POWER SYSTEM

Like the Brayton and Rankine systems, the thermionic system provides continuous power and is powered by a nuclear reactor. We assume the use of an in-core thermionic reactor; that is, the thermionic converters located inside the reactor are cylindrical in geometry and enclose nuclear fuel. A thermionic reactor will contain many thermionic converter elements. Nuclear fuel heats emitter surfaces which causes electrons to "jump" a gap between the emitter and collector. The collector collects the electrons which then pass through an electrical circuit to a load then back to the emitter. The collector surfaces are cooled by a mixture of sodium and potassium (NaK) which is in turn cooled by a space radiator. In terms of the number of major components, this is the simplest system. It consists of a reactor, power conditioning, and a radiator.

Our model for the performance of this system depends heavily on Angrist (1982). The saturation current from a thermionic emitter can be estimated using equation 52:

$$j_e = A_1 T_e^2 e^{-\phi_e/kT_e} \quad , \tag{52}$$

and the back current from the collector can be estimated using equation 53:

$$j_c = A_1 T_c^2 e^{-(\phi_c + \Delta V)/kT_c} \quad , \tag{53}$$

where
j_e is the emitter saturation current (A/m^2),
j_c is the back saturation current (A/m^2),
A_1 is a constant (1.2×10^6 a/m^2),
T_e is emitter temperature (K),
T_c is collector temperature (K),
ϕ_e is the emitter's work function (eV),
ϕ_c is the collector's work function (eV),
k is Boltzmann's constant (1.38×10^{-23} J/K, but it must be divided by 1.6×10^{-19} J/eV to get 8.62×10^{-5} eV/K), and
ΔV is the gap voltage drop (eV).

Angrist shows that the minimum voltage drop is 0.45 eV and that associated with it is a saturation current ratio of 0.4. That is, current is 0.4 times saturation current.

With this, the power per unit area, P, from a device is:

$$P = .4(j_e - j_c)(\phi_e - \phi_c - \Delta V) \quad . \tag{54}$$

We have assumed that $\phi_e - \phi_c - \Delta V$ is the useful voltage thus neglecting circuit and other voltage drops.

To calculate the efficiency of the device, we need to do an energy balance on the emitter. Energy carried away by electrons, Q_e (also called electron cooling), is given as follows:

$$Q_e = j_e(\phi_e + 2kT_e) - j_c(\phi_e + 2kT_c) \tag{55}$$

Radiation losses, Q_r, are:

$$Q_r = \frac{1}{\frac{1}{\varepsilon_e} + \frac{1}{\varepsilon_c} - 1} \sigma (T_e^4 - T_c^4) \quad , \tag{56}$$

ε_e is emitter thermal emittance (Angrist suggests 0.3),
ε_c is collector emittance (Angrist suggests 0.1), and
σ is the Stefan-Boltzmann constant (5.7×10^{-8} W/m^2k^4).

Conduction losses, Q_c, are:

$$Q_c = \frac{k}{g} (T_e - T_c) \quad , \tag{57}$$

where k is the thermal conductivity of cessium in the gap (Angrist suggests .0124 W/mk), and
g is the gap thickness (m).

Thus, the heat supplied to the emitter must be $Q_e + Q_r + Q_c$ and the efficiency of the device, η, is as follows:

$$\eta = P/(Q_e + Q_r + Q_c) \quad . \tag{58}$$

The thermal power, P_{th}, that must be generated by the reactor is given by equation 59:

$$P_{th} = P_e/(\eta\eta_{pc}) \quad , \tag{59}$$

where P_e is the electrical power required by the load, and
η_{pc} is power conditioning efficiency (we use .95).

The heat which must be dissipated by the radiator is Q_{rad}:

$$Q_{rad} = P_{th}(1 - \eta) \quad . \tag{60}$$

We assume that the coolant flow rate through the reactor, m, is 5 kg/s per MW_{th} of heat generated, and that the collector temperature is equal to the reactor coolant outlet temperature, T_{ro}. The reactor inlet temperature, T_{ri}, can be calculated using equation 61:

$$T_{ri} = T_{ro} - P_{th}/mC_p \quad , \tag{61}$$

where C_p is the NaK coolant's specific heat (950 J/kgK).

These algorithms were written into a computer program (TICYC) using FORTRAN/77. Collector temperature is optimized to get a minimum mass system. As collector temperature decreases, efficiency increases and the quantity of heat that must be rejected decreases, but radiator temperature decreases and the radiator rejects less heat per unit area. Thus, there is an optimum collector temperature.

Table 13 lists a typical input sequence for program TICYC. The user must specify a power level, an operation time, and then whether the program is to minimize mass or cost. Following that, default parameter values are listed and the user may change them. Table 14 shows a reactor inlet temperature (collector temperature) optimization first, then a listing of parameters for the optimized system.

The program estimates component mass values. Reactor and shield masses are estimated using algorithms constructed by Marshall (Ref. 1). The mass includes fuel, moderator (if any), structure, reflector, gamma shield, neutron shield, and miscellaneous mass. Power conditioning is assumed to weigh 0.2 kg/kw but this value should depend strongly on load characteristics. The power conditioning is assumed to have a 95% efficiency and is cooled using a 500 K isothermal radiator. The system's main radiator mass is summarized in Table 15 and its area is calculated using the algorithms in Appendix F. A miscellaneous mass of 10% is added for piping and structure.

Costs are also estimated, but they are not accurate enough to be taken seriously at this time.

TABLE 13

```
THIS PROGRAM MODELS A THERMIONIC SPACE POWER
SYSTEM.  THE SYSTEM CONSISTS OF A LIQUID METAL
COOLED THERMIONIC REACTOR,
A RADIATOR, AND POWER CONDITIONING.


ENTER VALUES FOR ELECTRICAL POWER IN MW AND
OPERATING TIME IN HOURS.   10 87600

ENTER "WEIGHT" OR "COST" AS PARAMETER TO BE
  MINIMIZED (IN CAPITAL LETTERS).   WEIGHT

THE FOLLOWING ARE DEFAULT PARAMETER VALUES.
THEY MAY BE CHANGED IF YOU WISH.


CYCLE PARAMETERS:
     1.     1800.00000000 EMITTER TEMPERATURE, K
     2.        2.90000010 EMITTER WORK FUNCTION, eV
     3.        1.50000000 COLLECTOR WORK FUNCTION, eV
     4.    5.00000024E-04 GAP DIMENSION, m
     5.    8.10000002E-02 GAP EMITTANCE
     6.        0.20000000 REACTOR PRESSURE, MPa
     7.        0.94999999 POWER CONDITIONING EFFICIENCY


REACTOR PARAMETERS:
     8.        0.93000001 FRACTIONAL FUEL ENRICHMENT
     9.       18.00000000 CRITICAL COMPACT MASS, Kg
    10.        0.27000001 FUEL + MODERATOR VOL FRACT
    11.    24000.00000000 FUEL POWER DENSITY, W/kg
    12.        0.10000000 FUEL BURNUP FRACTION LIMIT
    13.    0.00000000E-01 MODERATOR-TO-FUEL RATIO
    14.    0.00000000E-01 MODERATOR MOLECULAR WEIGHT
    15.        1.00000000 MODERATOR DENSITY, Kg/m3
    16.    4.99999992E+16 ALLOWED PAYLOAD NEUTRON DOSE, nvt
    17.       25.00000000 PAYLOAD SEPARATION DISTANCE, m
    18.       15.00000000 PROTECTION CONE HALF ANGLE, DEG
    19.        2.00000000 NEUTRON SHIELD MATL-B4C=1, LIH=2
    20.    1.00000000E+07 ALLOWED PAYLOAD GAMMA DOSE, R


RADIATOR PARAMETERS:
    21.        0.88000000 RADIATOR EMITTANCE


ENTER THE NUMBER OF PARAMETERS YOU WISH TO CHANGE.   0
```

TABLE 14

OUTLET TEMP (K)	INLET TEMP (K)	TI EFFIC	RCT+SHLD WT (Kg)	POW CONV WT (Kg)	RADIATOR WT (Kg)	TOTAL WT (Kg)	TOTAL COST (M$)
1250.000	1039.474	0.026	136720.	3119.	101993.	266015.	983.
1200.000	989.474	0.091	43689.	3119.	31211.	85822.	329.
1150.000	939.474	0.108	37355.	3119.	28794.	76195.	288.
1100.000	889.474	0.113	36021.	3119.	31035.	77193.	284.
1150.000	939.474	0.108	37355.	3119.	28794.	76195.	288.

CYCLE PARAMETERS

EFFICIENCY	=	0.10808214
THERMAL POWER-MW	=	97.39181519
MASS FLOW RATE-Kg/s	=	486.95907593
REACTOR OUTLET TEMP-K	=	1150.00000000
REACTOR INLET TEMP-K	=	939.47369385
REACTOR PRESSURE-MPa	=	0.20000000

REACTOR PARAMETERS

BURNUP MASS-Kg	=	397.94503784
INITIAL CRITICAL MASS-Kg	=	235.27148437
END CRITICAL MASS-Kg	=	260.43603516
TOTAL BRNUP+CRIT MASS-Kg	=	658.38110352
SPECIFIC POWER-W/Kg	=	24000.00000000
MASS FOR SPECIFIC POWER LIM-Kg	=	5275.38964844
MASS FOR ALLOWED BURNUP-Kg	=	4811.15527344
FUEL MASS-Kg	=	5275.38964844
MODERATOR MASS-Kg	=	0.00000000E-01
STRUCTURE MASS-Kg	=	11955.35156250
REFLECTOR MASS-Kg	=	2722.29345703
PRESSURE VESSEL MASS-Kg	=	309.63922119
MISCELLANEOUS MASS-Kg	=	5275.38964844
TOTAL REACTOR MASS-Kg	=	25538.06445312
NEUTRON SHIELD THICKNESS-m	=	0.19794284
NEUTRON SHIELD MASS-Kg	=	1241.26269531
GAMMA SHIELD THICKNESS-m	=	7.31635392E-02
GAMMA SHIELD MASS-Kg	=	10575.74707031
TOTAL SHIELD MASS-Kg	=	11817.00976562

RADIATOR PARAMETERS

RADIATOR INLET TEMPERATURE, K	=	1110.00000000
RADIATOR OUTLET TEMPERATURE, K	=	899.47369385
HIGH TEMPERATURE AREA, m2	=	829.06091309
MEDIUM TEMPERATURE AREA, m2	=	1155.91284180
LOW TEMPERATURE AREA, m2	=	0.00000000E-01
TOTAL AREA-m2	=	1984.97375488
TOTAL WEIGHT-kg	=	28794.05078125

POWER CONVERSION PARAMETERS

POWER CONDITIONING WEIGHT-kg	=	2000.00000000
PC RADIATOR WEIGHT-kg	=	1119.22570801
TOTAL WEIGHT-Kg	=	3119.22583008

TABLE 14 (cont.)

```
WEIGHT AND COST SUMMARY
   REACTOR WEIGHT-Kg                        =    25538.06445312
   SHIELD WEIGHT-Kg                         =    11817.00976562
   POWER CONVERSION WEIGHT-Kg               =     3119.22583008
   RADIATOR WEIGHT-Kg                       =    28794.05078125
   MISCELLANEOUS WEIGHT-Kg                  =     6926.83496094
   TOTAL WEIGHT-Kg                          =    76195.18750000

   REACTOR+SHIELD COST-M$                   =      164.36231995
   POWER CONVERSION COST-M$                 =       20.22384453
   RADIATOR COST-M$                         =        5.75881004
   LAUNCH COST-M$                           =       97.52983856
   TOTAL COST-M$                            =      287.87481689
Execution terminated : 0
```

TABLE 15
Thermionic System
Mass and Cost Algorithm Summary

Component	Weight	Cost
Reactor	Marshall's algorithm (Marshall, 1986)	\$4400/kg (estimate)
Power Conditioning	0.2 kg/kW (estimate)	\$10,000/kg (estimate)
PC Radiator	5 kg/m^2 (NASA estimate) multiply by 1.25 for meteoroid losses (estimate)	\$200/kg (estimate)
Radiator	12 kg/m^2 temp >1000 K 8 kg/m^2 temp 650 to 1000 K 5 kg/m^2 temp <650 K (NASA estimates) multiply by 1.25 for meteoroid losses (estimate) muliply by 1.2 for heat exchanger (estimate)	\$200/kg (estimate)

SUMMARY AND CONCLUSIONS

This document has described five multimegawatt space power system models:

Gas cooled reactor powered Brayton cycle,
Liquid metal cooled reactor powered Rankine cycle,
Liquid metal cooled reactor thermionic system,
Gas fooled reactor powered open turbine generator, and
Hydrogen-oxygen combustion open turbine generator.

The mathematical algorithms used to estimate system performance and mass have been described. These models have formed the foundation of our efforts to evaluate the many proposed multimegawatt space power systems.

Showing some examples of how these models have been used would be helpful here, but as an alternative, we refer the reader to other documents which describe system studies conducted using the models (Edenburn 1988-1 and 1988-2, and Edenburn 1990).

APPENDIX A

Specific Power Limit For A Gas Cooled Particle Bed Reactor

The specific power extracted from a reactor core can be limited by either fuel temperature or pressure drop considerations. The specific power limit determined by temperature is the maximum specific thermal power (power divided by fuel mass) that can be removed without causing the fuel's temperature limit to be exceeded. To determine this specific power limit we will consider a fuel particle comprised of a central fuel kernel which is coated by layers of other materials.

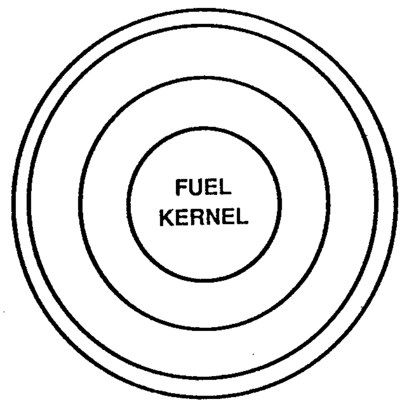

The temperature at the center of the fuel kernel can be found using a standard radial heat conduction analysis.

$$T_f = T_c + \frac{1}{3}\frac{q}{h}\frac{r_1^3}{r_n^2} + \frac{1}{6}\frac{q}{k_1} r_1^2 + \frac{1}{3} q r_1^3 \sum_{i=2}^{n} \frac{1}{k_i}\left(\frac{1}{r_{i-1}} - \frac{1}{r_i}\right) \quad , \qquad \text{(A-1)}$$

where T_f is the temperature at the center of the fuel kernel (K),
T_c is coolant temperature (K),
q is the volumetric heat generation in the fuel kernel (W/m^3),
h is the coolant's convection coefficient (W/m^2 K),
r_i is the radius of the i^{th} layer (m) (the fuel kernel is number 1), and
k_i is the thermal conductivity of the i^{th} layer (W/m K).

The term following T_c is the temperature rise from the coolant to the surface of the particle. Following that is the term representing the temperature rise from the edge to the center of the fuel kernel. The summation term is the temperature rise for all of the intermediate layers. If we let δ represent the kernel and layer temperature rise terms (divided by q), let R be the ratio of kernel to particle radius and D be the particle diameter Equation (A-1) can be abbreviated.

$$T_f = T_c + \frac{1}{6}\frac{q}{h} R^3 D + \delta q \quad . \qquad \text{(A-2)}$$

Solving this for q, we get equation A-3.

$$q = \frac{T_f - T_c}{\frac{R^3D}{6h} + \delta} \quad . \tag{A-3}$$

Since q is the volumetric heat generation, q/r_f is the fuel's specific power. r_f is the density of the fuel kernel. Its limiting value occurs when T_c is at its maximum - the reactor's outlet temperature, T_{out} - and when the fuel temperature is at its maximum value, T_{fmax}.

$$P_s = \frac{q_{max}}{r_f} = \frac{T_{fmax} - T_{out}}{\frac{r_f R^3 D}{6h} + \delta r_f} \tag{A-4}$$

P_s is the specific power limit due to temperature considerations. However, we have not yet evaluated h. Before evaluating h, we will define the rest of the terms to be used in the thermal analysis:

A is the bed's cross sectional area (m^2),
A_p is the total particle surface area (m^2),
C_p is the coolant's specific heat (J/kgK),
D is the fuel particle diameter (m),
h is the heat transfer coefficient between the fuel particles and the coolant (W/m^2K),
k is the coolant's thermal conductivity (W/mK),
L is the length of fuel bed through which the coolant flows (m),

$\dot{m}$ is the coolant flow rate (kg/s),
Pr is the coolant's Prandtl number,
R is the ratio of fuel kernel radius to fuel particle radius,
Re is the coolant's Reynolds number,
T_{in} is the coolant inlet temperature (K),
T_{max} is the maximum allowed fuel particle surface temperature (K),
T_{out} is the coolant outlet temperature (K),
U is the coolant's free stream velocity (m/s),
V_b is the total fuel bed volume (m^3),
V_f is the total fuel kernel volume (m^3) (a fuel particle consists of a UC fuel kernel surrounded by one or more carbon coatings),
V_p is the total fuel particle volume (m^3),
r is the coolant density (kg/m^3),
r_f is the fuel kernel density (kg/m^3), and
μ is the coolant's viscosity (kg/ms).

Eckert (1959), has an expression for h for a packed bed when Re > 500.

$$h = \frac{0.8k}{D} \left(\frac{UDr}{\mu} \right)^{0.7} Pr^{0.333} \quad . \tag{A-5}$$

The term in parenthesis is a Reynolds number and is generally greater than 500 for our applications.

We need to find U, the coolant's free stream velocity to evaluate h so we can determine the value of P_s. To find U, we will use the energy balance equation for the reactor, Equation (A-6).

$$P_s = \frac{\dot{m}C_p(T_{out} - T_{in})}{\rho_f V_f} \quad . \tag{A-6}$$

We can put this in a useful form using the following relations:

$$\dot{m} = \rho UA, \tag{A-7}$$
$$A = V_b/L, \tag{A-8}$$
$$V_f = R^3 V_p, \text{ and} \tag{A-9}$$
$$V_p = .65V_b. \tag{A-10}$$

This last equation assumes that the particle packing density is 65%.

(A-6) can now be written as.

$$P_s = \frac{U\rho C_p(T_{out} - T_{in})}{.65\rho_f R^3 L} \quad . \tag{A-11}$$

We can solve this for U, use this value of U to find h, and substitute the value of h into Equation (A-4) to evaluate P_s.

Letting

$$a_1 = \frac{.282\ \rho_f^{0.3} R^{0.9} D^{1.3}}{k\ P_r^{0.33}} \left[\frac{C_p \mu (T_{out} - T_{in})}{L} \right]^{0.7} \quad , \tag{A-12}$$

Equation (A-4) becomes:

$$P_s = \frac{T_{fmax} - T_{out}}{\dfrac{a_1}{P_s^{0.7}} + \delta\rho_f} \quad , \tag{A-13}$$

or

$$a_1 P_s^{0.3} + \delta\rho_f P_s = T_{fmax} - T_{out} \quad . \tag{A-14}$$

This equation can be solved for P_s.

That gives us the specific power limit associated with fuel temperature. Now we will turn to the specific power limit imposed by pressure drop considerations. The pressure drop across the particle bed is given by Equation (A-15) (Eckert and Drake, 1959).

$$\frac{\Delta P}{L}\frac{D}{(\overline{\rho U})^2}\frac{\varepsilon^3}{1-\varepsilon} = 150\,\frac{(1-\varepsilon)\mu}{\overline{\rho U D}} + 1.75 \quad , \qquad \text{(A-15)}$$

where ε is the void fraction of the bed (1-0.65 = 0.35); see Equation (A-10),
P is the outlet pressure from the reactor (P_a),
Δ is the allowed fractional pressure drop, and
bars over parameters denote mean values.

U will vary through the bed because density, ρ, changes with temperature, however ρU is constant (this is not precisely true for radial flow but is a reasonable approximation if the inside and outside fuel bed diameters are about the same). The coolant can be treated as an ideal gas, thus we can evaluate U as in Equation (A-16).

$$\overline{U} = \frac{U}{2}\left[1 + \frac{T_{in}}{T_{out}}\right] \quad , \qquad \text{(A-16)}$$

where U is the coolant velocity (m/s) at the bed's exit.

We have also estimated the pressure drop through flow channels from Powell (1985).

$$\Delta P = \left[2.9 \times 10^4\; T_{in}/T_{out} + 7.6 \times 10^3\right] \rho U^2 \quad \text{(moderated)}$$

(A-17)

$$\Delta P = \left[6 \times 10^4\; T_{in}/T_{out} + 7.6 \times 10^3\right] \rho U^2 \quad \text{(unmoderated)}$$

The two pressure drops are added to get the total pressure drop.

$$\Delta P = 740\left[1 + \frac{T_{in}}{T_{out}}\right]\frac{\mu L U}{D^2} + 13.3\left[1 + \frac{T_{in}}{T_{out}}\right]\frac{L\rho U^2}{D} + \Gamma\rho U^2,$$

(A-18)

where Γ is defined by the bracketed parts in Equation (A-17).

Again the energy balance Equation (A-11) must be satisfied. Substituting the value of U from the energy balance equation into (A-18) gives us an expression for the specific power limit based on the allowed pressure drop.

$$\Delta P = a_2 P_s + a_3 P_s^2 \quad , \qquad \text{(A-19)}$$

$$a_2 = 481\left[1 + \frac{T_{in}}{T_{out}}\right]\frac{\mu L^2}{D^2}\frac{\rho_f R^3}{\rho C_p (T_{out} - T_{in})} \quad , \qquad \text{(A-20)}$$

$$a_3 = \left\{ 13.3 \left(1 + \frac{T_{in}}{T_{out}} \right) \frac{LP}{D} + \Gamma\rho \right\} \left[\frac{.65\rho_f R^3 L}{\rho C_p (T_{out} - T_{in})} \right]^2 \quad \text{(A-21)}$$

For specified values of Δ and P we can find the value of P_s.

The two values of P_s will not be the same and the smaller of the two should be selected.

A summary of coolant properties is given in Table A-1.

TABLE A-1

Coolant Properties

Property	H_2	He
$k \left(\frac{W}{mK} \right)$	$0.49 \left(\frac{T_{out}}{1200} \right)^{0.43}$	$0.30 \left(\frac{T_{out}}{922} \right)^{0.4}$
$\mu \left(\frac{kg}{ms} \right)$	$23 \times 10^{-6} \left(\frac{T_{out}}{1200} \right)^{0.5}$	$41 \times 10^{-6} \left(\frac{T_{out}}{922} \right)^{0.4}$
$C_p \left(\frac{J}{kgK} \right)$	15,400	5188
$\rho \left(\frac{kg}{m^3} \right)$	$\frac{P}{R_G T_{out}}$	$\frac{P}{R_G T_{out}}$
Pr	0.72	0.72
$R_G \left(\frac{J}{kgK} \right)$	4126	2077
$\gamma \left(\frac{C_p}{C_v} \right)$	1.41	1.66

APPENDIX B

WRAPAROUND REACTOR SHIELD SIZE CALCULATION

Components behind the reactor are protected from radiation by a shadow shield. In Marshall's model (Marshall, 1986), the shield is shaped like a disc whose radius depends on the cone half-angle of protection. For cone half-angles above a certain value, a "wraparound" shield that protects a cone half-angle of 90° would be lighter than a disc shield.

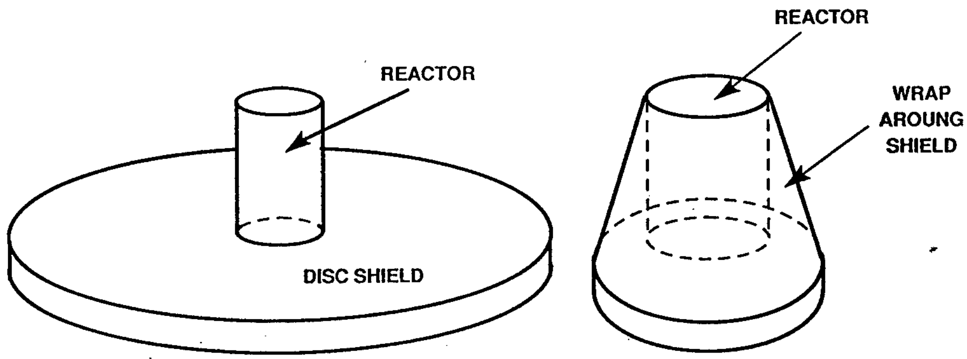

Marshall's model calculates the required thickness of alternating neutron and gamma shield layers t_1, t_2, t_3, and t_4. The wraparound shield calculation uses these thicknesses to calculate the weight of a disc bottom shield and a tapered side or "wraparound" shield as shown in Figure B-1. L_s is the reactor's length and r+T is its radius. The weights of the four layers are given as W_1, W_2, W_3, and W_4.

$\rho_{\gamma s}$ and ρ_{ns} are the densities of the gamma and neutron shields respecively.

If the weight of the wraparound shield is less than that of the disc shadow shield, its value is used as the shield weight.

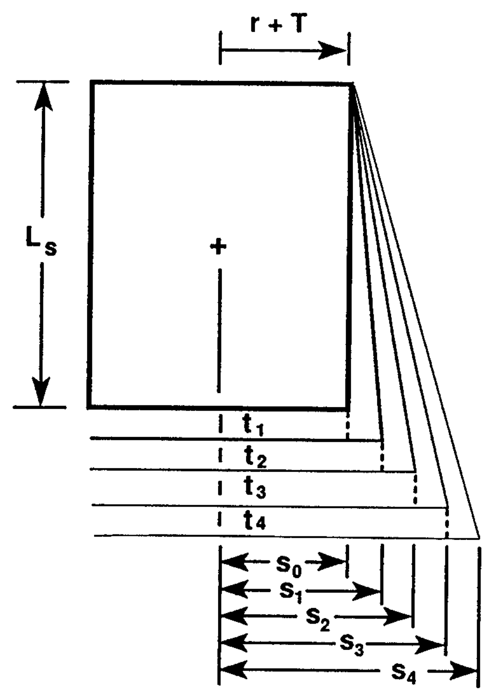

$$S_0 = r + T \quad . \tag{B-1}$$

$$S_1 = S_0 + t_1 \quad . \tag{B-2}$$

$$S_2 = S_1 + t_2 \quad . \tag{B-3}$$

$$S_3 = S_2 + t_3 \quad . \tag{B-4}$$

$$S_4 = S_3 + t_4 \quad . \tag{B-5}$$

$$W_1 = r_{\gamma s}\, \pi \left[t_1 S_0^2 + \frac{1}{2}(L_s + t_1)(S_1^2 - S_0^2) \right] \quad . \tag{B-6}$$

$$W_2 = r_{ns}\, \pi \left[t_2 S_1^2 + \frac{1}{2}(L_s + t_1 + t_2)(S_2^2 - S_1^2) \right] \quad . \tag{B-7}$$

$$W_3 = r_{\gamma s}\, \pi \left[t_3 S_2^2 + \frac{1}{2}(L_s + t_1 + t_2 + t_3)(S_3^2 - S_2^2) \right] \quad . \tag{B-8}$$

$$W_4 = r_{ns}\, \pi \left[t_4 S_3^2 + \frac{1}{2}(L_s + t_1 + t_2 + t_3 + t_4)(S_4^2 - S_3^2) \right] \quad . \tag{B-9}$$

APPENDIX C
Turbine Models

The gas turbine model described in this appendix was formulated by Hudson (1988). Modifications to his original formulation adjust material properties in each stage for temperature and add algorithms for blade cooling.

An axial flow gas turbine is composed of one or more stages which extract energy from a working fluid. Fixed nozzles accelerate the working fluid and direct it onto rotating blades which produce mechanical work. We determine the turbine's speed, disk (to which the blades are attached) radius, and blade length with help from four equations: 1) the blade stress equation (equation C-1); 2) the disk stress equation (equation C-2); 3) the working fluid continuity equation (equation C-3); and 4) the energy equation (equation C-4).

$$\sigma_b \frac{1}{T_f} = (R + L/2)\omega^2 L \quad , \tag{C-1}$$

$$\sigma_d \frac{1}{.9} = R^2 \omega^2 \quad , \tag{C-2}$$

$$\dot{m} = \rho V_a 2\pi \left(R + \frac{L}{2}\right)L \quad , \text{ and} \tag{C-3}$$

$$\dot{m} \left[\frac{1}{2} \left(V_{in}^2 - V_{out}^2\right) + C_p(T_{in} - T_{out}) \right] = \text{Power} \quad . \tag{C-4}$$

We will also need the isentropic expansion relation, an equation-of-state, and an efficiency algorithm.

where

σ_b is blade specific strength (strength divided by density),
T_f is a taper factor (.7),
R is disk radius,
L is blade length,
ω is turbine speed in rad/s,
σ_d is disk specific strength,

$\dot{m}$ is mass flow rate,
ρ is the working fluid's density,
V_a is the working fluid's axial velocity,
V_{in} is the working fluid's speed entering a stage,
V_{out} is the working fluid's speed leaving the stage,
T_{in} and T_{out} are corresponding temperatures, and
C_p is the fluid's specific heat.

Equation C-1 sets the blade's root tensile stress at its maximum allowed strength and equation C-2 sets the disk's greatest tensile stress at its maximum allowed strength.

Equation C-3 requires that the mass flow rate through a turbine stage be equal to the fluid's density multipled by its volume flow rate. V_a, in this equation, can be written in terms of the turbine's blade speed, U, by defining the turbine's work coefficient, ϕ.

$$\phi = \frac{V_{Tin} + V_{Tout}}{U} \quad , \tag{C-5}$$

where

$$U = (R + L/2)\omega \quad , \tag{C-6}$$

and by specifying that it is to be a 50% reaction turbine with constant axial velocity as in equation C-7.

$$V_{Tin} - V_{Tout} = U \quad . \tag{C-7}$$

This specification results in half of the stage's enthalpy drop occuring in the nozzles and half in the blades. A 100% reaction stage would extract all of the enthalpy drop in the blades and an impulse stage with 0% reaction would extract all in the nozzles.

V_{Tin} is the tangential fluid velocity and V_{Tout} is the leaving tangential velocity.

Equations C-5 and C-7 can be combined to evaluate V_{Tout}.

$$V_{Tout} = \frac{U}{2} (\phi - 1) \quad . \tag{C-8}$$

We must also introduce the angle, α, at which the fluid leaves the rotor relative to the rotor blades as in Figure C-1.

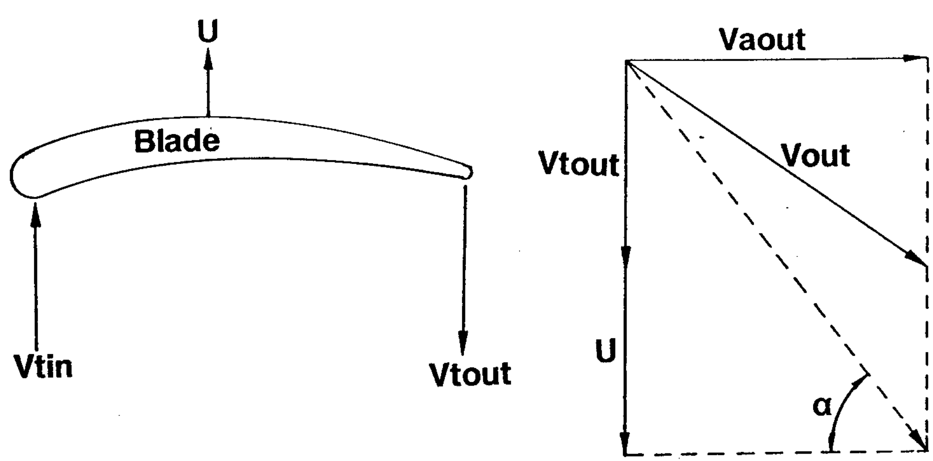

Figure C-1. Turbine Velocity Vector Diagram

Notice that U was added to V_{Tout} to get the tangential velocity relative to a blade. We can now get an expression for V_a to use in equation C-3.

$$V_{aout} = (V_{Tout} + U)/\tan\alpha \quad . \tag{C-9}$$

$$V_{aout} = U\,\frac{\phi + 1}{2\tan\alpha} \quad . \tag{C-10}$$

Using this, the ideal gas relation, and Equation (C-6), equation (C-3), the continuity equation, can be put in its final form.

$$\frac{\dot{m}R_g T_{out} \tan\alpha}{\pi\, P_{out}(\phi + 1)} = \left(R + \frac{L}{2} \right)^2 L\omega \quad , \tag{C-11}$$

where R_g is the fluid's gas constant,
T_{out} is its outlet temperature from a stage, and
P_{out} is its outlet pressure.

We can find a stage's blade length, L, disk radius, R, and angular speed ω, by simultaneously solving Equations (C-1), (C-2), and (C-11); however, there is a special process we must use. First, we need to know the turbine's outlet temperature and pressure. To find these we use a specified turbine pressure ratio, an estimate of turbine efficiency (Equation C-12), and the isentropic expansion relation, modified for a turbine efficiency of η_t (Equation C-13). η_s is the turbine's stage efficiency and is calculated using Equations (C-22) and (C-23) given later in this appendix. (These equations are for turbines with many stages.)

$$\eta_t = \frac{1 - \left(\frac{1}{R_p} \right)^{\eta_s R_g/C_p}}{1 - \left(\frac{1}{R_p} \right)^{R_g/C_p}} \quad , \tag{C-12}$$

$$T_{out} = T_{in} \left[1 - \eta_t + \eta_t R_p^{-R_g/C_p} \right] \quad , \tag{C-13}$$

where T_{out} is the turbine's outlet temperature,
T_{in} is its inlet temperature,
η_t is the estimated efficiency,
R_p is the specified pressure ratio, and
C_p is the working fluid's specific heat.
(C_p will be constant for helium, but for other gasses, it will vary with temperature and can be evaluated using the enthalpy relations in Appendix G. When C_p is not constant, an iterative process must be used to solve Equation (C-12).)

The turbine's last stage will be its largest stage, and since we assume that all of the stages must have the same angular speed, the blades in the last stage will experience the greatest stress. Because of this, we start our process with the last stage, using the turbine's outlet temperature and pressure, to find the turbine's speed. Thus, we calculate ω, R, and L for the last stage. These, of course, depend on blade and disk strength which are functions of temperature. Blade and disk temperatures for the last stage are presumed to be equal to the working fluid's outlet temperature or to a prescribed temperature if the blades are cooled. Material strength and its dependence on temperature are catalogued at the end of this appendix. The value of ω, which we have just calculated for the last stage, is the value of ω we will use for all of the turbine's stages unless we have prescribed a lower value for ω.

The next step in the process is to calculate R and L for each turbine stage starting with the first stage. We calculate R, disk radius, using Equation (C-2). Disk strength properties are evaluated at the stage's inlet temperature or at a prescried temperature if the disk and blades are cooled. To find L for the first and subsequent stages, we must require that energy and working fluid be conserved as working fluid flows through a stage. Equation (C-4) is the energy balance equation. The stage's power is equal to the force exerted on the blades by the fluid, due to its momentum change, multiplied by the blade's speed.

$$\text{Force} = \dot{m}(V_{tin} + V_{tout}) \quad . \tag{C-14}$$

$$\text{Power} = \dot{m}(V_{tin} + V_{tout})U \quad . \tag{C-15}$$

Using Equation (C-5) we get

$$\text{Power} = \dot{m}\phi U^2 = \dot{m}\phi(R + L/2)^2\omega^2 \quad . \tag{C-16}$$

V_{out} can be put in terms of U and finally L as follows:

$$V_{out}^2 = V_{tout}^2 + V_{aout}^2 = \left[(\phi-1)U/2\right]^2 + \left[(\phi+1)U/(2\tan\alpha)\right]^2 \quad . \tag{C-17}$$

These came from Equations (C-8) and (C-10).

With a little regrouping, and using $U = (R + L/2)\omega$, the energy equation can be rewritten as in (C-18).

$$\frac{V_{in}^2}{2} + C_p\,(T_{in} - T_{out}) = A\,(R + L/2)^2 \quad . \tag{C-18}$$

$$A = \left\{ \phi + \frac{1}{2}\left[\frac{(\phi - 1)^2}{4} + \frac{(\phi + 1)^2}{4\tan^2\alpha} \right] \right\} \omega^2 \quad . \tag{C-19}$$

The continuity equation, (C-11), restated here is as follows:

$$\frac{\dot{m}R_g T_{out} \tan\alpha}{\pi\, P_{out}(\phi + 1)} = \left(R + \frac{L}{2} \right)^2 L\omega \quad . \tag{C-11}$$

V_{in} and T_{in} are known from the outlet conditions of the previous stage or, for the first stage, from the turbine's inlet conditions. R and ω were already calculated and α and ϕ are specified values. The unknowns are T_{out}, L, and P_{out}. C_p is known as a function of temperature. To find the three unknowns, we guess values for P_{out} and C_p (our guess is that $P_{out} = P_{in}$ and $C_p = C_p(T_{in})$) and solve the two equations simultaneously to find T_{out} and L, using an iterative procedure. Then we find a new estimate for P_{out} using the isentropic expansion relation and the stage's efficiency, and we estimate a new C_p based on the enthalpy change between T_{in} and T_{out}.

$$P_{out} = P_{in} \left(\frac{T_{in}}{T^*_{out}} \right)^{C_p/R} . \tag{C-20}$$

$$T^*_{out} = T_{in} - \eta_s (T_{in} - T_{out}) . \tag{C-21}$$

η_s is stage efficiency. The value of stage efficiency was formulated by Steve Hudson (1987) using empirical data from a number of sources. T^*_{out} is the stage's outlet temperature for an ideal, isentropic expansion, and T_{out} is the real outlet temperature.

$$\eta_s = 2.49C - 1.623C^2 . \tag{C-22}$$

$$C = 2 \sin \alpha/(\phi + 1) . \tag{C-23}$$

The new values of C_p and P_{out} are used in the energy and continuity equations to calculate new values of L and T_{out}, and the iterative process is continued until it converges.

Notice that we have not used the blade strength equation. Since blade stress is greatest in the last stage, where it is equal to the blade's strength, blade stress will usually be less than strength in the other stages. But, since temperatures change from stage to stage, it is possible to exceed blade strength in an intermediate stage. We check to see if blade strength has been exceeded using Equation (C-1). If it has, a lower value for ω must be specified.

In this manner, we step stage-by-stage through the turbine and find blade length and disk radius. We stop when the turbine's outlet temperature is less than or equal to the desired outlet temperature from Equation (C-13). It is likely that we have overshot the desired outlet temperature substantially, and this is corrected by multiplying the disk radii by a number less than one to reduce the turbine's power extraction. We iterate the disk size until we get the desired outlet temperature.

Recall that we found the desired outlet temperature using an estimate for turbine efficiency in equation C-12. We can find a more accurate turbine efficiency using the modified isentropic expansion relation.

$$\eta_T = (T_{in} - T_{out} \text{ calculated})/(T_{in} - T_{out}^*) \quad . \qquad \text{(C-24)}$$

$$T_{out}^* = T_{in}/(R_p \text{ calculated})^{R/C_p} \quad . \qquad \text{(C-25)}$$

The above computations give us the disk radius, R, and blade length, L, for each stage. We find the mass of a stage by assuming that the stage's axial length depends on blade length. Aspect ratio, blade length divided by stage length, is given by equation C-26, and stage length is given by C-27.

$$A_R = 4 - 3.2e^{-.7L} \quad . \qquad \text{(C-26)}$$

$$S_L = L/A_R,\ R/25,\ \text{or } .004 \text{ m whichever is greater.} \qquad \text{(C-27)}$$

The rotor disk fills 100% of its associated volume plus 20% of the stator volume and the blades fill 30% of their associated volume for both the stator and rotor.

$$\text{disk mass} = 120\%\pi R^2 \rho_m S_L \quad . \qquad \text{(C-28)}$$

$$\text{blade mass} = 30\%\pi[(R+L)^2 - R^2]\rho_m 2S_L \quad . \qquad \text{(C-29)}$$

$$\text{casing mass} = 2\pi(R+L)t^r{}_m 2S_L \quad . \qquad \text{(C-30)}$$

η_m is the turbine material's density.

Casing thickness, t, is found using a hoop strength calculation.

$$t = \frac{(R+L)P_{in}}{\eta_m \sigma_b} \text{ or } \frac{R + L}{25} \text{ whichever is greater.} \qquad \text{(C-31)}$$

Recall that Brayton cycle efficiency depends on blade coolant flow rate, $\dot{m}$. A stage's blade coolant flow rate, $\dot{m}_s$, depends on the following parameters:

- h - the convection coefficient between the working fluid and the blade,
- A - total blade surface area,
- T_{in} - stage inlet temperature,
- T_b - maximum allowed blade temperature,
- C_p - working fluid specific heat, and
- T_c - coolant inlet temperature, (equal to compressor outlet temperature in a Brayton cycle).

El Wakil (1984) gives a graphic relation between $m_s C_p/hA$ and what he calls blade cooling effectiveness, $(T_{in}-T_b)/(T_{in}-T_c)$, for various types of blade cooling. The best was a combination of film and convective cooling, and, for this, a close fit to his data is given by Equation (C-32).

$$\frac{\dot{m}_s C_p}{hA} = 4 \left(\frac{T_{in} - T_b}{T_{in} - T_c} \right)^2 \qquad \text{(C-32)}$$

Thus, if we have values for h and A, we can calculate a value for $\dot{m}_s$. El Wakil proposes values of h between 200 and 500 B/ft^{2}hr F for air. In general, for laminar flow over exterior surfaces, h can be estimated using Equations (C-33) and (C-34) since Prandtl number is fairly constant among gases.

$$Nu \propto Re^{1/2} \quad \text{, and} \qquad \text{(C-33)}$$

$$h \propto k \sqrt{\frac{V\rho}{\mu L}} \quad , \qquad \text{(C-34)}$$

where Nu is Nusselt number,
Re is Reynolds number,
k is gas conductivity,
V is gas velocity
ρ is gas density,
μ is gas viscosity, and
L is the dimension of the surface.

If gas velocity and blade geometry are similar for turbines using two different gases, then Equation (C-34) can be simplified as follows:

$$h \propto k \sqrt{\frac{\rho}{\mu}} \quad . \qquad \text{(C-35)}$$

Thus, helium should have 1.4 times the convective coefficient of air since its $k\sqrt{\rho/\mu}$ is 1.4 times that of air (k is thermal conductivity, ρ is density, and μ is viscosity). We selected 400 B/ft^{2}hr F for air and multiplied by 1.4 to get an h of 560 B/hr ft^2 F or 3000 J/m^{2}sK for helium. For mixtures of He and X_e, k and μ are fairly constant until the mass fraction of Xe gets very large, greater than 0.8. Thus, we assume that h for a He-Xe mixture depends on density, and, since density is inversely proportional to the mixture's gas constant, we can estimate h for the mixture as follows:

$$h_{He\text{-}X_e} = h_{He} \sqrt{\frac{R_{He}}{R_{He\text{-}X_e}}} \quad . \qquad \text{(C-36)}$$

Thus,

$$h_{He-X_e} - 3000 \frac{J}{m^2 sk} \sqrt{\frac{2079}{R_{He-X_e}}} \tag{C-37}$$

Keeping in mind that each blade has two sides, that there are two sets of blades (nozzles and rotor blades) in each stage, and assuming that the spacing between blades is (1/3)L, we can find blade surface area, A.

$$A = 24\pi RS_L \quad . \tag{C-38}$$

From Equations (C-32), (C-36), and (C-38), we calculate m_s for each stage and add each of them to find the total coolant flow rate, $\dot{m}$. When the maximum allowed blade temperature is above the stage inlet temperature, no coolant is necessary.

Turbine Material Strength Catalog

We assume that if the blades are being cooled, the disk is maintained at the inlet coolant temperature.

These specific strength (strength divided by density) values are fits to data compiled by Steve Hudson and represent values that result in 1% creep over 7 years except for carbon composites where creep data is not available. For carbon composites, the values are estimates based on ultimate tensile strength.

Ni Superalloy:

below 875 K σ = 110 kJ/kg
875 to 1350 K $\sigma = 3.961 + 5.377 \times 10^5 e^{-0.00975T}$ kJ/kg (C-39)
above 1350 K - unusable

$$\rho_m = 8500 \text{ kg/m}^3 \quad \text{(C-40)}$$

TZM Mo Refractory:

below 1000 K σ = 40 kJ/kg
1000 to 1800 K $\sigma = -2.21 + 1.046 \times 10^3 e^{-0.00321T}$ kJ/kg (C-41)
above 1800 K - unusable

$$\rho_m = 10{,}200 \text{ kg/m}^3 \quad \text{(C-42)}$$

W-HfC W Refractory:

below 1375 K σ = 36 kJ/kg
1375 to 2000 k $\sigma = -67.2 + 2.567 \times 10^2 e^{-0.000663T}$ kJ/kg (C-43)
above 2000 K - unusable

$$\eta_m = 19{,}300 \text{ kg/m}^3 \quad \text{(C-44)}$$

Si_3N_4 Ceramic:

below 870 K σ = 124 kJ/kg
870 to 1590 k σ = 212 - .1014 T (C-45)
above 1590 K - unusable

$$\rho_m = 3{,}000 \text{ kg/m}^3 \quad \text{(C-46)}$$

Carbon Composite:

all temperatures σ = 167 kJ/kg (C-47)

$$\eta_m = 1800 \text{ kg/m}^3 \quad \text{(C-48)}$$

Simplified Turbine Algorithms

I have used the preceding turbine model to develop simple turbine mass algorithms for superalloy and carbon-carbon composite hydrogen--oxygen combustion, hydrogen and helium turbines, and similar algorithms were developed for potassium-vapor turbines by Steve Hudson.

Equation (C-49) shows the general form of the simplified mass algorithms, however, modifications are required for some specific turbines. Also, we at times used different sets of coefficients for different parameter ranges.

$$\text{mass (kg)} = M_o \, P^{\alpha} \, P_i^{\beta} \, R_p^{\gamma} \, \phi^{\delta} \, \omega^{\varepsilon} \, T_i^{\lambda+\mu} \, T_d^{-\mu} \, (1 + \nu e^{\rho T_d}). \qquad \text{(C-49)}$$

If $T_i < T_d$ then $T_d = T_i$.

The parameters are described as follows:

- P is the shaft power generated in MW,
- T_i is turbine inlet temperature in K,
- P_i is turbine inlet pressure in MPa,
- R_p is turbine pressure ratio,
- ϕ is the work coefficient,
- ω is turbine speed in RPM,
- T_d is disk temperature,

M_o, α, β, γ, δ, ε, λ, μ, υ, and ρ are coefficients to be derived for each type of turbine.

With blade and disk cooling, T_d is lower than T_i. If the blades and disk are not cooled then T_d, T_b and T_i are the same.

These simplified algorithms were constructed to replace the original turbine model which has been used in our reference system models. The original model does an excellent job of estimating the stage-by-stage mass and performance of a turbine, and it was a significant breakthrough for our modeling effort. But, it requires multiple iterations to converge on the proper pressure ratio within the system models, and it requires substantial computer time. The simplified models avoid all of these problems while using the original model as a basis. Thus, it is fast and simple, and it approximates the accuracy of the original basic phenomenological model over limited parameter ranges.

To formulate the simplified models, I assumed that the logarithm of turbine mass depends on the logarithm of each of the turbine parameters independently, and that the dependence on each is linear, except for the dependence on temperature. That is, if turbine mass is plotted as a function of an individual parameter on a log-log plot, the result is a straight line. The turbine's mass dependence on inlet temperature was assumed to be exponential when the blades and disk are not cooled. Coefficients for each of the parameters were found by making the best fit to the mass values obtained from Hudson's turbine model.

Using this procedure, we developed simplified mass algorithms for the following turbines:

Nickel -- H_2-O_2 combustion product
Carbon-Carbon Composite -- H_2-O_2 combustion product

Nickel -- Hydrogen
Carbon-Carbon Composite -- Hydrogen

Nickel -- Helium-Xenon
Carbon-Carbon Composite -- Helium-Xenon

Nickel -- Potassium vapor
Tantalum alloy -- Potassium Vapor

These aglorithms were fairly good over limited parameter ranges, and they have been used in our system models. However, extreme care must be taken in their use. Misleading results can be obtained outside appropriate parameter ranges. Even within appropriate ranges, problems can arise: blade and disk strength limitations can be exceeded, unrealistic blade lengths are possible, results may correspond to an excessive number of stages, and there are other potential problems associated with fluid velocity and blade length to disk diameter ratios. We always confirm system results with the original, more comprehensive model.

Because of the potential problems associated with using the simplified algorithms, I have not reproduced them in this report.

APPENDIX D

Cryogen Storage

The cryogenic storage subsystem consists of liquid hydrogen coolant or liquid oxygen used for combustion, a tank, multilayer tank insulation a refrigeration unit, and a meteoroid shield.

Hydrogen Weight

The mass of hydrogen to be stored is equal to its mass flow rate through the turbine or the weapon, whichever is greater, multiplied by the system operating time. The mass of liquid hydrogen is denoted by M.

$$M = \dot{m}T \quad . \tag{D-1}$$

T is system operating time in seconds and $\dot{m}$ is the hydrogen flow rate.

The volume of hydrogen is denoted by V.

$$V = \frac{M}{\rho} \quad . \tag{D-2}$$

ρ is the density of the stored liquid. The hydrogen is stored in a spherical aluminum tank at 20° K and 0.1 MPa (1 atm). The surface area of the tank is A.

$$A = 4\pi \left[\frac{3V}{4\pi} \right]^{2/3} = 4.84V^{2/3} \quad . \tag{D-3}$$

Hydrogen Tank Weight

The tank weight can be found using a stress analysis. The stress in the tank wall $\sigma(N/m^2)$ can be found as follows:

$$\sigma = \frac{\pi r^2 P}{2\pi r t} \quad , \tag{D-4}$$

where r is tank radius (m),
P is pressure (Pa), and
t is wall thickness (m).

$$t = \frac{rP}{2\sigma} \quad . \tag{D-5}$$

$$\text{tank weight} = 4\pi r^2 t\rho \quad . \tag{D-6}$$

$$\frac{\text{tank weight}}{\text{tank volume}} = \frac{1.5\ P\rho}{\sigma} \quad . \tag{D-7}$$

Values for these parameters for an aluminum tank follow. The tank is aluminum with an ultimate strength of 500 MPa and a safety factor of 2.5.

$$P = 10^5 \text{ Pa},$$

$$\rho = 2700 \text{ kg/m}^3,$$

$$\sigma = 200 \text{ MPa, and}$$

$$\frac{\text{tank weight}}{\text{tank volume}} = 2.03 \text{ kg/m}^3. \quad \text{(D-8)}$$

Refrigeration Unit Weight

The refrigeration unit consists of refrigeration equipment, a radiator, and a power supply. The refrigeration equipment comprises compressors, heat exchangers, turbines, and generators. The power required to run the refrigerator system is found by dividing the heat to be removed by the refrigerator's COP. We will assume that the COP is 15 percent of the Carnot COP for cooling loads above 500 W (Hudson, 1987).

$$COP = 0.15 \frac{T_L}{T_H - T_L} \quad , \quad \text{(D-9)}$$

$$P = \frac{Q}{COP} = Q \frac{T_H - T_L}{0.15 \; T_L} \quad , \quad \text{(D-10)}$$

where T_L is the low temperature in the refrigerator cycle -- the temperature at which the cryogen is stored, 20 K,
T_H is the high temperature in the cycle -- the radiator temperature, in K,
Q is the heat that must be removed, in W, and
P is the power required by the refrigeration unit in W/m^2.

The total heat that must be dissipated is equal to the sum of P and Q. The radiator's area can be found by dividing the heat to be dissipated by the radiator's emissive power. The radiator's weight can then be found by multiplying its area by 5 kg/m^2, the radiator's specific weight, and by 1.25, a factor that accounts for meteoroid losses.

$$\text{radiator weight} = \frac{6.25(P+Q)}{.88\sigma\left(T_H^4 - 250^4\right)} \quad . \quad \text{(D-11)}$$

Here, we assume that the radiating temperature of space is 250 K, and that the radiator's emittance is 0.88.

We calculate the refrigeration unit's power source weight using 30 kg/kW which is the specific weight of a proposed SP-100 power system.

Thus, the power source weight is given by Equation D-12.

$$\text{power source weight} = 0.03P = 0.2Q(T_H\text{-}T_L)/T_L \qquad \text{(D-12)}$$

We assume that the refrigeration equipment weight is given by equation D-13 (Hudson, 1987). This weight is based on a Garrett, reverse Brayton refrigerator.

$$\begin{array}{l}\text{refrigeration} \\ \text{equipment weight}\end{array} = 91.1\text{x}10^{0.0468(\log(Q))**2.9}(T_H\text{-}T_L)/280 \qquad \text{(D-13)}$$

The total refrigeration unit's weight is the sum of the radiator, power source, and refrigeration equipment's weight.

Weights for these components are shown in Table D-1 for various values of T_H, for T_L equal to 20 K, and for Q values of 100 and 1000 W.

The "optimum" radiator temperature, T_H, is 345 K at 100 W and 355 K at 1000 W. Thus, the optimum temperature is not very dependent on the cooling load, Q, and I selected 355 K to use for T_H. With this value of T_H, the refrigeration unit's weight is given by equation D-14.

$$\begin{array}{l}\text{refrigeration} \\ \text{unit weight}\end{array} = 4.52Q + 109\text{x}10^{0.0468(\log(Q))**2.9} \qquad \text{(D-14)}$$

<u>Insulation Weight</u>

CRC (1976) gives multilayer insulation conductivities ranging from 0.04 to 0.2 mW/m-K and an insulation density of 80 kg/m^3. The heat gain through this insulation depends on the difference between the cryogen's temperature (20 K) and the temperature of space (assumed to be 250 K).

$$Q = \frac{(250\text{-}20)kA}{t} , \qquad \text{(D-15)}$$

where k is the insulation's conductivity (we used 0.0001 W/mK),
A is the tank's surface area, and
t is the insulation's thickness in m.

$$\text{Insulation weight} = 80\ At \qquad \text{(D-16)}$$

Insulation thickness affects the weight of the refrigeration unit since it determines the value of Q. Thus, to optimize insulation thickness, we must minimize the combined insulation and refrigeration unit weight.

Table D-2 shows insulation and refrigeration unit weights as functions of insulation thickness for two tank sizes, 100 m^3 and 1000 m^3.

Table D-1
Refrigerator Unit Weights

Radiator Temperature T_H (K)	Power Source mass (kg)	Refrigeration Equipment mass (kg)	Radiator mass (kg)	Total mass (kg)
Cooling Load, Q = 100 W				
300	280	204	280	764
340	320	233	142	695
345	325	236	133	694
350	330	240	125	695
355	335	244	117	696
375	355	258	94	707
400	380	276	73	729
Cooling Load, Q = 1000 W				
300	2800	1235	2802	6837
345	3250	1433	1328	6011
350	3300	1455	1246	6001
355	3350	1476	1172	5998
360	3400	1500	1105	6005
365	3450	1522	1044	6016
375	3550	1566	937	6053
400	3800	1676	733	6209

Table D-2
Insulation Thickness Optimization

Insulation thickness (m)	Insulation weight (kg)	Refrigeration weight (kg)	Total weight (kg)
Tank volume, $V = 100\ m^3$			
.01	83	1492	1575
.02	166	808	974
.03	350	578	828
.035	291	512	803
.04	333	463	796
.045	374	424	798
.05	416	393	809
Tank volume, $V = 1000\ m^3$			
.01	386	6679	7065
.02	773	3326	4099
.03	1159	2247	3406
.035	1352	1942	3294
.04	1546	1714	3260
.045	1739	1537	3276

An insulation thickness of 0.04 m minimizes the total weight for both cases. Using this insulation thickness, we can specify the cooling load Q, power P, refrigeration unit weight, and insulation weight in terms of tank area A.

$$Q = 0.575\ A \text{ in watts} \quad \text{(D-17)}$$

$$P = 64.2\ A \text{ in watts} \quad \text{(D-18)}$$

$$\text{Insulation weight} = 3.2\ A \quad \text{(D-19)}$$

$$\text{Refrigeration unit weight} = 2.60A + 109\times10^{0.0468(\log(.575A))^{**}2.9} \quad \text{(D-20)}$$

Meteoroid Shield Weight

The thickness of an aluminum meteoroid shield that has only a 1 percent chance of being penetrated by a meteoroid during seven years in low earth orbit is specified by equation D-21.

$$t = 5.2 \times 10^{-6}(AT/-\ln P)^{0.29} \quad , \qquad \text{(D-21)}$$

where T is the exposure time in seconds (7 years),
P is the probability of no meteoroid penetrations (.99),
t is the shield's thickness in m, and
A is the tank's area in m^2.

This comes from Fras (1986) using parameters for an aluminum shield and low earth orbit. While the shield will stop natural meteoroids, it will not protect against space debris. Aluminum density (2700 kg/m^3) is multiplied by tank area and shield thickness to get shield weight.

$$\text{shield weight} = 14\ A^{1.29} \qquad \text{(D-22)}$$

Hydrogen Summary

Using equation D-3, the weights of the cryogen storage system can be summarized as follows:

$$\text{cooling load } Q = 2.78\ V^{2/3} \quad . \qquad \text{(D-23)}$$

$$\text{refrigeration power} = 311\ V^{2/3} \quad . \qquad \text{(D-24)}$$

$$\text{tank weight} = 2.03\ V \quad . \qquad \text{(D-25)}$$

$$\text{insulation weight} = 15.5\ V^{2/3} \quad . \qquad \text{(D-26)}$$

$$\text{refrigeration unit weight} = 12.6\ V^{2/3} + 109 \times 10^{0.0468(\log(2.78V**2/3))**2.9} \quad . \qquad \text{(D-27)}$$

$$\text{meteoroid shield weight} = 107\ V^{0.86} \quad . \qquad \text{(D-28)}$$

V is the tank's volume in m^3 and all weights are in kg.

The oxygen storage subsystem's mass was estimated in a similar manner to that used for hydrogen. We assumed that oxygen is stored at 90 K and 0.1 MPa in a spherical aluminum tank surrounded by multifoil insulation and an aluminum meteoroid shield. We also assumed that the oxygen's refrigeration system will be integrated with the hydrogen's refrigeration system.

Oxygen Mass

The density of liquid oxygen at 0.1 MPa is 1142 kg/m^3.

Oxygen Tank Mass

The algorithm for this is exactly the same as for a hydrogen tank.

Refrigeration System Mass

The oxygen will most likely not have a separate refrigeration system. It will "piggy-back" on the hydrogen's refrigeration system. We will assume that the added refrigerator mass can be estimated as follows:

$$O_2 \text{ refrigerator mass} = \frac{Q_O}{Q_H}\frac{COP_H}{COP_O} \times H_2 \text{ refrigerator mass.} \quad \text{(D-29)}$$

Q_O is the heat load to the oxygen tank.

$$Q_O = kA(T_S - T_O)/t \quad , \quad \text{(D-30)}$$

where
- k is insulation conductivity - .0001 w/mK,
- A is oxygen tank area - $4.84V^{0.667}$,
- V_o is oxygen tank volume in m^3,
- T_S is the background temperature - 250K,
- T_O is the oxygen temperature - 90K, and
- t is insulation thickness in m. $Q_O = 0.077V^{0.667}/t$
- Q_H is the hydrogen heat load. $Q_H = 2.8V_H^{0.667}$
- V_H is the hydrogen tank's volume.
- COP_H is the Carnot COP for the hydrogen refrigerator.

$$COP_H = \frac{20}{T_H - 20} \quad . \quad \text{(D-31)}$$

T_H is the refrigerator's radiator temperature, 355K.

COP_O is the Carnot COP for a refrigerator operating between T_H and the oxygen storage temperature, 90K.

$$COP_O = \frac{90}{T_H - 90} \quad . \quad \text{(D-32)}$$

Thus, refrigerator mass is estimated as follows:

$$\text{Refrigerator mass} = \frac{.0048}{t} \times \left[\frac{V_o}{V_H}\right]^{0.667} \times H_2 \text{ refrigerator mass} \quad \text{(D-33)}$$

<u>Insulation Mass</u>

Multifoil insulation has a density of 80 kg/m^3.

$$\text{Insulation mass} = 80 \times 4.84V_o^{0.667} \times t \quad . \quad \text{(D-34)}$$

To find the best insulation thickness, I assumed that the masses of oxygen and hydrogen are equal. (This is true if the combustion power generation system's turbine inlet temperature is around 1200K which requires the combustion of roughly equal portions of H_2 and O_2.)

The following table shows how refrigeration system mass and insulation mass trade-off for two oxygen tank sizes, 1.0 and 30.0 m^3.

	t (m)	O_2 refrig mass (kg)	insulation mass (kg)	total mass (kg)
1 m^3 O_2 tank	.010	16.3	3.9	20.2
	.015	10.9	5.8	16.7
	.020	8.2	7.7	15.9 *
	.025	6.5	9.7	16.2
	.030	5.4	11.6	17.0
30 m^3 O_2 tank	.010	84	37	121.
	.015	56	56	112. *
	.020	42	75	117.
	.025	34	93	127.
	.030	28	112	140.

2 cm is best for the smaller tank and between 1.5 and 2 cm is best for the larger tank. I will use 2 cm for all tanks.

$$\text{Insulation mass} = 7.7V_o^{0.667} \qquad \text{(D-35)}$$

$$\text{Refrigeration mass} = .25 \left[\frac{V_o}{V_H} \right]^{0.667} \times H_2 \text{ refrigeration mass} \qquad \text{(D-36)}$$

Meteoroid Shield

The algorithm for meteoroid shield mass is exactly the same as for the hydrogen tank.

APPENDIX E

Hydrogen-Oxygen Combustion

The heat of combustion for hydrogen and oxygen is $13.4x10^3$ KJ/kg of H_2O (gas reactants and gas products). Hydrogen is assumed to enter the combustion chamber at temperature T_i and it requires heat to be heated from T_i to the reaction temperature T_r which is 300 K. It is preheated when it cools the weapon, power conditioning unit, and generator. The oxygen, on the other hand, must use some of the combustion energy to heat it from a cryogenic liquid to T_r. The remaining combustion energy heats the combustion products, steam and hydrogen (since we are using excess hydrogen to reduce the combustion product temperature) from temperature T_r to temperature T. The energy balance equation for this process is given by equation E-1.

$$\begin{aligned} & m'_H[h_H(T)-h_H(T_r)] + m_S[h_S(T)-h_S(T_r)] \\ & = m_S(13{,}400) - m_O[h_O(T_r)-h_O(T_{so})] - m_H[h_H(T_r)-h_H(T_i)] + m_OS_{po} \; , \end{aligned} \quad \text{(E-1)}$$

where m'_H is the mass of noncombusted hydrogen in kg,
h_H is the enthalpy of hydrogen,
m_S is the mass of steam in kg,
h_S is the enthalpy of steam,
m_O is the mass of oxygen in kg,
h_O is the enthalpy of oxygen being heated through a supercritical process,
S_{po} is the oxygen pumping energy in J/kg,
T_{so} is the temperature at which oxygen is stored as a liquid -90 K, and
m_H is the mass of hydrogen entering the combustion chamber.

We want to find the mass ratio, M_R, of hydrogen to oxygen that results in combustion product temperature T, the turbine inlet temperature.

In the combustion process, 0.125 kg of H_2 combines with 1 kg of O_2 to form 1.125 kg of steam. Using this, we can rewrite equation E-1.

$$\begin{aligned} & (m_H-0.125m_O)[h_H(T)-h_H(T_r)] + 1.125m_O[h_S(T)-h_S(T_r)] \\ & = 1.125m_O(13{,}400)-m_H[h_H(T_r)-h_H(T_i)]-m_O[h_O(T_r)-h_O(T_{so})]+m_OS_{po} \; . \end{aligned} \quad \text{(E-2)}$$

m_H is the total mass of hydrogen entering the reaction. We can divide both sides of E-2 by m_O to get Equation E-3.

$$M_R = \frac{0.125[h_H(T)-h_H(T_r)]+1.125(13{,}400)-h_O(T_r)+h_O(T_{so})-1.125[h_S(T)-h_S(T_r)]+S_{po}}{h_H(T) - h_H(T_i)} \quad \text{(E-3)}$$

This defines the needed ratio of hydrogen-to-oxygen depending on hydrogen inlet temperature, pump power, and the desired combustion product temperature.

The properties of the combustion products depend on the masses of hydrogen and steam in the combustion products.

$$m'_H = (M_R - 0.125)m_O \quad . \tag{E-4}$$

$$m_S = 1.125\ m_O \quad . \tag{E-5}$$

Combustion product mixture properties are given by equations E-6, 7, and 8.

$$h = \frac{h_H m'_H + h_S m_S}{m'_H + m_S} = \frac{(M_R - 0.125)h_H + 1.125h_S}{1 + M_R} \quad . \tag{E-6}$$

$$\gamma = \frac{(M_R - 0.125)g_H + 1.125g_S}{1 + M_R} \quad . \tag{E-7}$$

$$R = \frac{(M_R - 0.125)R_H + 1.125R_S}{1 + M_R} \quad . \tag{E-8}$$

γ is the specific heat ratio
(1.4 for hydrogen, 1.24 for steam), and

R is the gas constant in kJ/kgK.
(4130 J/kgK for hydrogen, 46 J/kgK for steam)

Values for enthalpy are found in Appendix G.

APPENDIX F

Radiator Area

A radiator consists of side-by-side heat pipes. The evaporator end (the end where heat enters) of each pipe sticks into a heat exchanger where it absorbs waste heat from the working fluid of a thermodynamic power generation cycle.

Brayton Radiator

Working fluid from the turbine transfers heat to the finned evaporator ends of the radiator's heat pipes. Equations F-1 and F-2 describe the energy balance in the heat exchanger.

$$-\dot{m}C_p \frac{dT_f}{dX} = hP_x(T_f - T_e) \quad , \qquad \text{(F-1)}$$

$$hP_x(T_f - T_e) = P\varepsilon\sigma(T^4 - T_s^4) \quad . \qquad \text{(F-2)}$$

$\dot{m}$ is the working fluid flow rate,

C_p is the working fluid's specific heat,
T_f is the working fluid's temperature,
X is the dimension along the heat exchanger,
h is the convection coefficient in the heat exchanger,
P_x is the heat exchanger's surface area per unit length of heat exchanger,
T_e is the surface temperature of the heat pipe's evaporator,
P is the radiator's radiating surface area per unit length of heat exchanger,
ε is the radiator emittance (we use 0.88),
σ is the Stephan-Boltzmann constant,
T is the radiator's mean surface temperature, and
T_s is the radiating temperature of space (we use 250 K).

We assume that the temperature drop between the evaporator's surface and the mean radiating temperature is 20 K; that is, T_e - T = 20°K.

With this, we can solve equations F-1 and F-2 as follows:

$$hP_x(T_f - T - 20) = P\varepsilon\sigma(T^4 - T_s^4) \quad , \qquad \text{(F-3)}$$

$$T_f = \frac{P\varepsilon\sigma}{hP_x}(T^4 - T_s^4) + T + 20 \quad , \qquad \text{(F-4)}$$

$$\frac{dT_f}{dX} = \frac{4P\varepsilon\sigma}{hP_x} T^3 \frac{dT}{dX} + \frac{dT}{dX} \quad , \tag{F-5}$$

$$-\dot{m}C_p \left(\frac{4P\varepsilon\sigma}{hP_x} T^3 + 1 \right) \frac{dT}{dX} = P\varepsilon\sigma(T^4 - T_s^4) \quad . \tag{F-6}$$

Letting $a = \dfrac{\dot{m}C_p}{\varepsilon\sigma}$ and $b = \dfrac{\dot{m}C_p P}{hP_x}$

we get Equation (F-7).

$$PdX = -\left[\frac{a}{T^4 - T_s} + \frac{4bT^3}{T^4 - T_s^4} \right] \quad . \tag{F-7}$$

The integral of PdX is the radiation area, A, and can be found by integrating the right side of Equation (F-7).

$$A = \frac{a}{4T_s^3} \left\{ \ln \left[\frac{(T_{out} + T_s)(T_{in} - T_s)}{(T_{out} - T_s)(T_{in} + T_s)} \right] + 2\tan^{-1}\left[\frac{T_{out}}{T_s} \right] \right.$$

$$\left. - 2\tan^{-1}\left[\frac{T_{in}}{T_s} \right] \right\} - b\ln\left[\frac{T_{out}^4 - T_s^4}{T_{in}^4 - T_s^4} \right] \quad . \tag{F-8}$$

T_{out} is the mean radiator temperature at the radiator's fluid outlet end and T_{in} is its mean temperature at the inlet.

These values can be found by iterating to solve Equations (F-9) and (F-10).

$$T_{fin} = T_{in} + \frac{P\varepsilon\sigma}{hPx}(T_{in}^4 - T_s^4) + 20 \quad . \tag{F-9}$$

$$T_{fout} = T_{out} + \frac{P\varepsilon\sigma}{hPx}(T_{out}^4 - T_s^4) + 20 \quad . \tag{F-10}$$

T_{fin} and T_{fout} are inlet and outlet working fluid temperature.

Notice that the term $\frac{hPx}{P}$ is always grouped together. Px/P is the ratio of heat exchanger area to radiator area. Px/P is the most important factor in determining the difference between the fluid's temperature and the radiator evaporator's surface temperature.

The above analysis was first formulated by Al Juhasz at NASA LeRC.

Thermionic Radiator

This analysis is similar to the previous one but it assumes that the temperature difference between the reactor's cooling fluid and the radiator's evaporator surface is 20°K and that the temperature difference between the evaporator's surface and the mean radiator temperature is 20°K for a total difference of 40°K.

$$-\dot{m}C_p \frac{dT_f}{dX} = P\varepsilon\sigma(T^4 - 250^4) \quad . \tag{F-11}$$

Since $T_f = T + 40$, $dT_f = dT$, equation F-11 can be written as follows:

$$PdX = \frac{-\dot{m}C_p}{P\varepsilon\sigma} \frac{dT}{(T^4 - T_s^4)} \quad . \tag{F-12}$$

Integrating PdX gives us the radiator's radiating area, A.

$$A = \frac{\dot{m}C_p}{4\varepsilon\sigma T_s^3} \left[\ln\left(\frac{T_{out}+T_s}{T_{out}-T_s}\right) - \ln\left(\frac{T_{in}+T_s}{T_{in}-T_s}\right) \right.$$

$$\left. + 2\tan^{-1}\left(\frac{T_{out}}{T_s}\right) - 2\tan^{-1}\left(\frac{T_{in}}{T_s}\right) \right] \quad . \tag{F-13}$$

T_{in} and T_{out} are the mean radiating temperatures at the fluid inlet and outlet ends respectively.

$$T_{in} = T_{fin} - 40 \quad , \tag{F-14}$$

$$T_{out} = T_{fout} - 40 \quad . \tag{F-15}$$

T_{fin} and T_{fout} are the fluid inlet and outlet temperatures respectively.

Rankine Radiator

We assume that the radiator for a Rankine system extracts heat from an isothermal, condensing fluid and rejects it to space at an isothermal radiating temperature. The area for this radiator is given by equation F-16.

$$A = \frac{Q}{\varepsilon\sigma(T^4 - T_s^4)} \quad . \tag{F-16}$$

Q is the thermal power (watts) that must be dissipated.

We assume that the temperature drop between the condensing fluid and the evaporator's surface is 10 K and that the drop between the evaporator and mean radiating temperature is 20 K, thus $T = T_f - 30$.

APPENDIX G

Enthalpies for Hydrogen, Oxygen, and Steam

Hydrogen

Jones and Hawkins (1960) give the following expression for hydrogen's specific heat:

$$C_p = 12.1 + .00218T + 31.2/\sqrt{T} \text{ , in kJ/kg-K} \quad . \tag{G-1}$$

Their values were given in English units for 300 K and up. From this, we can find enthalpy by integrating:

$$h = 12.1T + .00109T^2 + 62.4\sqrt{T} + C \quad . \tag{G-2}$$

At low temperatures we used the following data from Reynolds (1979) for parahydrogen:

T (k)	P (MPa)	h (KJ/kg)
20	.1	50
100	10	1293
200	10	2984
300	10	4561

We used these because most of our processes start at 20 K and 0.1 MPa, are pumped to high pressure, then heated in various components. To the 300 K enthalpy we added 229 kJ/kg to account for 75% of the hydrogen changing from para to ortho. We assumed the transition came between 200 and 300 K although we realize the transition depends on many factors. We fit these data and obtained the following relation:

$$h = .007T^2 + 14.7T - 247 \text{ , in kJ/kg.} \tag{G-3}$$

We use this enthalpy expression below 300 K and Equation (G-2) above 300 K. To make them continuous, the constant term in Equation (G-3) is set equal to -15.

Because enthalpy is rather dependent on pressure at low temperatures, the accuracy of Equation (G-3) is not good for some pressure values at temperatures below 100 K.

Oxygen

For oxygen we fit data from Reynolds (1979). Again, we assumed that oxygen would start at 0.1 MPa and be pumped to high pressure before being used.

$$h = 1.0625T + 117.5 \quad , \qquad T > 200 \text{ K} \quad . \tag{G-4}$$

$$h = 2.455T - 161.3 \quad , \qquad T < 200\ K \quad . \tag{G-5}$$

These are in kJ/kg.

Steam

For steam, we used the expression for C_p from Jones (1960) and integrated to find enthalpy.

$$h = 4.61T - 206\sqrt{T} + 967 \ln T - 787 \tag{G-6}$$

This is in kJ/kg.

REFERENCES

Angrist, S.W., 1982. Direct Energy Conversion, fourth ed., Allyn and Bacon, Boston.

Aviation Week, March 18, 1985.

Bents, D., 1984. "Nonthermal Energy Storage for MMW Nuclear Systems," NASA/LeRC, PIR #65.

CRC Handbook of Tables for Applied Engineering Science, 2nd ed., 1976.

Eckert, E.R.G, and Drake, R.M., Jr., 1959. Heat and Mass Transfer, 2nd ed., McGraw Hill.

Edenburn, M.W., 1988-1. The Effect of Operating Temperature and Turbine Blade Cooling on Steady State Brayton Cycle Space Power Systems, SAND87-1921, Sandia National Laboratories.

Edenburn, M.W., 1988-2. The Effect of Operating Temperature on Open, Multimegawatt Space Power Systems, SAND86-1813, Sandia National Laboratories.

Edenburn, M.W., 1990. Reference Concepts for a Space Based Hydrogen-Oxygen Combustion Turboalternator, Burst Power System, SAND89-0423, Sandia National Laboratories.

El Wakil, 1984. Powerplant Technology, McGraw Hill.

Fras, A.P., 1986. Protection of Spacecraft from Meteoroids and Orbital Debris, ORNL/TM-9904, Oak Ridge National Laboratories.

Gerry, E.G., 1985. Advanced Weapon Concept Evaluation Study, Final Report (Appendix J), AFSTC-TR-84-03, Air Force Space Technology Center, Albuquerque, NM.

Hudson, S.L., 1987. Personal Communication, Sandia National Laboratories, Albuquerque, New Mexico, December 5, 1987.

Hudson, S.L., 1988. "Hydrogen Turbines for Space Power Systems: A Simplified Axial Flow Gas Turbine Model," 5th Symposium on Space Nuclear Power Systems, Albuquerque, NM.

Jones, J.B., Hawkins, G.A., 1960. Engineering Thermodynamics, Wiley & Sons, New York.

Marshall, A.C., 1986. RSMASS: A Preliminary Reactor and Shield Mass Model for SDI Applications, SAND86-1020, Sandia National Laboratories, Albuquerque, NM.

Powell, J.R., 1985. Strategic Defense Applications of Particle Bed Reactors (U), Brookhaven National Laboratories, informal report (SNSI).

Reynolds, W.C., 1979. Thermodynamic Properties in SI, Stanford University, Department of Mechanical Engineering, Stanford, CA.

DISTRIBUTION

Note: DOE/OSTI, UC 700 59 copies.

Julio C. Acevedo
PSIO/NASA
Lewis Research Center
21000 Brookpark Rd.
Cleveland, OH 44135

Dr. C. A. Aeby
WL/NTC
Weapons Laboratory
Kirtland AFB, NM 87117

Lt. Col A. Alexander
AFSTC/SW
Kirtland AFB, NM 87117

Douglas Allen
W. J. Schafer Associates
1901 No. Ft. Myers Drive
Suite 800
Arlington, VA 22209

L. Amstutz
U.S. Army Belvoir RDE Ctr.
STRABE-FGE
Fort Belvoir, VA 22060-5606

Larry Atha
U.S. Army Strategic Defense Com.
106 Wynn Drive
Huntsville, AL 35807

Lt. Dale Atkinson
WL/NTCA
Weapons Laboratory
Kirtland AFB, NM 87117

General Electric
Attn: H. S. Bailey
6835 Via del Oro
San Jose, CA 95153

Rick R. Balthaser
RETD
U.S. Department of Energy
Albuquerque Operations Office
Albuquerque, NM 87115

C. Perry Bankston
California Institute of Technology
Jet Propulsion Laboratory
4800 Oak Grove Drive
MS 122-123
Pasadena, CA 91109

Major W. Barattino
WL/TAS
Kirtland Air Force Base
New Mexico 87117-6002

J. O. Barner
Battelle Pacific Northwest Laboratory
P. O. Box 999
Richland, WA 99352

D. Bartine
Oak Ridge National Laboratory
P. O. Box Y
Bldg 9201-3, MS-7
Oak Ridge, TN 37831

Ormon Bassett
W. J. Schafer Associates
1901 No. Ft. Myers Drive
Suite 800
Arlington, VA 22209

Ms. Kathleen Batke
NASA Lewis Research Center
Research/Technology Branch
21000 Brookpark Road
MS 3350
Cleveland, OH 44135

J. Beam
AFWRDC/POOS
Wright-Patterson Air Force Base
Ohio 45433

J. A. Belisle
Manager, Energy Programs
Grumman Aerospace Corp.
MS B20-05
Bethpage, NY 11714

C. Bell
Los Alamos National Laboratory
P.O. Box 1663
MS-F611
Los Alamos, NM 87545

RP/Gary Bennett
NASA Headquarters
600 Independence Ave.
Washington, DC 20546

David Bents
NASA Lewis Research Center
21000 Brookpark Road
MS 301-5, Rm. 101
Cleveland, OH 44135

J. A. Bernard
Massachusetts Institute of Technology
1328 Albany Street
Cambridge, MA 02139

Dave Berwald
Grumman Aerospace Corporation
MS B20-05
Bethpage, NY 11714

F. Best
Assistant Professor
Texas A&M University
Nuclear Engineering Dept.
College Station, TX 77843-3133

Mark Bezik
NASA Lewis Research Center
MS 3160
21000 Brookpark Rd.
Cleveland, OH 44135

Samit K. Bhattacharyya
Argonne National Laboratory
9700 So. Cass Avenue
Bldg. 207
Argonne, IL 60439-4841

H. S. Bloomfield
Program Manager
NASA Lewis Research Center
MS 301-5, Rm. 103
21000 Brookpark Road
Cleveland, OH 44135

Ron Boatwright MS-L-8030
Attn: Document Control
Martin Marietta Space Systems
P O Box 179
Denver, CO 80201

Richard J. Bohl
Los Alamos National Laboratory
MS K560
P. O. Box 1663
Los Alamos, NM 87545

James Bolander
NASA Lewis Research Center
21000 Brookpark Road
Cleveland, OH 44135

William Borger
AFWRDC/POOA
Aeronautical Laboratory
Wright Patterson AFB
Ohio 45433

S. Borowski
NASA Lewis Research Center
MS: 501-6
21000 Brookpark Road
Cleveland, OH 44135

D. Bouska
U.S. Army Strategic Defense Command
106 Wynn Drive
Huntsville, AL 35807

T. Bowden
Brookhaven National Laboratory
P. O. Box 155
Upton, NY 11973

Robert Boyle
Garrett Fluid Systems Co.
P. O. Box 5217
Phoenix, AZ 85010-5217

Mr. Dick Bradshaw
CSSD-H-SAV
US Army Strategic Defense Command
106 Wynn Drive
P. O. Box 1500
Huntsville, AL 35807-3801

Jerry Bueck
W. J. Schafer Associates
2000 Randolph Road, SE
Suite 205
Albuquerque, NM 87106

Wade Carroll
U.S. Department of Energy
NE 52
Germantown Building
Washington, DC 20545

R. D. Casagrande
General Electric
Astro Systems
P. O. Box 8555
Philadelphia, PA

L. Caveny
SDIO/IST
Washington, DC 20301-7100

B. Chadsey
SAIC
1710 Goodridge Drive
McLean, VA 22101

T. S. Chan
General Electric
Astro Systems/SCO
P. O. Box 8555
35T15, Bldg. 20
Philadelphia, PA 19101

John W. H. Chi
Westinghouse Electric Corp.
Advanced Energy Systems
P.O. Box 158
Madison, PA 15663

W. Chiu
General Electric
Space Systems Division
Valley Forge Space Center
P. O. Box 8555
Rm. 35T20, Bldg. 20
Philadelphia, PA 19101

Paul Chivington
TRW, Inc.
Suite 200
2340 Alamo, Se
Albuquerque, NM 87106

Lynn Cleland
Lawrence Livermore National Laboratory
P.O. Box 808
MS L-144
Livermore, CA 94550

Robert Cooper
MS MS-241
Aerospace Corporation
P. O. Box 92957
Los Angeles, CA 90009-2957

E. P. Coomes
Battelle Pacific Northwest Laboratory
P. O. Box 999
Richland, WA 99352

Carl Cox
Westinghouse Hanford
MS C-27
P.O. Box 1970
Richland, WA 99352

Cecil Crews
MS M5-614
Aerospace Corporation
P. O. Box 92957
Los Angeles, CA 90009-2957

J. Crissey
W. J. Schafer Associates
1901 No. Ft. Myers Drive
Suite 800
Arlington, VA 22209

R. Dahlberg
General Atomics
P. O. Box 85608
San Diego, CA 92138

Dr. Gracie E. Davis
RAEE
HQ Defense Nuclear Agency
6801 Telegraph Road
Alexandria, VA 22213

R. Dewitt
Naval Surface Weapons Ctr.
Code F-12
Dahlgren, VA 22448-5000

N. Diaz
INSPI
202 NSC
University of Florida
Gainesville, FL 32611

P. J. Dirkmaat
U.S. Department of Energy/Idaho
785 DOE Place
Idaho Falls, ID 83402

M. P. Dougherty
Martin Marietta Corporation
Astronautics Group
Space Systems
P.O. Box 179
Denver, CO 80201

Rudy Duscha
NASA Lewis Research Center
PSIO
21000 Brookpark Rd.
Cleveland, OH 44135

Mr. Richard Dudney
CSSD-H-YA
US Army Strategic Defense Command
106 Wynn Drive
P. O. Box 1500
Huntsville, AL 35807-3801

D. S. Dutt
Manager, Fuel Design
Westinghouse Hanford
Engineering Development Lab.
P. O. Box 1970
Richland, WA 99352

G. Edlin
U.S. Army Strategic Defense Cm.
106 Wynn Drive
Huntsville, AL 35807

M. El-Genk
University of New Mexico
Chemical and Engineering Department
Albuquerque, NM 87131

Jeffrey George
MS 501-6
NASA Lewis Research Center
21000 Brookpark Road
Cleveland, OH 44135

Dr. David M. Ericson, Jr.
ERCE
7301-A Indian School Rd., NE
Albuquerque, NM 87110

D. Escher
TRW
One Space Park
Redondo Beach, CA 90278

J. Farber
Defense Nuclear Agency
RAEV
6801 Telegraph Road
Alexandria, VA 22310-3398

G. Farbman
Westinghouse
Advanced Energy Systems Division
P. O. Box 158
Madison, PA 15663

M. Firmin
Aerospace Corporation
P.O. Box 9113
Albuquerque, NM 87119

T. Fitzgerald
TRW
One Space Park
Redondo Beach, CA 90278

Terry Flannagan
JAYCOR
11011 Torreyana Road
P.O. Box 85154
San Diego, CA 92138-9259

Dr. Dennis Flood
NASA Lewis Research Center
Mail Stop: 302-1
2100 Brookpark Road
Cleveland, Ohio 44135

J. Foster
Defense Nuclear Agency
RAEV
6801 Telegraph Road
Alexandria, VA 22310-3398

E. P. Framan
California Inst. of Technology
Jet Propulsion Lab.
4800 Oak Grove Drive
MS 301-285
Pasadena, CA 91109

Dr. Mike Frankel
SPAS
HQ Defense Nuclear Agency
6801 Telegraph Road
Alexandria, VA 22213

Robert Franklin
U.S. Army Strategic Defense Cm.
106 Wynn Drive
Huntsville, AL 35807

Bob Gardner
Mission Research Corporation
1720 Randolph Road, SE
Albuquerque, NM 87106-4245

Dr. James Gee
MS M7-633
Aerospace Corporation
P. O. Box 92957
Los Angeles, CA 90009-2957

Jeffrey George
MS: 501-6
NASA Lewis Research Center
21000 Brookpark Rd.
Cleveland, OH 44135

R. Giellis
Martin Marietta Corp.
P. O. Box 179
MS 0484
Denver, CO 80201

Bruce Glasgow
R1/1070
TRW-ATD
One Space Park
Redondo Beach, CA 90278

Capt. J. Gray
WL/NTCA
Weapons Laboratory
Kirtland AFB, NM 87117

R. Gray
RADC/OCTP
Griffis Air Force Base
New York 13441

R. Gripshoven
Naval Surface Weapons Center
F12
Dahlgren, VA 22448-5000

R. L. Hammel
Product Line Manager
Spacecraft Engineering Division
TRW
One Space Park
Bldg. R-4/2190
Redondo Beach, CA 90278

R. Hammond
SDIO/DE
Washington, DC 20301-7100

W. R. Hardie
Deputy Group Leader
Los Alamos National Laboratory
MS F611
P. O. Box 1663
Los Alamos, NM 87545

Neal Harold
AFWAL/POOC-1
Wright-Patterson AFB
Ohio 45433-6563

Mr. Charlie D. Harper
CSSD-H-YA
US Army Strategic Defense Command
106 Wynn Drive
P. O. Box 1500
Hunstville, AL 35807-3801

Dr. M. Harrison
WL/NTCA
Weapons Laboratory
Kirtland AFB, NM 87117

S. Harrison
Office of Science & Technology
Executive Office of the President
Mailing Room 5013
New Executive Office Bldg.
Washington, DC 20506

J. K. Hartman
U. S. Department of Energy
San Francisco Operations Office
1333 Broadway Avenue
Oakland, CA 94612

L. Hatch
Rasor Associates
253 Humboldt Ct.
Sunnyvale, CA 94089

Col. C. Heimach
U. S. Air Force
SD/XR
P.O. Box 92960 WPC
Los Angeles AFB
CA 90009-2960

I. Helms
U. S. Department of Energy
NE-54
Washington, DC 20545

Mr. R. Herndon
AFSTC/SWL
Kirtland AFB, NM 87117

Lt. Col. C. Hill
SDIO/INK
Pentagon, Rm 1E178
Washington, DC 20301-7100

J. Hipp
S-Cubed
2501 Yale Blvd., SE
Suite 300
Albuquerque, NM 87106

E. E. Hoffman
U. S. Department of Energy
Oak Ridge Operations Office
P. O. Box E
Oak Ridge, TN 37830

H. W. Hoffman
Oak Ridge Nat'l Lab.
P.O. Box X
Oak Ridge, TN 37831

K. W. Hoffman
Air Force Foreign
Technology Division
TDTQ
Wright-Patterson AFB
Ohio 45433

R. L. Holton
U.S. Department of Energy
ALO/ETD
P.O. Box 5400
Albuquerque, NM 87115

J. L. Hooper
U. S. Department of Energy
Chicago Operations Office
9800 So. Cass Avenue
Argonne, IL 60439

CNSE/Capt. Howard
Space Systems Division
P. O. Box 92960
Worldway Postal Center
Los Angeles, CA 90009-2960

A. Huber
Air Force Space Technology Center
XLP
Kirtland Air Force Base
New Mexico 87117-6008

Dr. T. Hyder
Auburn University
202 Sanform Hall
Auburn, AL 36849-3501

D. E. Jackson
BDM Corporation
1801 Randolph Rd., SE
MS BV-24
Albuquerque, NM 87106

Jerry Jaggers
Attn: Document Control
for Bldg. 593
Lockheed Missiles and
Space Co. Inc.
P O Box 3504
Sunnyvale, CA 94088

Frank Jankowski
WL/TAPN
Kirtland AFB, NM 87117

Marshall Jew (MS: A02-105)
Grumman Aerospace Corporation
CDC (Ms: A04-35)
Bethpage, NY 11714

B. M. Johnson
Batelle Pacific Northwest Lab.
P.O. Box 999
Richland, WA 99352

R. Johnson
Rocket Dyne
HB-13
6633 Canoga Ave.
Canoga Park, CA 91303

A. Juhasz
NASA Lewis Research Center
MS 301-5, Rm. 101
21000 Brookpark Road
Cleveland, OH 44135

Col. John A. Justice
WL/NTN
Weapons Laboratory
Kirtland AFB, NM 87117

Ehsan Kahn
BDM Corp.
7915 Jones Branch Dr.
MS West Brach 5B37
McLean, VA 22102-3396

Robert Karcher, MS EA-22
Rockwell Int'l Space Transportation
Systems Division
12214 Lakewood Blvd.
Downey, CA 90241

W. Y. Kato
Deputy Chairman
Brookhaven National Laboratory
P. O. Box 155
Upton, NY 11973

D. Kelleher
Technical Director
Advanced Technology Division
AFWRDC/AW
Kirtland Air Force Base
New Mexico 87117

Peter Kemmey
DARPA
1400 Wilson Blvd.
Arlington, VA 22209

Lt. E. B. Kennel
AFWRDC/POOS
Bldg. 450
Wright Patterson AFB
Ohio 45433

K. Kennerud
Boeing Company
Boeing Aerospace System
P.O. Box 3707
Seattle, WA 98124

O. F. Kimball
Oak Ridge Nat'l Lab.
P.O. Box 2009
Bldg. 4508, MS 080
Oak Ridge, TN 37831-6080

F. King
U. S. Army Defense Command
106 Wynn Drive
Huntsville, AL 35807

W. L. Kirk
Los Alamos National Laboratory
P. O. Box 1663
Los Alamos, NM 87545

A. Klein
Oregon State University
Dept. of Nuclear Engineering
Corvallis, Oregon 97331

J. Krupa
U. S. Department of Energy
SAN-ACR Division
1333 Broadway
Oakland, CA 94612

K. D. Kuczen
Argonne National Laboratory
97000 So. Cass Avenue
Argonne, IL 60439

Gerald Kulcinski
University of Wisconsin
Fusion Technology Institute
1500 Johnson Drive
Madison, WI 53706-1687

A. S. Kumar
University of Missouri-Rolla
Department of Nuclear Energy
220 Engineering Research Lab.
Rolla, MO 65401-0249

W. Lambert
U. S. Department of Energy
SAN-ACR Division
1333 Broadway
Oakland, CA 94612

Dick Lancashire
PSIO/NASA
Lewis Research Center
21000 Brookpark Rd.
Cleveland, OH 44135

Lt. Col. F. Lawrence
HQ ASFPACECOM/XPXIS
Peterson Air Force Base
Colorado 80914-5001

R. J. LeClaire
Los Alamos National Laboratory
P. O. Box 1663
MS F611
Los Alamos, NM 87545

CNIS/Lt. Col. J. Ledbetter
Space Systems Division
P. O. Box 92960
Worldway Postal Center
Los Angeles, CA 90009-2960

J. P. Lee
U. S. Department of Energy
MS MA-206
Washington, DC 20545

Dr. James H. Lee, Jr.
SDIO/TNK
The Pentagon
Washington, DC 20301-7100

Lt. Col. R. X. Lenard
SDIO/KE
The Pentagon
Washington, DC 20301-7100

S. Levy
U. S. Army ARDC
Building 329
Picatinny Arsenal
New Jersey 87806-5000

R. A. Lewis
Argonne Nat'l Lab.
9700 So. Cass Avenue
Argonne, IL 60439

Larry Long
Westinghouse R&D
1310 Beulah Road
Bldg. 501-3Y56
Pittsburgh, PA 15235

L. H. Luessen
Naval Surface Weapons Center
Code F12
Dahlgren, VA 22448-5000

Bruce MacCabee
R/42
Naval Surface Weapons Laboratory
White Oaks
Silver Springs, MD 20910

Phil Mace
W. J. Schafer Associates
1901 North Ft. Myers Drive
Suite 800
Arlington, VA 22209

P. Mahadevan
MS M7-597
Aerospace Corporation
PO Box 92957
Los Angeles, CA 90009-2957

T. Mahefky
Group Leader, Thermal Systems
AFWRDC
Aeronautical Laboratory
Wright Patterson Air Force Base
Ohio 45433

B. J. Makenas
Westinghouse Hanford Company
P. O. Box 1970
Richland, WA 99352

P. Margolis
Aerospace Corporation
P. O. Box 92957
El Segundo, CA 90009

Lee Mason
NASA Lewis Research Center
MS: 501-6
21000 Brookpark Road
Cleveland, OH 44135

L. D. Massie
AFWRDC/POOC-1
Aeronautical Laboratory
Bldg. 450
Wright-Patterson AFB
Ohio 45433

Bill Matoush
AFSPACESOM/XPXY
Peterson AFB
Colorado Springs, CO 80915-5001

Maj. Tom McDowell
SDIO/INK
Pentagon, Rm 1E178
Washington, DC 20301-7100

Glen McDuff
Texas Tech. University
Dept. of Electrical Engr.
Lubbock, TX 79409

Barbara McKissock
NASA Lewis Research Center
MS 301-5
21000 Brookpark Road
Cleveland, OH 44135

D. McVay
United Technologies
International Fuel Cells
195 Governor's Highway
So. Windsor, CT 06074

M. A. Merrigan
Los Alamos National Laboratory
P. O. Box 1663
Los Alamos, NM 87545

Ira Merritt
CSSD-H-LS
US Army Strategic Defense Command
106 Wynn Drive
P. O. Box 1500
Huntsville, AL 35807-3801

B. Meyers
Naval Space Command
Dahlgren, VA 22448

J. Metzger
Los Alamos National Laboratory
P. O. Box 1663
Los Alamos, NM 87545

Tom Miller
ASAO/NASA
Lewis Research Center
21000 Brookpark Rd.
Cleveland, OH 44135

J. Mims
S-Cubed
2501 Yale Blvd., SE
Suite 300
Albuquerque, NM 87106

J. F. Mondt
Deputy Project Manager
California Institute of Technology
Jet Propulsion Laboratory
4800 Oak Grove Drive
Pasadena, CA 91109

Capt. J. Moody
AFSTC/SWW
Kirtland AFB, NM 87117

J. C. Moyers
Oak Ridge National Laboratory
P. O. Box Y
Bldg. 9201-3, MS-7
Oak Ridge, TN 37831

D. M. Mulder
AFWL/TAPN
Kirtland Air Force Base
New Mexico 87117-6008

Mr. J. Mullis
WL/NTCA
Weapons Laboratory
Kirtland AFB, NM 87117

I. T. Myers
NASA Lewis Research Center
MS 301-2, Rm. 116
21000 Brookpark Road
Cleveland, OH 44135

Joseph Nainiger
MS 501-6
NASA Lewis Research Center
21000 Brookpark Road
Cleveland, OH 44135

D. F. Nichols
AFWL/TAPN
Kirtland AFB
NM 87117-6008

J. P. Nichols
Oak Ridge National Laboratory
Bldg. K-1030, Room 110
P. O. Box 2003
Oak Ridge, TN 37831-7312

M. Nikolich
W. J. Schafer Associates
1901 No. Ft. Myers Drive
Suite 800
Arlington, VA 22209

Commander R. Nosco
Naval Space Command
Dahlgren, VA 22448

George Novak
Cost Analysis Org.
NASA/Lewis Research Center
21000 Brookpark Rd.
Cleveland, OH 44135

Capt. P. D. Nutz
USAF-SD/CNSD
P.O. Box 92960
LA-AFS
Los Angeles, CA 90009-2960

Tuong Nguyen
MS FB25
Rocketdyne
6633 Canoga Ave.
Canoga Park, CA 91303

C. Oberly
AFWRDC/POOC-1
Wright-Patterson AFB
Ohio 45433

M. Olszewski
Oak Ridge National Laboratory
P. O. Box Y
Oak Ridge, TN 37831

D. Palac
NASA Lewis Research Center
MS: 501-6
21000 Brookpark Road
Cleveland, OH 44135

Dr. D. Payton
EOS Technologies Inc.
200 Lomas NW, Suite 1121
Albuquerque, NM 87102

Capt. G. Peredo
U. S. Air Force
SD/XR
P.O. Box 92960 WPC
Los Angeles AFB
CA 90009-2960

Ed Peterson
Code 4611
Naval Research Laboratory
4555 Overlook Drive
Washington, DC 20375-5000

W. Portnoy
Texas Tech University
Dept of Electrical Engineering
Lubbock, TX 79409

J. Powell
Office of Reactor Systems
Brookhaven National Laboratory
MS 820M, Bldg. 701, Level 143
P. O. Box 155
Upton, NY 11973

J. L. Preston, Jr.
United Technologies
International Fuel Cells
195 Governor's Highway
South Windsor, CT 06074

Eric Proust
Commissariat A L'Energie Atomique
Dept. des Etudes Mechaniques
et Thermiques
33 Rue de La Federation
75015 Paris
FRANCE

Lt. Col. H. Pugh
AFSTC/SWL
Kirtland AFB, NM 87117

C. Purvis
NASA Lewis Research Center
MS 302-1, Rm. 101
21000 Brookpark Road
Cleveland, OH 44135

C. Quinn
U. S. Department of Energy
ALO/ETD
P. O. Box 5400
Albuquerque, NM 87115

William A. Ranken
Los Alamos National Laboratory
Mail Stop: E552
P. O. Box 1663
Los Alamos, NM 87545

N. Rasor
Rasor Associates
253 Humboldt Ct.
Sunnyvale, CA 94089

D. Reid
Los Alamos National Laboratory
MS H811
P. O. Box 1663
Los Alamos, NM 87545

CNBSS/Maj. L. Rensing
Space Systems Division
P. O. Box 92960
Worldway Postal Center
Los Angeles, CA 90009-2960

Dick Renski
AFWRDC/AA
Wright-Patterson AFB
Ohio 45433

J. R. Repp
Westinghouse R&D
1310 Beulah Road
Bldg. 501-3Y56
Pittsburgh, PA 15235

W. H. Roach
S-Cubed
2501 Yale Blvd., SE
Suite 300
Albuquerque, NM 87106

Carlos D. Rodriquez
ASAO/NASA
Lewis Research Center
21000 Brookpark Rd.
Cleveland, OH 44135

Frank Rose
Auburn University
Space Power Institute
231 Leach Center
Auburn, AL 36849-3501

J. H. Saloio
ERCE
7301-A Indian School Road, NE
Albuquerque, NM 87110

S. L. Samuelson
U. S. Department of Energy
San Francisco Operations Office
1333 Broadway Avenue
Oakland, CA 94612

R. T. Santoro
Oak Ridge National Laboratory
P. O. Box 22008
Oak Ridge, TN 37831-6363

Mike Saunders
Booz-Allen and Hamilton Inc.
4330 East-West Highway
Bethesda, MD 20814

L. Schmid
Assistant Project Manager
Battelle Pacific Northwest Lab.
P. O. Box 999
Richland, WA 99352

Paul Schmitz
MS: 301-5
NASA Lewis Research Center
21000 Brookpark Road
Cleveland, OH 44135

Lt. Col. Schneider
WL/NTC
Weapons Laboratory
Kirtland AFB, NM 87117

Col. Garry Schnelzer
SDIO/SATKA
Washington, DC 20301-7100

A. D. Schnyer
NASA Headquarters
Room 600, Code: RP
600 Independence Ave., SW
Washington, DC 20546

Col. J. Schofield
SDIO/SY
Washington, DC 20301-7100

J. Scholtis
Directorate of Nuclear Safety
AFISC/SN
DET 1, AFISC/SNRA
Kirtland AFB
New Mexico 87117-5000

M. J. Schuller
WL/TAPN
Kirtland Air Force Base
New Mexico 87117-6008

G. Schwarze
NASA Lewis Research Center
MS 301-2, Rm. 117
21000 Brookpark Road
Cleveland, OH 44135

Jim Scott
Los Alamos National Laboratory
Mail Stop: E552
P. O. Box 1663
Los Alamos, NM 87545

Clarence Severt
AFWRDC/POOC-1
Wright-Patterson AFB
Ohio 45433-6563

Lt. Col. John Seward
WRDC/AAW
Wright Patterson Air Force Base
Ohio 45433

D. C. Sewell
DCSCON Consulting
4265 Drake Court
Livermore, CA 94550

C. Sharn
SDIO/SY
Washington, DC 20301-7100

B. J. Short
Babcock & Wilcox
Nuclear Power Division
3315 Old Forest Road
P.O. Box 10935
Lynchburg, VA 24506-0935

M. Simon-Tov
Oak Ridge Nat'l Lab.
Bldg. 9201-3, MS-7
Oak Ridge, TN 37831

CNIWT/Capt. Simpson
Space Systems Division
P. O. Box 92960
Worldway Postal Center
Los Angeles, CA 90009-2960

Dr. B. K. Singaraju
WL/NTCA
Weapons Laboratory
Kirtland AFB, NM 87117

Henry Smith
Nichols Research Corp.
4040 So. Memorial Pkwy
Huntsville, AL 35802

John Smith
NASA Lewis Research Center
MS 301-5
21000 Brookpark Road
Cleveland, OH 44135

S. Solomon
Aerospace Corp.
P. O. Box 92957, MS: M1-131
Los Angeles, CA 90009-2957

R. J. Sovie
NASA Lewis Research Center
MS 301-5, Rm. 105
21000 Brookpark Road
Cleveland, OH 44135

O. Spurlock
NASA Lewis Research Center
MS 501-6
21000 Brookpark Road
Cleveland, OH 44135

G. Staats
U. S. Department of Energy
Pittsburgh Energy Tech. Center
PM-20
P. O. Box 18288
Pittsburgh, PA 15236

M. L. Stanley
EG&G Idaho, Inc./INEL
P. O. Box 1625
Idaho Falls, ID 83415

Steve Stevenson
NASA Lewis Research Center
ASAO
21000 Brookpark Rd.
Cleveland, OH 44135

D. C. Straw
W. J. Schafer Associates
2000 Randolph Road, SE
Suite 205
Albuquerque, NM 87106

O. Spurlock
NASA Lewis Research Center
MS: 501-6
21000 Brookpark Road
Cleveland, OH 44135

T. P. Suchocki
Los Alamos National Laboratory
P. O. Box 1663
Los Alamos, NM 87545

L. H. Sullivan
Los Alamos National Laboratory
P. O. Box 1663
Los Alamos, NM 87545

A. Sutey
Spacecraft Subsystems
Boeing Company
P. O. Box 999
MS 8K-30
Seattle, WA 98124-2499

D. W. Swallom
AVCO Research Laboratory
2385 Revere Beach Parkway
Everett, MA 02149

Major P. Talty
HQ USAF/RD-D
Washington, DC 20330-5042

Owen Taylor
Westinghouse R&D
1310 Beulah Road
Bldg. 501-3Y56
Pittsburgh, PA 15235

Charles Terrell
WL/TA
Kirtland AFB,
NM 87117-6008

R. Thibodeau
AFWRDC/POOC-1
Bldg. 450
Wright Patterson Air Force Base
Ohio 45433

J. C. Trocciola
United Technologies
International Fuel Cells
195 Governor's Highway
South Windsor, CT 06074

V. C. Truscello
California Institute of Technology
Jet Propulsion Laboratory
4800 Oak Grove Drive
Bldg. 264-770
Pasadena, CA 91109

John Uecke
S-Cubed
Suite 300
2501 Yale Blvd., SE
Albuquerque, NM 87106

T. H. Van Hagan
General Atomics
10955 John Jay Hopkins Dr.
P. O. Box 85608
San Diego, CA 92121-1194

G. B. Varnado
Int'l Energy Associates Ltd.
1717 Louisiana NE
Suite 202
Albuquerque, NM 87110

R. Verga
SDI Organization
The Pentagon
Washington, DC 20301-7100

D. C. Wade
Applied Physics Division
Argonne National Laboratory
9700 So. Cass Avenue
Argonne, IL 60439

John Wagner
SAIC
2109 Air Park Road, SE
Albuquerque, NM 87106

E. J. Wahlquist
U. S. Department of Energy
NE-54
F415/GTN
Germantown, MD 20545

C. E. Walter, P.E.
Lawrence Livermore National Lab.
P. O. Box 808
MS L-144
Livermore, CA 94550

J. Warren
U. S. Department of Energy
NE-52
GTN
Germantown, MD 20545

C. W. Watson
Los Alamos National Laboratory
MS F607
P. O. Box 1663
Los Alamos, NM 87545

Robert C. Webb
RAEE
HQ Defense Nuclear Agency
6801 Telegraph Road
Alexandria, VA 22213

R. Weed
Nichols Research Corporation
2340 Alamo SE
Suite 105
Albuquerque, NM 87106

Eric Wennas
JAYCOR
11011 Torreyana Road
P. O. Box 85154
San Diego, CA 92138-9259

J. R. Wetch
President
Space Power, Inc.
621 Riverside Pkwy.
San Jose, CA 95134

J. F. Wett
Space & Defense Program
Westinghouse
Advanced Energy Systems Div.
Route 70, Madison Exit
Madison, PA 15663

Dan Whittener
U.S. Army Strategic Defense Cm.
106 Wynn Drive
Huntsville, AL 35807

R. D. Widrig
Human Factors Projects
Battelle Pacific Northwest Laboratory
P. O. Box 999
Richland, WA 99352

F. W. Wiffen
Oak Ridge National Laboratory
P. O. Box Y
Bldg. 9201-3, MS-7
Oak Ridge, TN 37831

Major J. Wiley
Naval Space Command
N5
Dahlgren, VA 22448

Robert Wiley
5998 Camelback Lane
Columbia, MD 21045

E. L. Wilkinson
U. S. Army Strategic Defense Command
106 Wynn Drive
Huntsville, AL 35807

Dr. Ken Williams
SAIC
2109 Air Park Road, SE
Albuquerque, NM 87106

N. Wilson
U. S. Army Lab. Com.
SLKET/ML
Pulse Power Technology Branch
Ft. Monmouth, NJ 07703-5000

Jerry Winter
NASA Lewis Research Center
21000 Brookpark Road
Cleveland, OH 44135

William Wright
Ballena Systems Corporation
1150 Ballena Blvd., Suite 210
Alameda, CA 94501

T. S. Wuchte
AFWL/TAPN
Kirtland AFB
NM 87117-6008

E. R. Zercher
Martin Marietta Corporation
MS L8060
P. O. Box 179
Denver, CO 80201

J. Zielinski
U. S. Department of Energy
SAN-ACR Division
13333 Broadway
Oakland, CA 94612

G. L. Zigler
Science & Engineering Associates
6301 Indian School NE
Albuquerque, NM 87110

Internal Distribution

1200 J. P. Van Devender
1240 K. Prestwich
1248 M. Buttram
1270 R. Miller
1271 M. Clauser
1810 G. Kepler
1830 M. Davis
1832 W. Jones
1840 R. Eagan
3141 S. A. Landenberger (5)
3141-1 C. L. Ward (8) for DOE/OSTI
3151 W. L. Klein (3)
6201 M. Edenburn (20)
6400 D. J. McCloskey
6410 D. Dahlgren
6420 W. Gauster
6421 P. Pickard
6422 J. Brockmann
6450 T. Schmidt
6453 J. Philbin
6460 J. Walker
6461 G. Allen
6461 F. Wyant
6461 L. Sanchez
6461 D. Dobranich
6461 V. Dandini
6461 W. McCulloch
6465 J. Lee (5)
6465 L. Cropp
6465 D. Gallup
6465 R. Peters
6471 L. Bustard
6474 W. Wheelis
6690 D. Berry
6900 A. W. Snyder
8400 R. Wayne
8442 M. Stoddard
8524 J. A. Wackerly
9000 R. Hagengruber
9010 W. Hines
9014 J. Keizur
9014 R. Zazworski
9015 R. Preston
9015 J. Purvis
9100 R. Clem
9110 P. Stokes
9140 D. Rigali
9340 W. Beezhold

*U.S. GOVERNMENT PRINTING OFFICE 1991-0-573-038/20040

Org.	Bldg.	Name	Rec'd by	Org.	Bldg.	Name	Rec'd by

Sandia National Laboratories